UNIVERSITY OF CALGARY

Avalanche Terrain Modeling in Glacier National Park, Canada

BY

Donna M. Delparte

A THESIS
SUBMITTED TO THE FACULTY OF GRADUATE STUDIES
IN PARTIAL FULFILMENT OF THE REQUIREMENTS FOR THE
DEGREE OF DOCTOR OF PHILOSOPHY

DEPARTMENT OF GEOGRAPHY
CALGARY, ALBERTA
JANUARY, 2008

Abstract

Snow avalanches are a significant natural hazard that impact roads, structures and threaten human lives in mountainous terrain. Snow avalanche hazard mapping has the potential to reduce this risk by modeling, mapping and visualizing hazardous terrain using Geographic Information Systems (GIS). The Rogers Pass area in Glacier National Park, British Columbia, Canada provides an ideal location for studying well documented avalanche paths that impact the Trans-Canada Highway. Modeling of terrain in a GIS is typically done by utilizing a digital elevation model (DEM). DEM resolution has traditionally been a limiting factor in the evaluation of terrain at a slope scale. The best available DEM data for this area has a resolution of 25 m. Using a procedure of digital stereo photogrammetry, an improved DEM of higher resolution was generated for this research. This technology allows a GIS operator wearing stereo goggles to digitally resample surface heights using stereo-photo pairs. Topographic parameters such as slope, aspect, curvature and distance from ridges were derived from the DEM.

To evaluate what terrain parameters are most likely to contribute to avalanche activity, expert knowledge from known avalanche paths was documented and statistically evaluated for these key factors. In addition, the alpha-beta statistical model, first used by the Norwegian Geotechnical Institute, was adapted for estimating maximum snow avalanche runout in the Rogers Pass area based upon the detailed avalanche record from the highway corridor. Along roadways or in areas where there is a human presence, details of avalanche runout distance are often recorded; however areas in the backcountry typically traveled by recreationists may not have a recorded history of avalanche activity or runout distances. Patterns from well known avalanche occurrences along the highway corridor were transferred to map avalanche hazard in more remote areas of the region using the derived terrain characteristics, runout model and a GIS algorithm (Avalanche Terrain Exposure Scale) to map avalanche terrain into clear categories of terrain exposure. The results are useful in supplementing traditional field based methods of avalanche hazard mapping as well as providing a tool for risk assessment.

Preface

This thesis explores the use of Geographic Information Systems (GIS) for avalanche hazard and terrain mapping. GIS and digital elevation data offer a means to explore the nuances of terrain that contribute to avalanche formation and release. This thesis describes the process of developing an avalanche runout model for the Columbia Mountains and a preliminary algorithm for determining avalanche exposure. The research presented in this thesis offers a foundation for GIS and avalanche experts to build further understanding and applications in the use of GIS and digital data to aid in decision-making with respect to avalanche terrain.

The GIS maps produced in this thesis are not verified representations of avalanche exposure and no attempt should be made to navigate or make route decisions based on the maps presented in this paper. This thesis is not intended as a guide for backcountry users. Backcountry travel has inherent risks and there is always the potential for avalanches in the terrain described.

Acknowledgements

I would like to gratefully acknowledge Dr. Nigel Waters and Dr. Bruce Jamieson for their contributions, insight, guidance and support throughout the process of completing this PhD thesis. I would also like to thank the other members of my examination committee, Drs. Shawn Marshall, Tak Fung and Karl Birkeland for their time in reviewing this thesis and their constructive comments.

This research would not have been possible without the support provided by an anonymous donor grant through the University of Calgary and is gratefully acknowledged. I would like to thank Graham Bruce for acting as facilitator for this anonymous grant.

I would like to acknowledge and thank Bruce McMahon for the many hours he contributed to identifying topographic features in the GIS for this study and to both his and Grant Statham's input on developing a GIS algorithm based on how experts think about classifying avalanche terrain.

I would also like to thank Dr. Tak Fung of the University of Calgary for statistical analysis support and to Janet Rose for her technical knowledge and assistance with regards to digital elevation mapping. In terms of computer and software support, I'd like to acknowledge Bruce Park for his tremendous and timely assistance as well as his words encouragement at many stages of this research. Thanks also to Ron Perla for his insightful comments and discussion on avalanche runout models.

In April of 2007, I received a Graduate Conference Travel Grant from the University of Calgary Research Grants Committee which allowed me to make two presentations at the European Geosciences Union General Assembly in Vienna, Austria. This opportunity allowed me to present the runout model and the algorithm for avalanche hazard mapping in the Columbia Mountains.

I would like to extend my appreciation to Dr. Nigel Waters for creating the opportunity to present this PhD research at the Core-to-Core Workshop at Schloss Dagstuhl, Germany in July of 2006 and for providing assistance with my travel expenses.

The support of the Selkirk College Professional Development Committee is gratefully recognized for providing one year of professional development funding as well as additional funds to cover travel expenses for numerous conferences, training opportunities and events. In addition, I would like to thank Selkirk College and the Selkirk Geospatial Research Centre for the use of leading-edge technical equipment and data support. My former colleagues at Selkirk College were always supportive and encouraging of my research efforts and future plans and for this I am very appreciative.

I would like to acknowledge the support and encouragement of my parents, Don and Kay Delparte as well as all my friends who encouraged me in the pursuit of my PhD and with whom I have shared many special times in the outdoors, especially on skiing and whitewater kayaking adventures. Particular thanks to Paula Vaananen, Dave Larocque, Laura Adams, Rob D'Eon, Brendan Wilson and Marnie Laser.

Finally, thanks to my husband Rick Richardson for his support and for being my partner in a life of adventure on rock, snow and water.

Table of Contents

List of Tables

List of Figures

List of Symbols, Abbreviations and Nomenclature

α	Angle measurement on the avalanche profile centreline from the top of the avalanche to the maximum runout position
β	Angle measurement on the DEM avalanche profile centreline from the top of the avalanche to the point at which the slope declines to 10˚ in the runout zone
C	Curvature value derived from a DEM using GIS to describe the amount terrain cross-slope and down-slope deviates from being flat
θ	Angle measurement on the avalanche profile centreline from the top of the avalanche to a point on the slope 100 vertical metres below. Measurement of the starting zone slope angle
H	Vertical measurement from the top of the avalanche to a point on the parabola that best fits the avalanche profile at which $y' = 0$
y''	Curvature of the parabola for the alpha-beta runout model
E_A	Avalanche exposure
H_A	Avalanche hazard
P_A	Probability of avalanches
R_A	Avalanche risk
S_A	Avalanche severity
AHMS	Avalanche Hazard Mapping System (Swiss Federal Institute for Snow and Avalanche Research)
AT	Aerial triangulation
ATES	Avalanche Terrain Exposure Scale
BMGS	Base Mapping and Geomatics Service (Province of British Columbia)
CAA	Canadian Avalanche Association
CAC	Canadian Avalanche Centre
CADS	Canadian Avalanche Data System
CPR	Canadian Pacific Railway
ESSF	Englemann Spruce Sub-Alpine Fir
DEM/DTM	Digital Elevation Model
GCP	Ground Control Point
GIS	Geographic Information Systems
GNP	Glacier National Park
GPS	Global Positioning Systems
ICAR	International Commission for Alpine Rescue
ICH	Interior Cedar Hemlock
IMA	Interior Mountain-heather Alpine
NGI	Norwegian Geotechnical Institute
RAAMS	Rapid Mass Movements (Swiss Federal Institute for Snow and Avalanche Research)
SAMOS	Snow Avalanche Modeling and Simulation (Austrian Institute for Avalanche and Torrent Research)

SAR	Search and Rescue
SLF	Swiss Federal Institute for Snow and Avalanche Research
TCH	Trans Canada Highway
TIN	Triangulated Irregular Network
TRIM	Terrain Resource Information Management
VIP	Very-important-point

Chapter One: Introduction

1.1 Background and rationale

Snow avalanches are a significant natural hazard that impact roads, structures and threaten human lives in mountainous terrain. In Canada, despite avalanche control measures such as active triggering of avalanches with explosives and the presence of protection structures, interruptions to transportation on the Trans Canada Highway (TCH) total about 100 hours per winter and have significant economic impacts. Villages in the Alps, Iceland, Kashmir, Northern Afghanistan, Canada and the North Caucasus, Russia have been hit by avalanches resulting in damage to infrastructure and loss of human lives (Egilsson, 1996; George, 1999; NATO, 2006; Sigurdsson et al., 2000). Internationally, based on a reporting period from 1985 to 2005 of the International Commission for Alpine Rescue (ICAR) countries, 138 avalanche fatalities are recorded on average each year for the Alps and North America, with most fatalities resulting from winter recreational activity. Since the 1990s, an increase in the number of winter backcountry users in Canada and Europe is being linked to an increase in the number of avalanche fatalities. In Canada, within the past two decades, fatalities peaked in the winter of 2002/2003, a year noted for an unstable snowpack, with a total of 29 that included the tragic loss of seven students from Strathcona-Tweedsmuir Secondary School in Glacier National Park.

Snow avalanches occur as a result of the interaction of the snowpack, weather and terrain; these three factors are referred to as the avalanche triangle (Fredston and Fesler, 1994) (Figure 1). To create circumstances favourable to avalanching, the weather conditions must be suitable to create snowpack instability and most importantly, the terrain must possess the characteristics necessary for the avalanche to initiate. Terrain is a vital component of the avalanche triangle and is only one that backcountry users can control by selecting appropriate terrain for travel. Terrain influences on avalanche activity include: slope steepness necessary to create a slide, the presence of gullies or

channels into which snow can collect and distance to ridgelines which are prone to wind scouring of snow on the windward side and snow deposition on the leeward side. Terrain also offers areas of refuge. Locations where slopes are less steep or areas of dense forest cover offer a measure of protection. Flat ridge tops and other high points in the terrain also provide options for safer routes of travel.

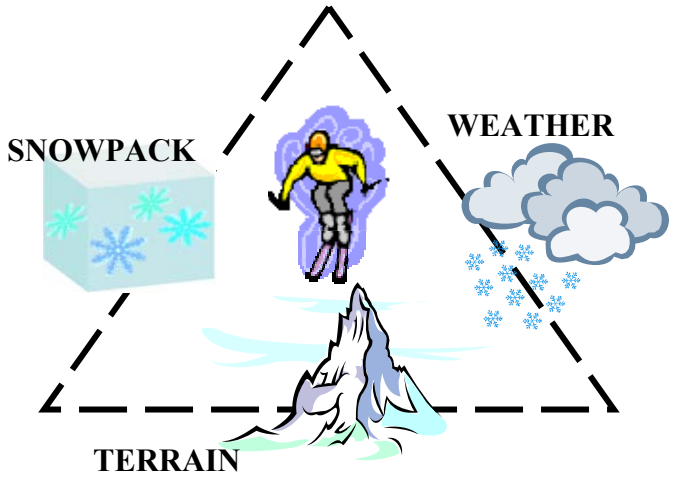

Figure 1. The avalanche triangle. Adapted from Fredston and Fesler (1994)

The importance of terrain in the formation of avalanches and the potential for backcountry users to reduce their risk by selecting safer terrain for travel and skiing illustrates the need for improved terrain description and recognition. Parks Canada (2007) has recognized this need and, as part of an effort for public education and communication, has introduced avalanche terrain maps on trailhead signage with printable versions on their website that highlight terrain hazards by coloured shading on 'bird's eye perspective' photographic maps for popular backcountry skiing areas within the national park system. Further, Parks Canada has introduced the Avalanche Terrain Exposure Scale (ATES) that aids users in identifying Simple, Complex and Challenging avalanche terrain based upon terrain criteria such as slope angle, forest cover and slope shape (Statham et al., 2006a). ATES is used in combination with the Canadian Avalanche Centre's AVALUATOR™ Trip Planner card, where users can select travel routes based upon the current avalanche bulletin advisory, terrain rating and guidelines on

environmental observations (Obvious Clues Method). Together these decision aids would have prevented up to 98% of historical avalanche accidents in Canada (McCammon and Haegeli, 2006).

Geographic Information Systems (GIS) have the capacity to model, analyze, predict, map and visualize avalanche terrain to build and improve upon avalanche terrain recognition and education for backcountry users. The capacity for GIS to produce maps visualizing terrain features and improvements in web-based mapping software has led several European countries to make avalanche hazard based maps available for the public, particularly in the form of on-line solutions. In Norway, searchable on-line maps highlight areas of avalanche potential (http://www.skrednett.no/). Swiss avalanche bulletins along with maps of snow depth, snow profiles and related weather information can be browsed on-line by region (Stoffel et al., 2001). A European Union funded project (PARAMOUNT) combined GIS analysis capabilities with mobile devices in the field to provide avalanche information, weather, tracking and routing and guidance for locations in the Alps and Pyrenees (Löhnert et al., 2004). Research in Canada is underway on how to organize and structure on-line educational exercises facilitated with 3D GIS applications and virtual reality to interactively educate users on route selection through avalanche terrain and hazard identification based on the guidelines of the AVALUATOR™ (Kowalczuk, 2007).

The Canadian Avalanche Association (CAA) has recently recognized the potential of GIS for their operations. The CAA has launched an initiative called the Canadian Avalanche Data System (CADS), encouraged and supported by the Canadian avalanche community, to build a comprehensive database of avalanche and avalanche related information with a planned GIS component to georeference terrain-based information such as mountain features, avalanche paths and ski runs (Tomm, 2006). The CADS project builds upon existing data collected from avalanche operators and is expected to incorporate GIS within the next two years.

Complementing the capacity of GIS to visualize terrain, produce cartographic representations and store information, is the power in GIS for avalanche modeling and prediction or the scientific visualization of those models. For example, the Snow Avalanche Modeling and Simulation (SAMOS) project based out of the Austrian Institute for Avalanche and Torrent Research, is a computer-aided model that uses granular and turbulent flow models to calculate avalanche force and velocities (Buckley et al., 2004). The Norwegian Geotechnical Institute has employed GIS to aid in maximum runout calculations (Toppe, 1987). At the Swiss Federal Institute for Snow and Avalanche Research, numerical simulation models were imbedded in a GIS tool to simulate avalanche dynamics. GIS was the logical tool as it enabled the preparation of digital data for the model's terrain inputs and facilitated map outputs (Haeberli et al., 2004). Critical to the modeling of avalanche terrain are good digital representations of topography. These high quality digital elevation models or DEMs provide an approximation of the terrain surface with sufficient detail for both modeling and visualization.

The emphasis of this thesis is on using GIS and high quality digital terrain data to scientifically model avalanche terrain and visualize the results. The need has been established for better analysis, communication, and visualization of avalanche terrain to aid decision-making. This thesis aims to contribute new findings to the existing body of knowledge by contributing a made-in-Canada avalanche runout model and by developing a GIS based algorithm to map avalanche terrain exposure. In order to outline the purpose of this study, the following section provides a background on the fundamentals of snow avalanches, a discussion of hazard and risk in relation to avalanches and classification of avalanche terrain as it applies in Canada. This is followed by a description of the study area, to provide context, and concludes with a detailed outline of the specific goals and objectives of this thesis.

1.2 Snow avalanches

Snow avalanches threaten lives and infrastructure; the result is lost economic revenue in mountainous regions due to highway and rail closures. In order to understand avalanche phenomena, a review of avalanche fundamentals is necessary, particularly with regards to defining, describing and classifying avalanches. This discussion will aid in outlining the objectives and goals of this thesis. Avalanche researchers and experts have developed a rich background of knowledge from which to further avalanche study. This background information contributes to the understanding of the complexities involved in avalanche activity and helps to describe avalanches through the use of related nomenclature that is relevant to this thesis.

1.2.1 Description and classification

Snow avalanches occur when a mass of snow resting on a surface begins a rapid motion downslope. There are two basic types of snow avalanche: loose snow avalanche and slab avalanche. These two types can be further described as to whether they are wet or dry. Wet snow avalanches have a water content of >3% (McClung and Schaerer, 2006). Snow avalanches are also described based upon their release mechanism. An avalanche may be said to be actively triggered, meaning a release initiated due to a disturbance such as the presence of a skier, cornice fall, snowmobile, or explosive. Natural or spontaneous avalanches occur without an obvious physical stimuli or presence but are likely due to a natural cause such as precipitation or solar radiation; however, the precise cause may be difficult to determine.

Loose snow avalanches start from an initial point in surface or near surface snow that lacks cohesion and can be either wet or dry (Figure 2). Loose snow avalanches are also known as point release avalanches. A slope angle that is sufficient to induce motion is required, typically greater than 40˚ (McClung and Schaerer, 2006). On the descent, loose snow avalanches are characterized by a triangular pattern. Loose snow avalanches often occur naturally due to factors such as solar radiation, snowfall or rain. For the purposes

of this thesis, loose snow avalanche characteristics are not being integrated into any of the GIS modeling or analysis procedures.

Dry slab avalanches pose a greater threat to backcountry users. From a period of 1984 to 1996, slab avalanches accounted for 95% of all recreational accidents (Jamieson and Geldsetzer, 1996); thus, for this thesis, an emphasis is placed on the evaluation of terrain parameters necessary for the formation of dry slab avalanches.

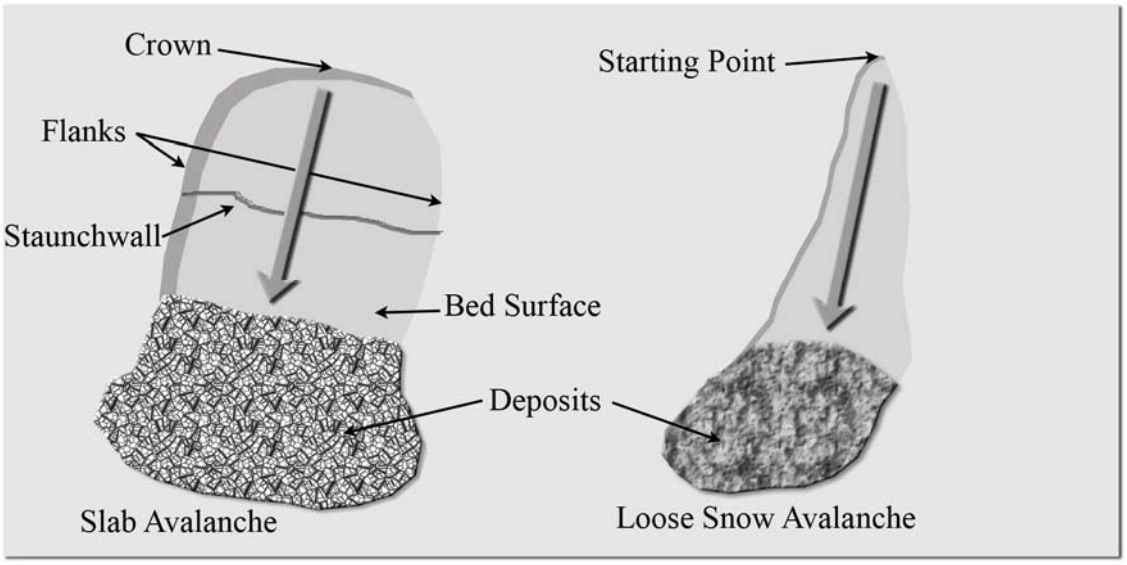

Figure 2. Slab and loose snow avalanches. (Source: author)

Slab avalanches (Figure 2) form when a cohesive block of snow rests upon a weaker layer that can be composed of either wet snow, dry snow or the ground surface. At the moment of release, slab avalanches are roughly rectangular in shape, typically four times as wide as long and less than one metre in thickness and move downslope over the bed surface which can be either the ground or a stationary snow layer. The sides of the slab are referred to as the flanks. The stauchwall is the lowest downslope portion of the slab formed before the slab moves downslope (McClung and Schaerer, 2006). Dry hard slab avalanches result in blocks of snow in the runout zone while soft slab avalanches break up into small clumps during the descent.

Human triggered slab avalanches result mainly from recreational activities in mountainous terrain. To protect transportation corridors, ski areas and other infrastructure, artificial control measures such as explosives are used to mitigate avalanche activity. Dry slab avalanches constitute the main threat to recreationists, so they form the focus of this research.

An avalanche path describes terrain boundaries of known or potential avalanches (Mears, 1992) and is characterized by a starting zone, track and runout zone (Figure 3). The starting zone of an avalanche path is where avalanches begin, the track is where large avalanches achieve maximum velocity and mass and the runout zone is where large avalanches begin to decelerate and deposition occurs. The avalanche track is the area where maximum velocity of large avalanches is reached and is typically in the 15˚- 30˚ slope range (Mears, 1992). The track can be confined, unconfined or a combination of both. A confined track is characterized by small drainages or gullies and has the effect of increasing flow depth and runout distances. Unconfined tracks occur on large open slopes where increased deposition may be observed at abrupt slope transitions such as benches along the avalanche path. This research uses GIS to identify the top of the starting zone of avalanches and to model maximum runout extent.

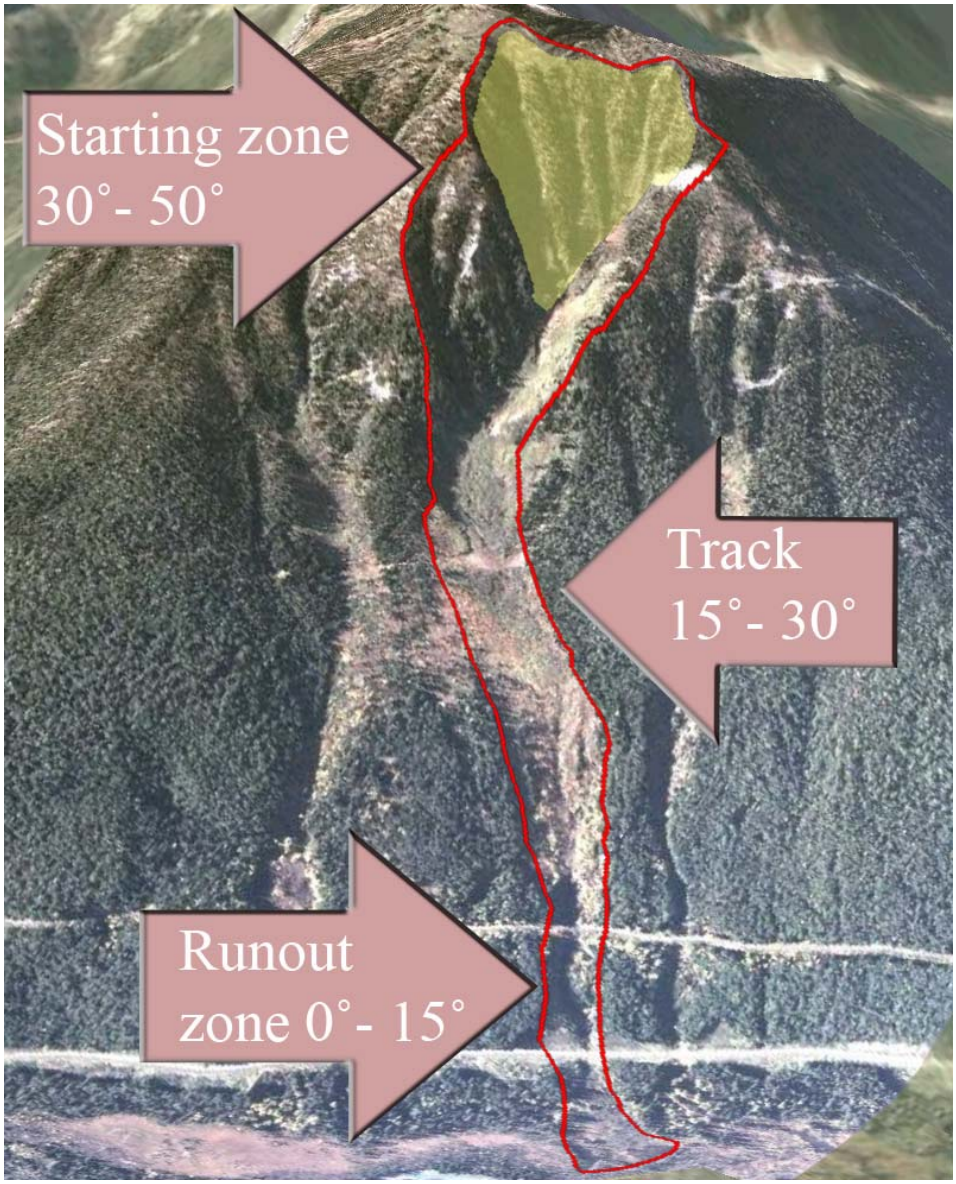

Figure 3. Avalanche path showing the typical slopes of the starting zone, track and runout zone (Source: Parks Canada 2004 air photographs from Glacier National Park draped on a manually generated DEM data with an expert identified avalanche path outline and starting zone digitized by author)

In Canada, the snow avalanche classification system, which categorizes snow avalanches based upon the potential destructive effects, is the means of describing the size and characteristics of an avalanche occurrence. There are five categories ranging from a size 1 avalanche that is relatively harmless to people to a size 5 avalanche that has the capacity to destroy a village or forest of 40 hectares (Table 1).

Table 1. Canadian Snow Avalanche Classification System (McClung and Schaerer, 1993)

Size	Description	Typical Mass	Typical Path Length	Typical Impact Pressures
1	Relatively harmless to people	< 10 t	10 m	1 kPa
2	Could bury, injure, or kill a person	10^2 t	100 m	10 kPa
3	Could bury a car, destroy a small building, or break a few trees	10^3 t	1,000 m	100 kPa
4	Could destroy a railway car, large truck, several buildings or a forest with an area up to 4 hectares	10^4 t	2,000 m	500 kPa
5	Largest snow avalanches known; could destroy a village or forest of 40 hectares	10^5 t	3,000 m	1,000 kPa

1.2.2 Avalanche formation and release

Snowpack characteristics, meteorological factors and terrain features, are significant in influencing snow stability, avalanche release, avalanche motion and runout. The multifaceted interaction of these factors that initiate avalanche release is referred to as avalanche formation (Schweizer et al., 2003). To assess snow stability, avalanche practitioners search for the presence of weak layers within the snowpack. Snowpack stability is defined as the chance of avalanches not starting and in Canada consists of five classes: very good and good stability, fair stability and poor and very poor stability (Canadian Avalanche Association, 2002c). Snowpack stability is forecast for elevation bands of alpine, treeline and below treeline. Stability does not indicate size or potential consequences of avalanches.

Meteorological factors impacting stability include: air temperature, wind, relative humidity, solar radiation, longwave radiation, snow accumulation rates, snow depth and

rainfall. These factors contribute to the formation of weak layers within the snowpack thus influencing the overall stability. Alternatively, new precipitation on top of a snowpack may trigger a weak layer to initiate an avalanche. In the Columbia Mountains, layers of surface hoar crystals are the most common type of weak layer found in fatal slab avalanches (Jamieson and Johnston, 1992).

Expounding on the presence of weak layers and snow stability, the snowpack characteristics that influence avalanche formation relate to the effects of snow metamorphism, which is dependent on snow temperature, density, snow grain characteristics, the temperature gradient within the snowpack and on properties such as snow hardness and the potential for fracture propagation (McClung and Schweizer, 1999). Schweizer and Jamieson (2002), show that snowpack variables of failure layer snow grain size and hardness and the differences in hardness and grain size across the failure interface are key properties in predicting slab failure triggered by skiers. These are time dependent characteristics that change over the winter season, in contrast, terrain characteristics, over a winter season, are time independent characteristics suitable to support static mapping.

This thesis will place an emphasis solely on the terrain factors that lead to slab avalanche formation and potential for release. These terrain characteristics include key factors such as slope angle, distance to ridges, slope curvature and vegetation cover. Terrain factors do not change or play a significant role in slab avalanche formation and release. A brief discussion of slab mechanics provides a background to assist further discussion pertaining to avalanche activity and its relationship to terrain.

Although the mechanics of slab avalanching are not precisely known, the release is generally described as a shear failure that occurs under the slab at the bed surface followed by deformation that occurs rapidly enough to initiate fractures, which leads to a tensile fracture at the crown, lateral breaks on the flanks and a compressive failure at the staunchwall (Figure 4) (McClung and Schaerer, 2006; Schweizer, 1999; Weir, 2002).

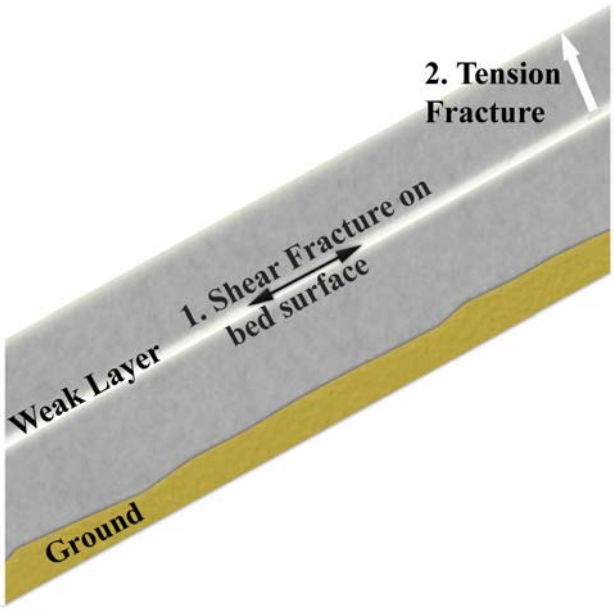

Figure 4. Mechanism of slab release. First a shear fracture of the slab occurs on the weak layer (1) which is followed by a tension fracture at the crown (2). (Adapted from McClung and Schaerer, 2006).

1.2.3 Avalanche frequency, return period and encounter probability

Snow avalanches in mountainous terrain result from a combination of meteorological and snowpack factors. Yet major storms occurring in the same mountain range may produce avalanche activity on some avalanche paths and not others. This variation is due to terrain characteristics such as starting zone topography and orientation to wind. The result is that some paths may produce a large number of smaller avalanches each year while others may only produce a major avalanche event much less frequently. Avalanche "return period" (Figure 5) refers to the expected average time in years between natural avalanche events reaching or exceeding a specified point on an avalanche path, similar to flood return periods (Canadian Avalanche Association, 2002b). An avalanche path with a 10 year return period thus translates into an annual average probability of 0.1. Avalanche frequency is the average number of avalanches that occur per year and is the reciprocal of the return period (e.g.1:100). After slope, snow supply is the greatest determinant of frequency (McClung, 2000; Smith and McClung, 1997) and is further

influenced by terrain characteristics of slope angle, aspect, elevation and ground cover (McClung and Schaerer, 2006).

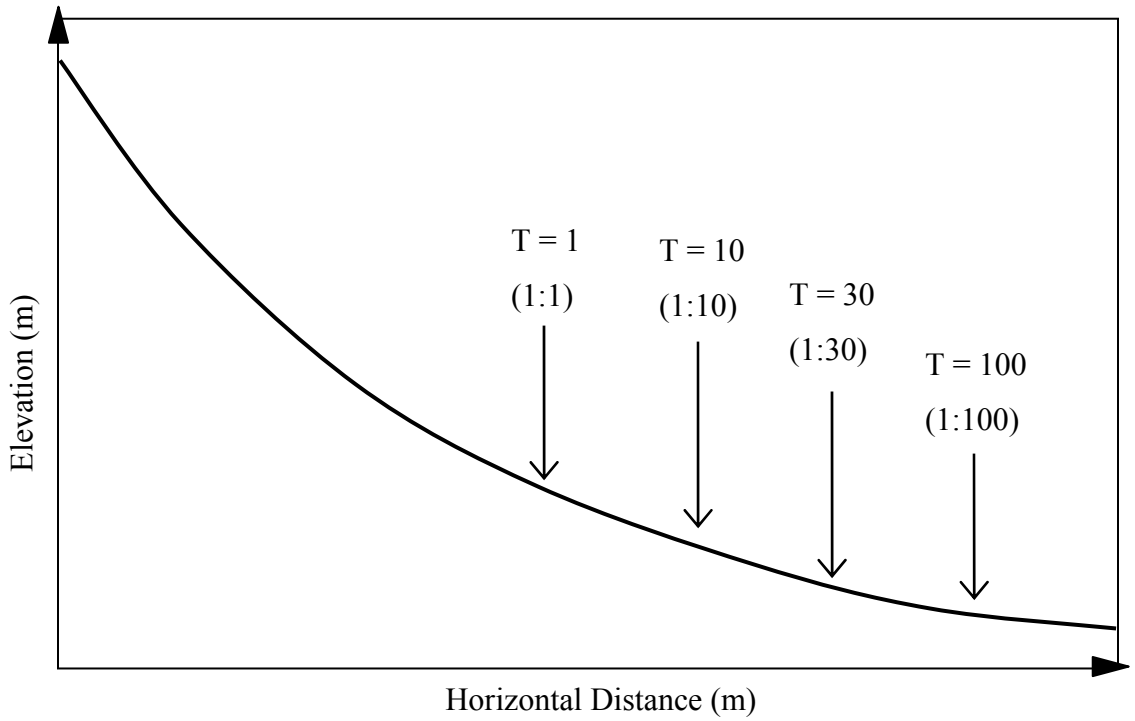

Figure 5. Avalanche return period where T is the average time in years that an avalanche reaches a given point on an avalanche path

The Rogers Pass Snow Avalanche Atlas lists several terms related to avalanche occurrence. Average avalanche activity per year represents the yearly average of all recorded avalanches for the path. Average avalanche effectivity per year represents the yearly average number of avalanches that impact the Trans Canada Highway or the CPR. Lastly each avalanche path is given an effective avalanche hazard rating which is based on the general size of avalanches with some consideration given to the impact of time on road closure required for clearing the avalanche debris (Schleiss, 1989).

Artillery fire can artificially inflate avalanche frequency. In order to estimate the effects of avalanche control, a study was conducted in Rogers Pass based upon observations at 15 avalanche paths along the highway corridor. The results indicated that artillery

produced avalanches, on average, 1.9 times more than would be expected naturally (Schaerer, 1977). This research does not adjust for the effect of explosive control on avalanche frequency in runout calculations or how it may relate to frequency of avalanches on similar slopes in the backcountry that are not controlled. An assumption is made that paths with avalanche control have more frequent events and may reflect a shorter maximum runout than similar avalanche paths that are not controlled.

Encounter probability, E, describes the chance of an avalanche with a return period of T years occurring during some time period, L, and is expressed in the formula below (Mears, 1992) (Eq. 1.1).

$$E = 1 - (1 - 1/T)^L \tag{1.1}$$

For example, an avalanche with a return period of 40 years ($T = 40$) given the chance of occurring within a 40 year time period ($L = 40$) has an encounter probability (E) of 0.64. Compared to the European historical avalanche record of in many cases more than 100 years, the North American historical record of avalanches for many locations is less than 50 years and for longer records relies upon a study of vegetation if available. Thus for many sites in Canada the extreme avalanche events in the range of 100 years or more have simply not been observed.

1.3 Understanding risk, hazard and danger in avalanche terrain mapping

Concise definitions are required to clarify the meaning of certain terms with regards to risk, hazard and danger in avalanche terrain; these terms are often combined or used interchangeably. Each of these terms has a specific meaning in relationship to avalanche activity. These terms have further significance when discussing the type of map that is represented. Is it a risk map or hazard map or is it an indication of some kind of danger that will be draped over the terrain? The following discussion will attempt to clarify

these terms and their relationships with respect to a description of avalanche activity or avalanche terrain.

1.3.1 Risk and hazard

Any outdoor activity constitutes some level of risk. These activities expose the individual to the chance that they may lose something that is of value to them. Risk is a measure of the probability and severity of an adverse effect that can include a potential injury including death, loss of money or loss of possessions (CSA, 1997. (R2002)). Alternatively, it must be recognized that risk also affords an opportunity for the individual to experience something that they highly value. Risk thus provides an opportunity for gain with the consequence of a potential for loss. Risk seems to be an essential part of the human experience, as demonstrated by an increasing number of people who are participating in outdoor adventure, extreme sports or wilderness activities.

Whereas risk is the likelihood or chance that potential harm occurs, hazard describes the source of potential harm, damage or adverse effects (CSA, 1997. (R2002)). Specific to the avalanche environment, a working group in Canada (Statham, G., personal communication, August 21, 2007) is working towards devising expressions to describe both avalanche risk (R_A) and avalanche hazard (H_A). In Equation 1.2, avalanche risk (R_A) is determined by the physical exposure (E_A) of a person or thing to avalanche hazard (H_A). Equation 1.3 shows that avalanche hazard (H_A) is a function of the probability of avalanche(s) (P_A) and the severity of the avalanche (S_A). A key difference between the definitions is that risk involves exposure while hazard assumes the potential to effect people but does not explicitly denote physical exposure.

$$R_A = f(H_A, E_A) \tag{1.2}$$

$$H_A = f(P_A, S_A) \tag{1.3}$$

A hazard rating scale would describe the potential harm from an avalanche for individuals, infrastructure and the environment in the path of an avalanche, particularly in terms of high, moderate and low. For example, the Canadian Hazard Rating Scale for Roads and Highways ranges from Low to Extreme and is a function of the likelihood of avalanches to run onto the highway and the potential impacts to traffic.

Traditional forms of risk assessment for avalanche hazard mapping in Canada seek to protect transportation routes, energy and communication structures, occupied structures, resort ski areas, work sites and are also used for forest harvest planning such as the avalanche likelihood mapping conducted for the BC Ministry of Forests (Kelly and Stevens, 1997). This form of mapping uses topographic maps, air photos and field observations along with a sound knowledge of snow climate characteristics (Canadian Avalanche Association, 2002a). There are four common forms of traditional snow avalanche mapping that include locator maps, avalanche atlas maps, zone maps and risk based maps (Canadian Avalanche Association, 2002b). Locator maps identify potential avalanche terrain for human infrastructure or natural resources at a 1:20,000 or 1:50,000 scale and are generally supplemented with field studies. One of the objectives of this research is to create a visually appealing map of the backcountry using GIS to indicate varying levels of avalanche terrain (Simple, Challenging and Complex). An avalanche atlas provides a detailed catalogue of avalanche paths and terrain characteristics. For this thesis the *Rogers Pass Snow Avalanche Atlas* (Schleiss, 1989) was an indispensable resource for collecting detailed information on avalanche paths in the highway corridor. Zone maps identify avalanche terrain areas based on characteristics such as slope angle and snow depth. Risk maps provide a formal assessment of risk that indicate some level of avalanche frequency, damage and assumed exposure (Canadian Avalanche Association, 2002a). Risk maps may include: risk determination for structures, linear features and natural resources that describe risk in terms of impact pressures and return periods and zone maps for human occupied infrastructure with shading of red (high risk), blue (moderate risk) and white (low risk). These maps are generated at a scale of

1:50,000 or 1:20,000 or larger. Probable exposure is critical for applications of risk mapping as in the case of transportation corridors.

To reduce risk, risk management strategies can be implemented. Risk management is a process for managing or optimizing risks and hazards (Cloutier, 2000). The goal of risk management is to avoid high-risk, high consequence activities and to optimize risk management strategies to decrease the probability of an accident and to reduce its severity should one occur. Specific to avalanche operations, risk management for a spatially variable snowpack involves pre-season planning, daily planning and travel and field studies (Jamieson, 2003).

1.3.2 Avalanche danger

In an effort to communicate avalanche risk to the backcountry recreationist, the Canadian Avalanche Centre (CAC) uses a five level danger scale (Table 2) that is based on the probability of natural or human triggered avalanches. The scale also provides recommended actions for each level. Avalanche danger refers specifically to the effect of avalanches on backcountry recreationists. In Canada, public avalanche bulletins and avalanche education are the primary means of aiding the public in reducing avalanche exposure risk. More recently, regulations for custodial groups in National Parks have been introduced for winter activities to reduce exposure of custodial groups to avalanche hazards. All avalanche bulletins may be accessed via the web at the Canadian Avalanche Centre website and all use the five level danger scale and the Backcountry Avalanche Advisor, (Figure 6) as described below (http://www.avalanche.ca).

The capacity for Geographic Information Systems to produce maps visualizing terrain features as well as improvements in web-based mapping software has led to an interest in providing avalanche risk based maps for the public, particularly in the form of on-line solutions. To display avalanche danger provided by the CAA bulletin or a stability rating on a slope-by-slope scale, the temptation is to drape these rating systems on terrain maps

such that a backcountry user could visualize safe slopes to use. Important issues in examining the potential of providing risk based maps to the public are: scale issues, limitations of data and technology, verification and issues around liability. Scale presents a substantial challenge in producing avalanche risk based maps for visualizing a complex interaction of terrain, weather and snowpack. Of primary interest to a backcountry user would be snowpack stability at the scale that would allow a skier to determine if a particular slope is safe to ski. Unfortunately, snowpack stability can vary within a few metres while the resolution of commercially available digital data to represent terrain is at best 25 m and weather required for the inputs into stability models would require a density of weather stations that does not exist in Canada. Even with a dense network of weather stations, stability maps at a slope scale would still be difficult to generate as there is not a complete understanding of all the processes involved that lead to avalanche release.

The lack of a dense network of meteorological and snowpack stations in the backcountry in Glacier National Park prohibit the ability to map snowpack stability at a small process scale (slope-level). Within the region, there is a continuously manned weather observation station and study plot at Rogers Pass and periodic monitoring of a weather station and study plot at Mount Fidelity. As well, there are seven other locations consisting of field test sites or automatic weather stations that supply weather data. With the observation network that exists, it would be impossible to estimate meteorological input variables for specific avalanche slopes or known slab release points. Insufficient data points are available for spatial interpolation methods. Local variations in stability due to wind, ground cover and subtle variations of terrain would pose the greatest challenge in these estimations. Due to the lack of understanding related to the patterns of snowpack stability and the data currently available to model the complex interactions of weather and terrain factors to predict snowpack stability, it would be impossible to map slope-scale danger, risk or hazard (Campbell et al., 2004). Conversely, Switzerland has a large automated weather network supplementing direct human observations that can be related to the local scale. Hourly data from the network, which includes over 80 high

alpine automated weather and snow stations, builds a snowpack model for each station and the information is stored in a central database for avalanche forecasters to review (Lehning et al., 2002b). Further developments involve looking at generating a physical model of snow cover instability and a statistical model of avalanche release probability (Lehning et al., 2002a; Schweizer et al., 2006a).

Table 2. Canadian Avalanche Centre Danger Scale (2006)

Danger Level and colour	Probability and Trigger	Recommended Action
Low	Natural avalanches very unlikely. Human triggered avalanches unlikely.	Travel is generally safe. Normal caution advised.
Moderate	Natural avalanches unlikely. Human triggered avalanches possible.	Use caution in steeper terrain on certain aspects.
Considerable	Natural avalanches possible. Human triggered avalanches probable.	Be increasingly cautious in steeper terrain.
High	Natural and human triggered avalanches likely.	Travel in avalanche terrain is not recommended.
Extreme	Widespread natural or human triggered avalanches certain.	Travel in avalanche terrain should be avoided and confined to low angle terrain, well away from avalanche path runouts.

BACKCOUNTRY AVALANCHE ADVISORY

A general summary of avalanche conditions in Western Canada is produced daily throughout the winter. You'll find it in the weather pages of most daily newspapers, and on most TV and radio weather forecasts. More precise information can be found in the Public Avalanche Bulletins at **www.avalanche.ca or call 1800 667 1105.**

AVALANCHE CONDITIONS	TRAVEL ADVICE	GUIDANCE FOR AMATEUR RECREATION
GOOD	NORMAL CAUTION	Avalanches are infrequent but possible. Appropriate conditions for informed backcountry travel.
SERIOUS	EXTRA CAUTION	Avalanches will occur with human and other triggers. Avalanche training and experience are essential for safe backcountry travel.
POOR	NOT RECOM-MENDED	Avalanches are occurring frequently. Inappropriate conditions for backcountry travel without extensive avalanche training and experience.
VARIABLE	EXTRA CAUTION	Conditions change from good with frozen snow to poor with melted snow. Avalanche training and experience are essential to monitor conditions for safe travel.

Users of this information assume their own risk.

Figure 6. Parks Canada Backcountry Avalanche Advisory

In response to recommendations made in the Parks Canada Backcountry Avalanche Risk Review (O'Gorman et al., 2003) , the CAA has attempted to simplify the five levels of relative avalanche potential in its danger scale (Table 2) to a simpler warning system for the general public. Thus, the backcountry avalanche advisory (Figure 6) has been devised for use on TV, radio, the CAA website and newspaper weather forecasts. Concerns over the subjectivity of the "considerable" category in the five level danger scale led to this recommendation. The objective is to aid the general public in understanding avalanche risk in the mountains. This backcountry advisory is intended as a general summary of avalanche conditions. Recreational users are requested to seek further information from the Canadian Avalanche Centre website that provides more detailed avalanche bulletins.

The purpose of the bulletins is to provide current and relevant information regarding avalanche danger, snowpack and weather conditions to the general public so that the

information provided can be used by recreationists to make better and more informed decisions. The information used to compile the bulletins is synthesized from a network of over 80 commercial, private and government operations collectively known as "InfoEx". Located in the seven regions covered by the CAC bulletins, these organizations record daily avalanche, weather and snowpack observations that are submitted to InfoEx online. The avalanche bulletin is the first avenue of support for recreational backcountry users to obtain information that may aid them in making more informed decisions.

1.3.2.1 Avalanche Terrain Exposure Scale (ATES)

The ATES scale (Table 3) was initially developed by Parks Canada personnel in order to identify terrain suitable for custodial groups. This is an expert system that uses terrain features to determine challenges presented by the terrain in an area for backcountry travel. The ratings consist of Simple, Challenging and Complex terrain. In referring back to the avalanche risk calculation (1.2), if determining avalanche risk (R_A) using GIS represents scale challenges, perhaps another approach to reduce risk is to reduce the level of exposure (E_A) in the terrain used by backcountry recreationists. GIS has been used in other countries to map avalanche hazards such as starting zones and runout at a slope scale that may be of relevance to the backcountry user. Parks Canada has introduced its Avalanche Terrain Exposure Scale that includes reference to vegetation, slope, starting zones and runout which could be modeled in a GIS. Table 3 provides a summary of the ATES terrain categories that is suited for public consumption. The detailed technical model of ATES used to aid experts in categorizing terrain is discussed in chapter five.

The current procedure to rate popular recreation routes is to have one or more avalanche experts, who have knowledge of the area, to categorize it as Simple, Challenging or Complex terrain according to ATES criteria. This judgement relies heavily on personal knowledge of the terrain being rated. This local expert knowledge is a limitation on providing accurate and consistent ratings across large and/or multiple areas which this thesis addresses by utilizing the ATES expert approach in combination with GIS to

produce maps that reveal areas of exposure based on the critical terrain characteristics. An ATES rating by recreation route does not reveal variations of exposure; for example, a recreation route may be entirely within Simple terrain with the exception of one or more crossings of challenging terrain, so the rating becomes Challenging for the entire route. GIS maps can show how, over a specific route, the terrain rating may change from Simple to Complex. By utilizing a higher resolution DEM (5- 10 m), GIS has the capacity to produce maps at a local scale to reveal areas of Simple, Challenging and Complex terrain. The resulting terrain exposure map has the potential to assist experts in making their assessment of recreation trails and routes as well as being a decision-making tool for backcountry recreationists to reduce their risk by making wise use of terrain to minimize avalanche exposure.

Table 3. Avalanche Terrain Exposure Scale (ATES) v.1/04 (ParksCanada, 2004) (also http://www.pc.gc.ca/pn-np/ab/banff/visit/visit7a1_E.asp)

Level	Description
Simple	Exposure to low angle or primarily forested terrain. Some forest openings may involve the runout zones of infrequent avalanches. Many options to reduce or eliminate exposure. No glacier travel.
Challenging	Exposure to well defined avalanche paths, starting zones or terrain traps; options exist to reduce or eliminate exposure with careful route finding. Glacier travel is straightforward but crevasse hazards may exist.
Complex	Exposure to multiple overlapping avalanche paths or large expanses of steep, open terrain; multiple avalanche starting zones and terrain traps below; minimal options to reduce exposure. Complicated glacier travel with extensive crevasse bands or icefalls.

Slope angle is a critical component of terrain analysis in GIS as well as for backcountry skiers who are encouraged to select ski slopes of less than 30˚ or “Simple terrain” in

conditions of high and extreme avalanche danger. This is an important part of the recommendations in Canada's new Avaluator Avalanche Accident Prevention Card (Haegeli and McCammon, 2006). GIS has the capacity to reveal this terrain through maps and other forms of visual aids to assist users in identifying safer areas in avalanche country. In combination with a higher resolution DEM (< 10 m), the ability of GIS to examine subtle terrain features is enhanced. A GIS analysis utilizing compatible ATES criteria and is an area of inquiry that this research explores in chapter five.

1.4 Location and general description of the study area

The study area is in Glacier National Park (GNP), British Columbia, Canada. GNP is located along the Trans Canada Highway (TCH) and the main line of the Canadian Pacific Railway, approximately 350 km west of Calgary, in the Rogers Pass area between Golden and Revelstoke (Figure 7). The TCH provides easy access to backcountry skiing within Glacier National Park. Situated in the Columbia Mountains of western Canada and mainly within the sub-range known as the Selkirk Mountains, with only the eastern park boundary edging into the Purcell Mountains sub-range, GNP covers an area of approximately 1,300 km^2. The terrain of GNP is characterised by steep-sided glaciated valleys, rugged high peaks and expansive glaciers. Elevations in the Park range from 820 m in the valley bottom to approximately 3377 m for Hasler peak on Mount Dawson in the southern part of the Park and 3284 m for the more famous Mount Sir Donald located adjacent to the Trans Canada Highway. During the winter, avalanche activity in GNP results in frequent road closures and over the years fatalities in the backcountry have been recorded.

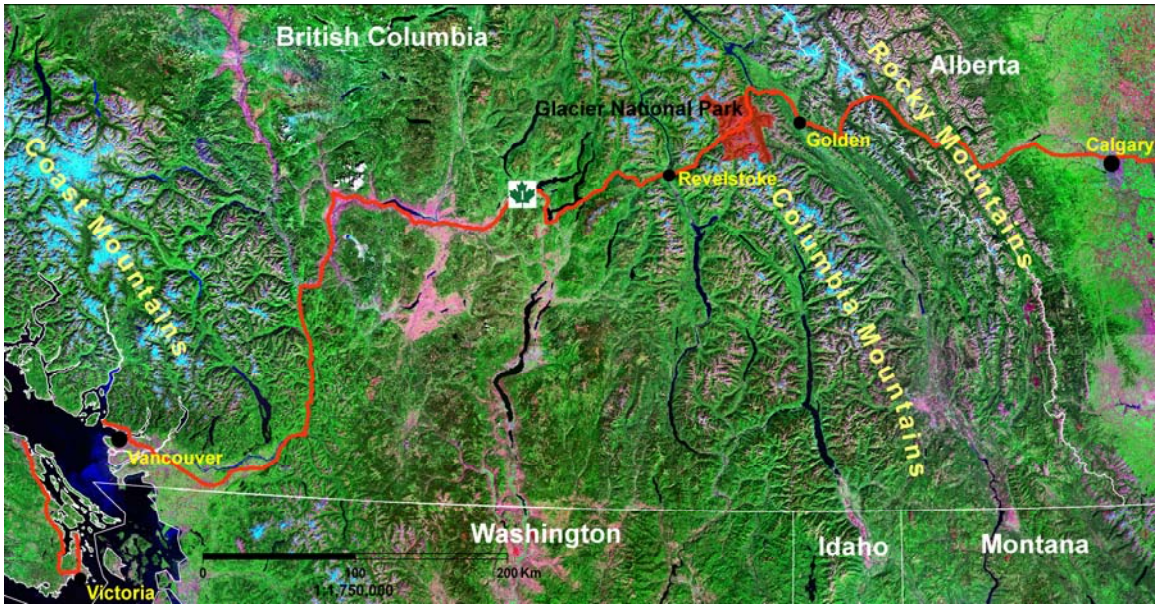

Figure 7. Location of study area (Data source: NASA Landsat 7 Imagery, 2000)

Along the highway corridor, covering a distance of 45 km, there are 144 avalanche paths that are monitored by the Parks Canada avalanche control program (Figure 8). The combination of heavy snowfall and a steep sided U-shaped valley through which the highway passes leads to frequent avalanche activity. For example, the 40 highway avalanche paths analyzed for this study have a per path avalanche frequency ranging from 1 to 70 avalanches per year, a mean frequency of 23 avalanches per year and a median of 9 avalanches for each path per winter season. The mean length of these avalanche paths is 2115 m with mean starting and end elevations of 2175 m and 1220 m, respectively. Starting zones have a mean elevation range from 1870 m to 2200 m and mean surface area of 1.4 ha.

Parks Canada operates one of the world's largest mobile avalanche control programs to keep the Trans Canada Highway (TCH) and the Canadian Pacific Railway (CPR) operating through Rogers Pass. The exposure of the highway and railway and their importance as a transportation corridor led to the formation of an avalanche control program prior to the highway's construction in 1959. Avalanche problems in this corridor were well known based on a historical record of accidents dating back to the

construction of the railway in 1885. Between 1885 and 1911, over 200 deaths of railway workers were recorded, caught by avalanches as they cleared snow and debris from previous avalanche events (Woods, 1983). To avoid the high avalanche hazard along Rogers Pass, the Connaught Tunnel was built, diverting 16 km of surface rail line underground to an 8 km tunnel which was completed in 1916. A second tunnel was completed in 1988, the 14.6 km Mount Macdonald Tunnel.

To counteract the impact of avalanches hitting the highway and exposed sections of the rail line, additional defensive structures including snow sheds, diversion dams, mounds and other barriers have been constructed. Despite these measures, there are many avalanche paths where avalanche debris reaches the highway in the valley bottom and in some cases will cross the valley floor and run-up the opposite slope. To control avalanche paths that impact the transportation corridor, weather, snowpack and avalanche observations are evaluated by avalanche forecasters and, if necessary, the TCH and CPR are closed while avalanches are triggered artificially with assistance from the Canadian artillery. Stationed at the Pass during the winter months, the soldiers use a 105 mm Howitzer from 18 separate gun positions to shell targets identified by the Parks Canada avalanche forecasters. Road crews then clear snow from the highway. Significant costs are associated with the avalanche forecasting and control along the transportation corridor. In addition, despite the sizable expenditure on the construction of defensive structures, there are economic impacts when the highway is shut down for avalanche control and snow removal.

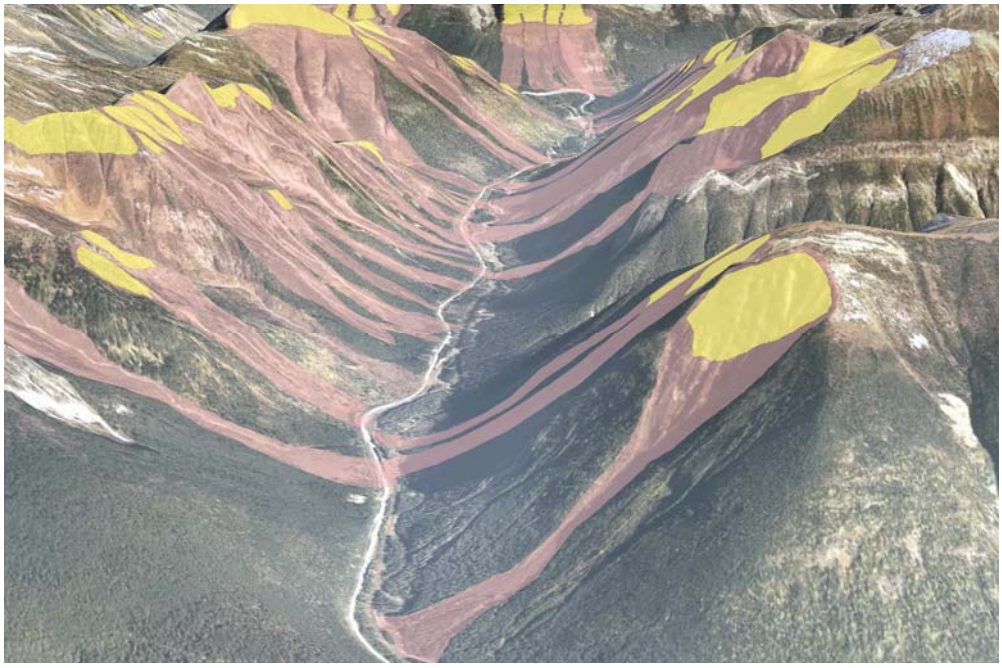

Figure 8. Starting zones (yellow) and avalanche paths (pink) along part of the Trans Canada Highway in Glacier National Park (Data source: Parks Canada Air Photos, 2004 and digitized avalanche paths, author)

With an average snow fall of over 1000 cm annually and accessible ski terrain due to the presence of the highway, GNP has become a destination for backcountry skiers and snowboarders. Although there are no precise user numbers of recreationists heading into the backcountry, park visitation numbers, winter permits to access restricted areas and use of Alpine Club of Canada huts in the park show an increasing trend (O'Gorman et al., 2003). The increasing backcountry usage highlights a need for avalanche exposure mapping in the backcountry. This study creates a Rogers Pass specific runout model, in chapter four, which is based upon a historical database of highway corridor avalanche paths and subsequently applies it in selected backcountry areas. In chapter five, a GIS algorithm, in part based on terrain characteristics from ATES, is used to generate an avalanche exposure map for a backcountry area.

Glacier National Park is characterized by a transitional (or intermountain) snow climate, located between the Coastal Mountains (maritime or coastal snow climate) to the west and the Rockies (continental snow climate) bordering on the east. These snow climate

zones are generally described as follows: the coastal zone is typified by abundant heavy snowfall, high temperatures and a more stable snowpack; the continental zone exhibits cold temperatures, lower snowfall and a persistently unstable snowpack; and the intermountain zone exhibits milder temperatures, an average snowfall that is greater than the average for the Rockies and a snowpack displaying varying stability from year to year (Armstrong and Armstrong, 1987; LaChapelle, 1966; McClung and Schaerer, 1993; Mock and Birkeland, 2000). In an examination of avalanche characteristics specific to the Columbia Mountains in Canada and related to the local snow climate, Hägeli and McClung (2003) showed that the Columbia Mountains are typified by a transitional snow climate consistent with characteristics previously defined in the aforementioned studies. However, they are impacted by a strong maritime influence and specific snowpack conditions that relate to persistent weak layers due to rain on the snow layers in the early part of the winter season or surface hoar layers which develop during the core winter months that can persist for long periods through the season. In their subsequent paper, Hägeli and McClung (2007) showed a strong variation in the snow climate regimes for Rogers Pass where some winters exhibited a more continental climate regime and others were more maritime influenced leading to a suggestion of the term 'avalanche winter regime' to better classify seasonal variability and more clearly describe the impact of seasonal weather variation on the snowpack and resulting avalanche activity.

Vegetation in the valley bottoms and valley sides is composed of coniferous forest species. Above tree line, the land cover ranges from scattered tree patches and alpine tundra to barren rock, moraine deposits and ice covered mountains tops and glaciers. In British Columbia, a Biogeoclimatic Ecosystem Classification system is used to identify areas with similar vegetation, soils, climate and topography (Krajina, 1972; Mah et al., 1996). GNP contains three biogeoclimatic zones (Figure 9): Interior Cedar Hemlock (ICH) in the valleys (one of the most productive and biologically diverse zones), Englemann Spruce-Sub-Alpine Fir (ESSF) in the mid-elevations and the Interior Mountain-heather Alpine zone (IMA) in the higher elevations. The ICH zone in the valleys consists of a dense forest of Western Red Cedar (*Thuja plicata*) and Western

Hemlock (*Tsuga heterophylla*) along with Douglas-Fir (Pseudotsuga menziesii), Western Larch (*Larix occidentalis*), Lodgepole Pine (*Pinus contorta*) and Western White Pine (*Pinus monticola*), Sub-Alpine Fir (*Abies lasiocarpa*) and Englemann Spruce (*Picea engelmanii*) (Egan, 1998). The ESSF zone is identified with the mid-elevations and is recognized as a zone with deep snowfall, presence of avalanche paths and the highest recreation value for skiing in the Columbia Mountains (Alldritt-McDowell, 1998). Forest cover includes: Englemann Spruce and Sub-Alpine Fir along with additional species of Whitebark Pine (*Pinus albicaulis*), Limber Pine (*Pinus flexilis*) and Alpine Larch (*Larix lyallii*). Above the tree line, the IMA zone begins at 1800 m elevation, the land cover ranges from scattered tree patches and alpine tundra to barren rock, moraine deposits and ice covered mountains tops and glaciers such as the Illecilliwaet Neve and Avalanche Glacier (Mackenzie, 2006). Major rivers in GNP include the Illecilliwaet and Beaver Rivers.

Glacier National Park has the terrain features and a snow climate regime necessary for significant avalanche activity every year. According to Environment Canada's (2002) Climate Normal's from 1971 to 2000, average annual snowfall, as measured at Mount Fidelity weather station at an elevation of 1905 m, is 1471 cm. The maximum snowpack depth of 465 cm during this period was measured in April 1991. For the purposes of this thesis, terrain and land cover characteristics are vital considerations for GIS to model and map avalanche terrain. For example, slopes of a sufficient angle are required to initiate avalanche activity but slopes with sufficient tree cover will not release avalanches. The digital data sources required for the analysis of avalanche terrain are discussed in the following section.

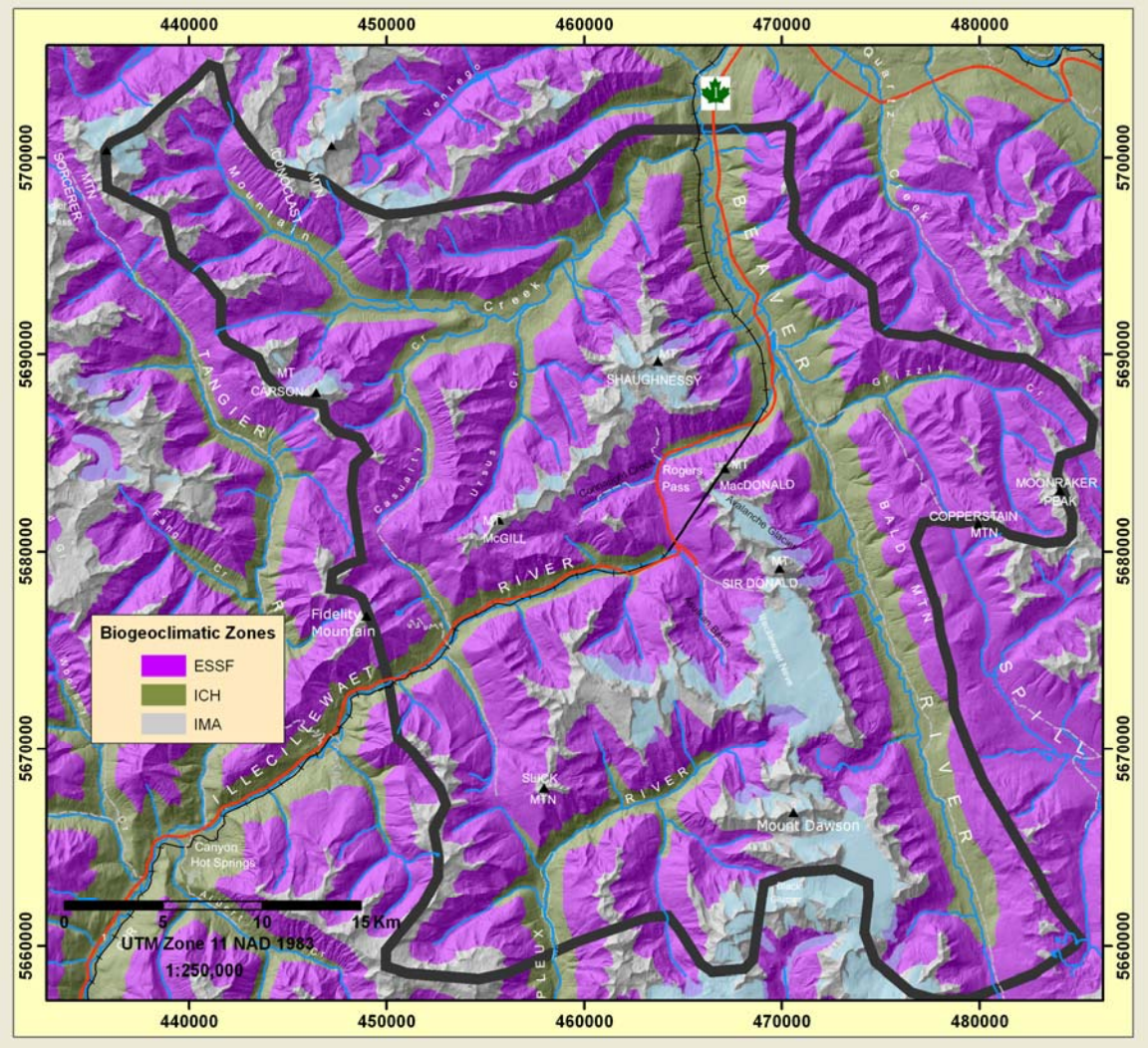

Figure 9. Biogeoclimatic zones of Glacier National Park. The three biogeoclimatic zones include: Englemann Spruce and Sub-Alpine Fir (ESSF), Interior Cedar Hemlock (ICH), and Interior Mountain-heather Alpine (IMA).

1.4.1 Datasets and avalanche database of the study area

This study utilized both digital data and avalanche records from a database collected in Glacier National Park over a 40 year period. The digital data consisted of base map information, digital elevation data and scanned colour air photos. The source digital data sets for this study are highlighted in the table below (Table 4).

Table 4. Digital data sources for Glacier National Park

Digital Data Set	Description
BC Terrain Resource Information Management Base Maps (TRIM 1:20,000)	Data Custodian: Base Mapping and Geomatic Services Branch (BC Ministry of Agriculture and Lands - Integrated Land Management Bureau) Last Revision: 2004-04-16 Data Layers: Topography, Planimetry, Elevations, Toponymy and Digital Elevation Model (DEM) Reference System: British Columbia Albers NAD83 File Format: ESRI ARC Coverage TRIM tiles: 082N002-004, 082N012-014, 082N022-024, 082N031-034, 082N041-044
Parks Canada Air Photos (1:30,000)	Data Custodian: Parks Canada Date Flown: 2004-09-27 Contractor: Geodesy Remote Sensing Inc. Reference System: UTM 11 NAD83 Camera: Zeiss/Jena LKM 15 Focal: 152.092 mm Exposure: 4.5/125 Altitude: 22,500 m (a.s.l) Scan Resolution: 25 microns File Format: TIF

BC TRIM (Terrain Resource Information Management) digital data is the base map product available for the Province of BC that consists of topography, planimetry (line features), toponymy (geographic place names) and digital elevation data. TRIM products are created by stereo compilation from air photos flown at a maximum scale of 1:70,000 and are sold in tiles that measure 6 minutes of latitude by 12 minutes of longitude. The BC Ministry of Agriculture and Lands, through the Integrated Land Management Bureau,

Base Mapping and Geomatics branch, manages the TRIM product. The digital elevation model (DEM) component of TRIM is discussed in chapter three.

Parks Canada contracted Geodesy Remote Sensing Inc. of Calgary, Alberta to collect air photos at a 1:30,000 scale during the fall of 2004. These photos were subsequently scanned at a resolution of 25 microns which results in a raw ground pixel size of 0.75 metres. The coverage of air photos along with flight lines, air photo centres and control points are displayed in chapter three. To enable an avalanche terrain analysis at a local scale it was assumed that higher resolution data would improve the GIS analysis. From these air photos, a higher resolution DEM and enhanced forest cover were generated as well as orthophotos, the methodology of which is discussed further in chapter three.

An extensive avalanche database for the 144 avalanche paths along the Trans Canada Highway has been collected for over 40 years by Parks Canada. The database contains information pertaining to the maximum runout recorded, avalanche size, path name, avalanche frequency and hazard rating. As part of this research, the avalanche paths have been digitized in GIS and linked to the relevant information collected from the database (Figure 10).

From the original data sources, new digital datasets were created for the purpose of this thesis. Drawing from avalanche expert knowledge of the highway corridor, a series of data layers were digitized using stereo photogrammetry to accurately represent starting zones, runout extents and avalanche paths. Stereo photogrammetry also aided in developing a higher resolution DEM and forest cover for portions of the study area. Further, GIS analysis using these derived datasets yielded a multitude of primary topographic attributes ranging from slope, curvature, flow direction and flow accumulation which were used to model a representation of ATES terrain categories for a popular backcountry skiing area. Table 5 briefly highlights the main digital data contributions of this research.

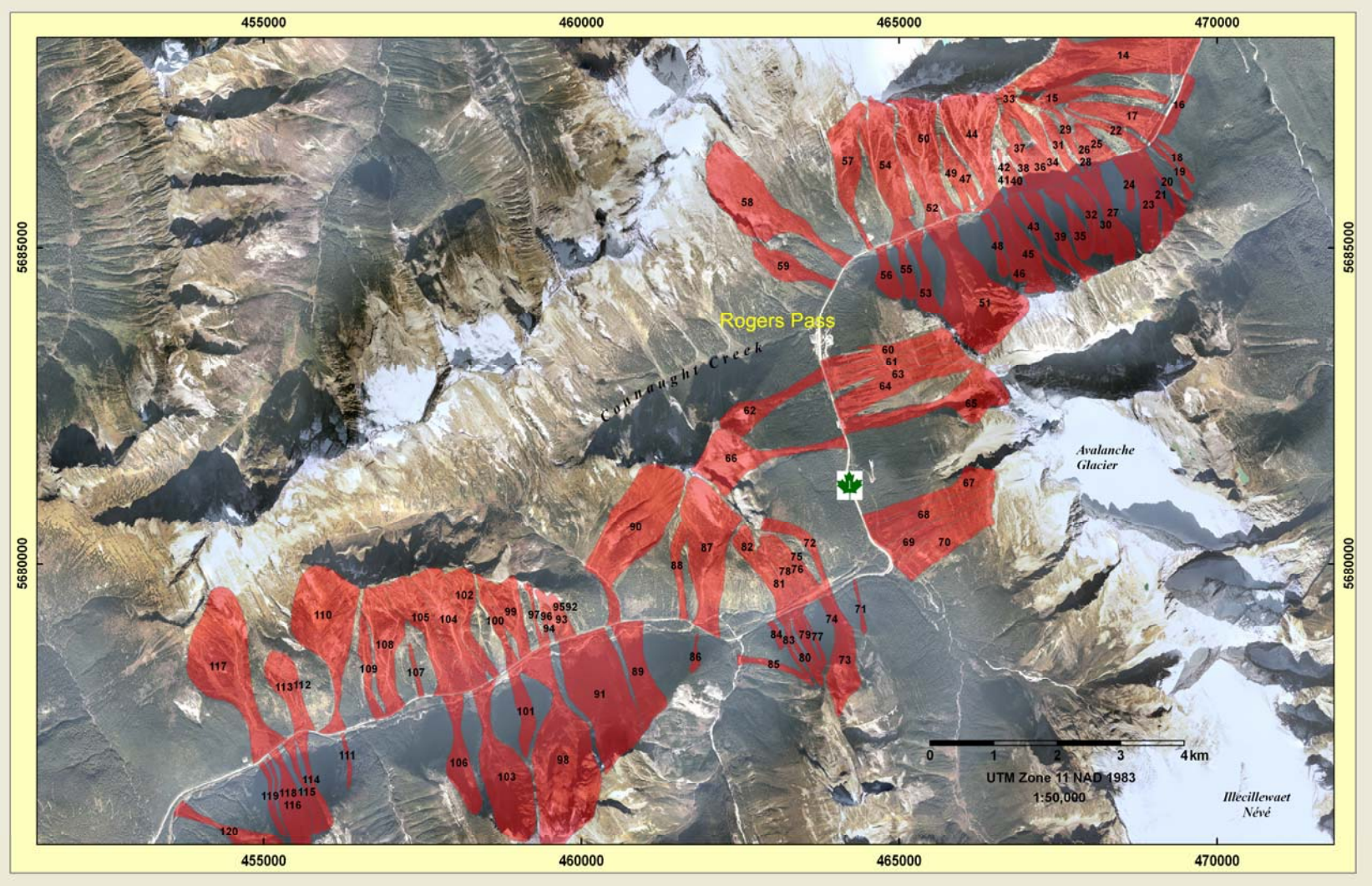

Figure 10. The main group of controlled avalanche paths along the Trans Canada Highway in Glacier National Park

Table 5. Digital data contributions

Data Layer	Description
Highway corridor avalanche paths	Stereo digitized avalanche paths based upon expert delineation
Highway corridor starting zones	Stereo digitized starting zones for each avalanche path based upon expert knowledge
Highway corridor centreline of avalanche flow profile lines	Stereo digitized profile lines of avalanche flow for each avalanche path with the end of the line representing the maximum recorded avalanche extent
Highway corridor start of runout	Stereo digitized line indicating the avalanche expert's knowledge of the point at which runout is expected
Forest cover for the Asulkan Basin	Stereo digitized forest cover of the Asulkan Basin based on dense forest, mixed vegetation and open areas.
Higher resolution digital elevation model	Enhanced digital elevation model created from softcopy stereo photogrammetry methods
ATES hazard map for the Asulkan Basin	Hazard map highlighting areas of Simple, Challenging and Complex avalanche terrain

1.5 Statement of goals and objectives

While GIS is useful for cartographic reproductions and visualizations, this study aims to focus on the use of GIS for modelling avalanche terrain. Specifically, a runout model is derived to predict maximum runout for avalanche paths in the Rogers Pass highway corridor and selected areas in the backcountry and an avalanche terrain algorithm is developed based upon the ATES system that has been modified to be compatible with GIS. There is potential to apply the model in other backcountry areas and transportation corridors in the Columbia Mountains.

Research objectives:

1. Build a detailed digital avalanche atlas for the avalanche paths along the Trans Canada Highway within Glacier National Park. This involves incorporating expert knowledge to accurately digitize runout, starting zones and avalanche paths.

2. Construct a high resolution digital elevation model (DEM) for selected portions of the study area. By employing digital stereo photogrammetry a high resolution DEM can be created from digital air photographs.

3. Develop an avalanche runout zone model specific to the Columbia Mountains in Glacier National Park. A statistical runout model procedure has been successful in determining maximum runout in other mountainous ranges around the world. This model can be adapted to the unique topographic parameters specific to the Columbia Mountains to determine maximum runout.

4. Compare high and low resolution DEM runout model equations. To determine an maximum runout model, topographic parameters from both a high and low resolution DEM will be utilized. Tests will be carried out to determine if there is a difference between the runout models derived from low and high resolution DEMs.

5. Verify the runout model and assess sources and margin of error within the model. To determine the veracity of the model, statistical tests will be performed to estimate error.

6. Use the runout model with avalanche paths along the highway corridor which are outside the dataset to determine maximum runout position. To provide an example, the runout model will be applied to a known avalanche path along the

highway corridor that is outside the dataset used to derive the model. The observed maximum runout will be compared to predicted runout extent.

7. Apply the runout model to selected popular backcountry recreation areas within Glacier National Park. A popular backcountry area will be used to demonstrate the use of the runout model and map predicted maximum runout location.

8. Identify avalanche terrain according to an ATES classification system that is compatible with GIS to assist recreationists in recognizing avalanche terrain in winter backcountry areas. A GIS compatible framework will be devised to map Simple, Challenging and Complex avalanche terrain based upon topographic parameters used in ATES.

1.6 Thesis structure

The structure of this thesis is as indicated below:

- **Chapter two** provides a review of the literature that is relevant to this thesis. Topics include: a background on avalanche formation and release, the methods of creating digital elevation models and the process of extracting topographic parameters from DEMs, an examination of avalanche terrain characteristics, statistical runout modeling procedures and a review of GIS applications related to avalanche modeling worldwide.

- **Chapter three** delves into the methodology used to build a higher resolution DEM for the study area and the process used for vector capture of expert knowledge related to avalanche activity along the Rogers Pass highway corridor.

- **Chapter four** presents the procedure used for modeling maximum runout and the application of the model to avalanche paths along the highway corridor and in the backcountry.

- **Chapter five** draws upon the ATES model and uses GIS to map snow avalanche terrain for selected backcountry areas

- **Chapter six** reviews the thesis findings and conclusions and then proposes new opportunities for further research.

Chapter Two: Literature Review

2.1 Introduction

Identifying avalanche terrain can be a difficult process, especially for those areas where no records exist and there is a lack of vegetative evidence, particularly in regards to estimating maximum avalanche runout. With high resolution digital elevation data, GIS offers an opportunity to use topographic information to assist in the identification and modeling of avalanche terrain. Although digital elevation data with resolutions of 25-30m are commonly available for many parts of the world, higher resolution DEM data facilitates terrain evaluation at a scale that is of interest to backcountry users – the slope scale. The procedures for building a higher resolution digital elevation model from air photographs or acquiring high resolution data from airborne sensors are discussed in this chapter. Further, geomorphometric or topographic parameters derived from digital data are essential for the identification of avalanche release areas and the analysis of snow avalanche runout. A review of the literature summarizes findings pertaining to these topographic parameters and the influence they have in avalanche formation. Finally, GIS has great potential in the visualization, mapping and modeling of avalanche terrain as evidenced by a review of GIS applications from around the world.

2.2 Digital elevation models and topographic attributes

Terrain modeling in GIS is fundamentally dependent upon the availability of Digital Terrain Models (DTM) or Digital Elevation Models (DEM). The terms DTM and DEM are often used interchangeably to describe a digital representation of the variation in relief over a surface. Several divergent definitions exist in the literature. In many countries the terms are synonymous. In Maune et al. (2001a), DTMs differ from DEMs: rather than a regular grid of elevation points, as found in a DEM, a DTM consists of irregularly spaced elevation points, elevations of significant terrain features and breaklines that indicate abrupt changes in terrain such as ridgelines, roads, or cliffs. The

result is that DTMs represent the actual terrain surface more accurately than DEMs. Li et al. (2005), broadly define a DTM as representing topography of the terrain and objects in the terrain that include both terrain and non-topographic information, beyond simple elevation points, such as landforms, terrain features, natural resources and socioeconomic data. Conversely, Paparoditis and Polidori (2001), define a DEM as a mathematical and digital representation of elevation in the environment and of objects that may include layers above the ground such as buildings or forest canopy; whereby, a DTM is data confined to points on the ground or water surface. For this thesis, the generic term DEM will be used to refer to all forms of digital elevation products.

Most digital elevation data are derived from stereo photogrammetry capture which is based on the interpretation of aerial photographs using either manual or automated means that allows the representation of geometric properties of the earth's surface (Wilson and Gallant, 2000). As mentioned above, many DEMs consist of regularly spaced grid points; a TIN (triangulated irregular network), on the other hand, represents an irregular network of digital elevation points representing surface features such as peaks, ridges and breaks in slope that are represented with triangular facets.

The following discussion will highlight the methods of building a DEM using softcopy photogrammetric methods (softcopy is based on digital images as opposed to hardcopy that is based on film images) and a review of the procedures for extracting terrain parameters from a DEM using GIS.

2.2.1 Building a digital elevation model

The horizontal resolution of the DEM is critical for portraying avalanche hazard mapping at a scale that is reasonable for route finding and selecting suitable slopes to ski. A DEM of at least 20-30 m is required to meet this purpose (Schweizer et al., 2003); however, even at this resolution, small-scale variations in slope may not be evident. The denser the horizontal resolution, the more vertical (elevation) data points that are captured, resulting

in a more detailed picture of terrain variation. This thesis involved the development of a higher resolution terrain model to improve the capacity of the GIS for modeling and analysis. Modern stereo mapping methods for terrain are facilitated by softcopy photogrammetry or digital stereo mapping. This technology was essential for this study. A review of these methods is provided so as to describe how they work and to highlight possible sources of error.

Once air photographs have been digitally scanned, they can be viewed and processed by softcopy photogrammetry software. What was once accomplished with stereo plotters has now become a digital operation. The photogrammetry software facilitates a process whereby the digital air photos are georeferenced to allow stereo viewing and manipulation in a digital environment. After the process of correction has accurately placed the images into real world coordinates, the generation of a DEM can begin.

There are three main methods of generating a high resolution Digital Elevation Model from aerial photographs: a procedure that is performed manually by a human operator, auto-generated models that are calculated using image autocorrelation algorithms and finally methods that include some combination of both techniques. Manual DEM generation requires a human operator to manually trace in contour lines, enter elevation points or trace breakline features such as ridgelines, roads, rivers or other abrupt changes in slope. This process is slow and time consuming. An automated DEM is generated quickly and once an automated DEM is generated, the photogrammetry software allows an operator to correct DEM points that are incorrectly placed. However, in some cases the editing process may take longer than generating a DEM solely with human interpolation.

In densely forested mountainous regions computer generated DEMs can result in misplaced elevation points. Forest cover, shadows and snow or ice cover can interrupt the processing whereby points are placed on the tops of trees in the forest canopy or placed incorrectly in shadowed areas or areas covered by snow and ice. Although the manual

method of interpretation is time consuming, a skilled human operator is able to execute a high level of accuracy. According to Molander (2001), automatically deriving elevations with digital correlation may require editing time that exceeds what would be required by a skilled operator. As well, the elevations sampled are not sensitive compared to what a human operator would capture in regards to breaklines and an efficient capture of data points that model the terrain.

LiDAR (Light Detection And Ranging) is emerging as a highly useful tool for generating high resolution DEM. LiDAR remote sensing equipment is installed on the base of an aircraft and is flown over an area of interest. Pulses of light from a laser are emitted to the ground and the distance is calculated as the pulse bounces off an object and returns to the sensor. Different pulses can be measured such as the reflection of a first pulse from the forest canopy, followed by subsequent pulses that would record the distance to the ground (Fowler, 2001). LiDAR is not commonly available for Canadian terrain; however, as it becomes more widely available in the future, it will further enable the use of high resolution DEMs to advance terrain modeling with GIS. Eventually, it is expected that the access to LiDAR data will be such that manual methods of generating a DEM will be replaced. Although the research conducted in this study uses a mostly manually generated digital elevation model, the analysis techniques using the DEM would certainly mirror operations that would utilize LiDAR data.

2.2.1.1 Potential sources of error

In the process of softcopy photogrammetry and DEM generation, sources of error include: camera error, scanner error, control error, error in geocorrection and operator error. Knowledge of the camera error is mitigated by camera calibration reports which detail any anomalies and specific camera parameters that can be entered into the softcopy image processing software. Scanning introduces a potential source of error. An analog photographic image is converted to a digital image using a scanner. The resolution of the scanned image file is critical for high resolution photogrammetric operations of feature

identification and extraction. Coarser scanner resolution results in loss of detail. Scanners themselves can have mechanical errors and thus result in error; however with improvements in scanner technology the error is usually minimal in nature (ISM, 1997).

Geocorrection is the process of rectifying an image to 'real world' coordinates. Control points used for this purpose must be as accurate as possible in order to ensure that images are referenced as close as possible to the ground surface. For remote areas, control data may be difficult to obtain as surveyed points in these areas are dispersed and their level of precision may be questionable. In these circumstances the only option may be to use what is available or to survey new control points with GPS.

Operator error can influence the photogrammetry process during the geocorrection phase and during DEM capture. An important consideration for the optimal performance of a human operator is a comfortable and technologically sufficient photogrammetric workstation. For example, the operator must have a monitor capable of viewing high resolution stereo scanned images such that a monitor pixel when zoomed in on will cover image pixels scanned at the level captured by the scanning device. In this regard, the operator's ability for pointing acuity is compromised by image magnification. Ideally, the operator can function with an accurate and high image magnification in order to accurately select points for ground control or during the process of DEM capture. Photogrammetric operators may also read terrain differently which can be another source of error, one of interpretation. A common error in one style of manually generated DEMs is a "corn row" effect that is evident when visualizations are generated in GIS. This effect is generated when an operator moves uniformly along spaced profiles of the stereo model and the result is a striping effect in the shaded image (Daniel and Tennant, 2001)

Determining accuracy in a DEM involves a comparison of the measure of closeness between a point or points in a DEM and the surveyed or accepted correct value(s) in terms of both the horizontal (x, y) plane and the vertical (z). Vertical accuracy for a DEM is determined by the root-mean-square-error (RMSE) representing the square root of the

average set of squared differences between the dataset coordinate values and the coordinate values from an independent source such as ground control points (Maune et al., 2001b). While vertical accuracy represents error in elevation, horizontal accuracy is represented by RMS error in planimetric survey points. Testing the accuracy requires comparisons of the DEM points with surveyed ground points of high accuracy. Data standards exist for federal and provincial agencies on the tolerances of positional accuracy and data must be captured to meet those standards, see, for example, the British Columbia specifications for DEMs (BMGS, 2002).

2.2.2 Extracting terrain attributes from a DEM

To describe the terrain of a landscape, primary terrain features such as slope, aspect, catchment area, profile and plan curvature and length can be derived from DEM data (Wilson and Gallant, 2000). These are common procedures available in most commercial GIS software packages. Primary terrain attributes are computed directly from a DEM, while secondary attributes involve combinations of the primary attributes. An example of a secondary terrain attribute would be the calculation of sediment transport for a watershed that involves a combination of primary attributes such as slope, length into an algorithm in order to compute an estimate. ArcGIS® software from Environmental Systems Research Institute (ESRI) was used to extract these primary topographic parameters from the DEM datasets.

2.3 Avalanche terrain characteristics

The Europeans have been pioneers in exploring the use of GIS for avalanche related applications, particularly in Switzerland, Norway and France. GIS has been utilized for the mapping of potential starting zones and evaluating the terrain characteristics with respect to avalanche occurrence or frequency (Maggioni and Gruber, 2003; Stoffel et al., 1998). GIS has also been useful in extracting terrain parameters for dynamic avalanche runout calculations (Gruber et al., 1998) and statistical runout models (Lied et al., 1989).

In addition, expert systems have been partnered with GIS for avalanche forecasting (Bolognesi, 1998; Buisson and Charlier, 1993). The common link is the importance of terrain as an essential factor in influencing avalanche frequency and runout and as a factor that remains relatively constant over time.

2.3.1 Starting zone or potential release area modeling

Modeling of starting zones in a GIS requires a digital elevation model (DEM) and a digital land cover layer, usually depicting forest cover. Terrain parameters such as slope, aspect, length, area and distance from ridges, can be derived from the DEM. To evaluate which terrain parameters are most likely to contribute to high frequency, known avalanche paths have been documented and evaluated for these key factors (Gruber, 2001; Gruber and Sardemann, 2002; Maggioni and Gruber, 2003; Maggioni et al., 2001). The results are useful in conducting and improving avalanche hazard mapping as well as a tool for avalanche hazard risk assessment. Patterns from paths with known avalanche frequency can be transferred to less known areas based on the terrain characteristics that have been identified as strong factors.

In Maggioni and Gruber (2003), potential release areas are defined based on terrain parameters that have been derived from historical avalanche occurrences (slopes between 30^{o}-60^{o}, proximity to ridges, curvature of slope, altitude, and aspect) to build maps using GIS that relate the terrain features to avalanche frequency. One of their main findings was to confirm that highly concave cross-slope curvature in combination with steep down-slope curvature (>36˚) and proximity to ridgelines were factors that lead to high avalanche frequency. Furthermore, a study at Zuoz, Switzerland also took the approach of evaluating the spatial characteristics of daily avalanche activity based on GIS mapping of potential starting zones. This study used all slopes from 30^{o}-50^{o} and then compared this information in the GIS with 14 years of daily avalanche observations and a database of daily weather parameters (Stoffel et al., 1998). One of the results of the terrain analysis revealed that starting zones with more northerly aspects had higher avalanche frequency.

The following discussion will review the literature for key starting zone terrain factors that are applicable in the Rogers Pass region. Table 6 summarizes the terrain factors associated with avalanche formation in starting zones.

Table 6. Summary of terrain factors in avalanche formation

Factor	Description
Slope (Mears, 1992; Schweizer et al., 2003; Smith and McClung, 1997)	25˚ – 50˚ : range of slope angles for starting zones 30˚ – 40˚ : starting zone slope angles for large long return period avalanches
Exposure to wind (Gleason, 1994) (Feick et al., 2007)	Lee slopes subject to loading by wind lead to avalanche formation Wind impacts the formation and destruction of weak layers (surface hoar) creating spatial variability in snow stability
Cross slope curvature (Gleason, 1994; Gruber and Sardemann, 2002; McClung, 2001)	Concave cross slope curvature facilitates avalanche formation
Down slope curvature (Jamieson and Geldsetzer, 1996)	Convex down slope curvature is susceptible to skier triggering
Size of zone area (Schweizer et al., 2003)	Start zones with an open area of 10 m wide and 10-20 m in length are required for slab avalanches
Elevation (Smith and McClung, 1997)	Higher elevations receive more snow and are subject to the effects of wind loading on lee slopes
Aspect with respect to solar radiation (Schweizer and Jamieson, 2000)	Northerly aspects are more likely to have facets, depth hoar and surface hoar weak layers. South slopes are susceptible to rapid warming and avalanche release.
Forest cover (Mears, 1992; Weir, 2002)	Dense forest cover inhibits avalanche formation and release

2.3.1.1 Slope

The primary characteristic for a starting zone is the presence of a suitable inclination (typically 25˚– 45˚) that allows an avalanche to start and move down slope. For dry snow slab avalanches, a slope angle of >30˚ is typically required (Schweizer et al., 2003). Slope angles greater than 60˚ are prone to frequent sloughing of snow thus accumulation of snow for large avalanche formation is reduced. An analysis of over 800 human triggered avalanches in the Columbia Mountains of Canada and the Swiss Alps found a median maximum slope angle of investigated cases of 38˚ for Switzerland and 40˚ for Canada (Schweizer and Jamieson, 2001). Figure 11 is a graph showing the frequency of average slope angle in the starting zones of 40 avalanche paths from the Rogers Pass highway corridor used for analysis in this thesis. The average slope angle was calculated using zonal statistics to determine mean slope for grid cells within an expert delineated starting zone polygon. In agreement with the aforementioned studies, slope angles falling between 35˚ and 45˚ are most characteristic of avalanche starting zones.

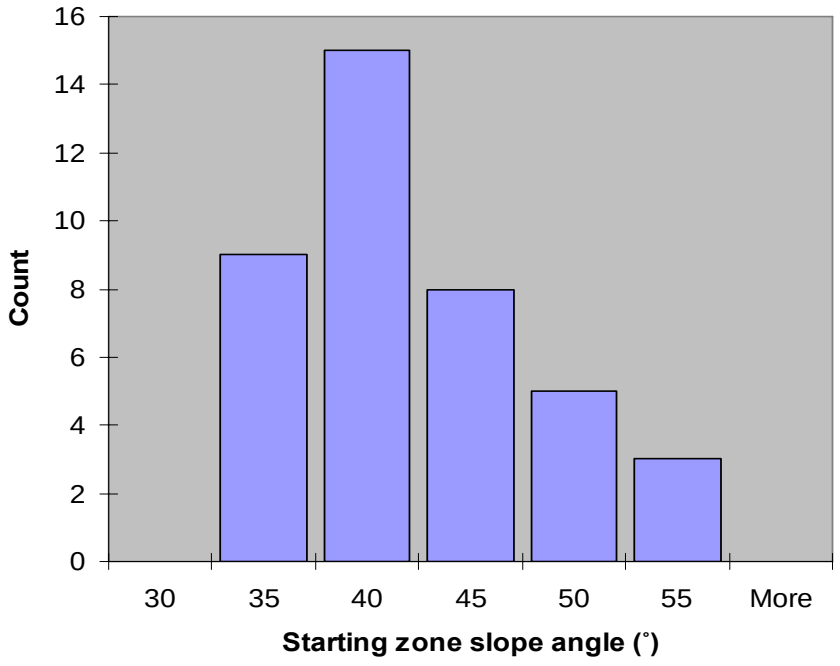

Figure 11. Frequency of average starting zone slope angle from 40 avalanche paths in the Rogers Pass highway corridor (N= 40, mean: 39.8˚, median: 38.6˚, standard deviation: 6.1˚) (Source: author, from digitized data)

2.3.1.2 Exposure to wind

After slope angle, exposure to wind is the second most important factor, as exposed starting zones on lee slopes are subject to loading of wind transported snow that is transported from windward slopes (McClung and Schaerer, 2006). Higher density and cohesive snow deposits from wind action provide an opportunity for the formation of slab avalanches when overlying a snowpack that contains a weak layer. Wind deposits add shear stress to the snowpack. In studies conducted in Montana, aspect with respect to wind was considered one of the most significant terrain parameters contributing to avalanche formation (Gleason, 1994). Schweizer et al. (2006b), make the observation that topography and meteorological conditions of wind and sun are the most important factors in the spatial variability of snow stability and that wind causes random spatial variation above tree line. Feick et al. (2007) observed that wind was the most crucial factor for predicting surface hoar formation and destruction and its resulting impact on spatial variation of snow stability; it was nearly impossible to predict unless the local wind regime was known at a high resolution of at least 10 m. These considerations make the impacts of wind on snow stability a very difficult process to model, especially in mountainous terrain where topography can alter wind direction at a micro-climatic or local scale level.

Modeling the impact of wind has been attempted utilizing DEM data along with wind and snow information. In Mases et al. (1998), the spatial snow distribution in avalanche terrain is based on a wind coefficient that represents a relationship between snow accumulation at the end of a given wind period and the snow available for transport at the beginning of the wind period. For the model to produce an accurate simulation of the distribution of snow (scouring of windward slopes and loading of lee slopes) it is reliant upon wind periods with a constant direction. In the Western Highlands of Scotland, Purves et al. (1998), used GIS to model snow transport by wind using a rule-based model over topography which showed good agreement with what experts in the field would expect such as the accumulation on lee-ward slopes and in sheltered zones like gullies.

However, the complexity of southerly winds proved challenging to model based upon a lack of field measurements and the divergent nature of the wind in the mountains.

Categories of wind exposure were devised in examining starting zones in snow avalanche terrain in Rogers Pass (Schaerer, 1977). Five categories expressed the action of wind nominally (Table 7). Wind categories ranged from a category of 1 represented by a starting zone sheltered from wind to a wind category 5 represented by starting zone on a lee side of a ridge where the presence of open windward areas provided snow for transport and deposition (loading) into the starting zone. Wind was determined to have a significant effect in relation to avalanche frequency, especially where wind loaded specific fracture points.

Table 7. Exposure to wind. Adapted from (Schaerer, 1977)

Wind Category	Description
1	Starting zone completely sheltered by dense forest
2	Starting zone sheltered by open forest or facing the direction of prevailing wind
3	Starting zone is an open slope with rolls or terrain features where localized snow drifting can occur
4	Starting zone is on the leeward side of a steep ridge
5	Starting zone is on the leeward side of a large rounded ridge where large amounts of snow are available for transport

2.3.1.3 Slope curvature

Variations in terrain such as curvature of the slope have been recognized as significant to avalanche formation. Depositions of snow from wind can collect irregularly in varied terrain or deposition can occur from multiple directions, as may occur in a cirque. For an avalanche starting zone, wind can deposit snow in concave areas and deplete snow from convex areas (Gleason, 1994). Figure 12 displays an avalanche that has occurred on a

cross-slope as a function of wind scouring and deposition. A cross-slope curvature of a concave nature has been observed to be a characteristic of frequent performing starting zones in terrain that has been logged (McClung, 2001). Down-slope convex curvatures are susceptible to skier-triggered avalanche release at the top of the roll where a susceptibility to failure often exists (Jamieson and Geldsetzer, 1996).

Figure 12. Cross-slope curvature. Cross-slope winds have depleted snow from a convex area and deposited it in a concave starting zone that resulted in a slab avalanche. (Photo: Bruce Jamieson)

2.3.1.4 Aspect with respect to solar radiation

Aspect, with respect to solar radiation, influences the radiation balance which then impacts the snowpack temperature and temperature gradient. Bakermans and Jamieson (2006) observed that differences in snow surface warming can result from even small changes in aspect. Radiation is further impacted by slope angle and elevation. In the northern hemisphere, in general, shady north slopes are characterized by strong

temperature gradients and thus are more prone to the presence of weak layers (depth hoar, surface hoar and facets). In the winter months of December and January, a negative energy balance can dominate preventing a warming of air temperature that would act to aid snowpack stabilization (Schweizer et al., 2003). However, rapid warming in the spring or after a snow storm can generate avalanche releases on sunny slopes.

In mountainous terrain, the impacts of the variation in solar radiation over the course of the winter and the effects of shading or reflecting of surrounding mountains and the presence or absence of cloud cover make it difficult to ascertain the impact of solar radiation for any particular slope without direct measurement. In Rogers Pass, aspect to sun did not reveal any strong relationship with avalanche frequency (Schaerer, 1977). However, in examining the relationship between skier-triggered avalanches and aspect, Schweizer and Jamieson (2000) report more cases on northerly aspects. Thus skier-triggering is more common on shady or lee slopes and may be due to skiers selecting slopes to ski that have more favourable snow conditions.

A computer-based system that largely uses aspect for avalanche forecasting and modeling avalanche risk is the SAFRAN, CROCUS, MÉPRA (SCM) three-model system. SCM estimates meteorological parameters to simulate snowpack characteristics and associated avalanche activity. SAFRAN performs an analysis of observed weather data available over the elevations and aspects of the forecasting area; the results are used by Crocus to simulate the snowpack and its stratigraphy. MÉPRA is an expert system that deduces avalanche risks based upon an assessment of snowpack stability (Brun et al., 1992; Brun et al., 1989; Durand et al., 1993; Durand et al., 1999; Durand et al., 1998; Giraud, 1992; Giraud et al., 1994; Giraud et al., 1998). This automatic system is used to model snow cover evolution and its stability for typical slopes, elevations and aspects representative of different massifs in the French Alps and Pyrenees. The results of the model are used by avalanche forecasters to aid them in determining avalanche risks for operational avalanche forecasting.

2.3.1.5 Elevation

The elevation of a starting zone is significant in that more snow falls at higher elevations and there is more snow loading due to wind by the process of windward slopes being scoured and deposition occurring over ridges onto lee slopes. Temperatures are typically cooler, vegetation can be sparser and exposure to solar radiation may be greater than lower slopes. The combined impact can produce conditions that are favourable for avalanche formation. In Rogers Pass, in addition to wind exposure, elevation in the starting zone was a significant factor with respect to avalanche frequency (Smith and McClung, 1997)

2.3.1.6 Size of starting zone area

The main impact of the size of the starting zone is the increased capacity to capture snow for avalanche formation. Typically this would be a wide open area where snow accumulates. The larger the starting zone area, the larger the potential avalanche. Generally, for slab avalanches, the width of the slab is greater than the downslope length of the slab. After the slab releases it often entrains additional snow.

2.3.1.7 Forest cover

Terrain surface cover or terrain roughness impact avalanche formation in several ways. A thin snowpack of less than 1 m may be weakened by the presence of a rough, irregular surface where rocks and rock outcrops promote instability by creating higher temperature gradients which foster a very locally weaker snowpack. At over a depth of 1 m most terrain roughness is smoothed out (Schweizer et al., 2003). For Glacier National Park the early season snowpack quickly exceeds the 1 m threshold and thus smoothes out terrain roughness. However, of particular consideration for this thesis is the presence of forest cover.

Forests of sufficient size and density inhibit avalanche formation by anchoring the snow to the ground in the starting zone (Mears, 1992). Estimations in the Province of British Columbia ICH forest zone are that 1000 stems per 1 hectare with trees possessing a diameter at chest height of 12-15 cm are sufficient to prevent avalanching or that 30-50 years after replanting a forest cutblock, avalanche potential decreases provided that no avalanching damages the stand during that time (Weir, 2002). Other estimates suggest that forest cover with canopies of a density greater than 80%, composed of conifers and a height three times the snow depth is sufficient to inhibit avalanche formation (Canadian Avalanche Association, 1998). Forest cover in Canada plays a more significant role than in Europe where the treeline is often absent due to historical clearing of the land.

2.3.2 Avalanche runout modeling and prediction

Determining the potential avalanche runout distance has been a problem that countries with communities, transportation, resources, and recreation in mountainous terrain prone to snow avalanches have been trying to solve for several decades. To address the serious concern of avalanche runout, research efforts into modeling the impact and extent of snow avalanche runout have fallen in to two main categories: statistical runout modeling and dynamic or physical-based avalanche runout models. Statistical or topographical runout models were pioneered in Norway with seminal research (Lied and Bakkehoi, 1980) based upon field observations and derived regression equations. Dynamic models mathematically simulate avalanche motion from initiation to rest and can yield information on snow flow height, velocity and runout distance; however, these models require inputs such as snow fracture height and friction coefficients that may be difficult to estimate especially for areas where a record of avalanche activity is absent. Some of these dynamic models such as AVAL-1D (Gruber and Margreth, 2001) and RAAMS have emerged as snow avalanche modeling tools that incorporate GIS and facilitate avalanche hazard mapping. Harbitz et al., (1998) provide an overview of the development and diversity of dynamic models that have been employed to describe the physics of dense and powder snow avalanche phenomena. This thesis builds upon the statistical

model approach developed in Norway and the following discussion focuses specifically on the alpha-beta statistical model and its potential for application in the Columbia Mountains.

2.3.2.1 Statistical runout model – the Alpha-Beta approach

The statistical approach used by the Norwegian Geotechnical Institute (NGI) was introduced in 1980 as method of calculating maximum runout based on topographic parameters. This approach has since been refined to develop maps for the entire country that are available online (Bakkehoi et al., 1983; Lied, 1998; Lied and Bakkehoi, 1980; Lied et al., 1989; Lied et al., 1995). Starting and runout zones (includes track) have been mapped at a 1:50,000 scale by the NGI to produce avalanche hazard maps. Starting zones (red) were identified in a GIS based upon slope and areas above tree line or with sparse forest cover; maximum and minimum runout zones (pink) were calculated with a regression equation based upon terrain parameters. The intention of these maps is to protect structures, settlements and military or recreation users from avalanche danger.

Through an initial regression analysis of eight topographic parameters based on 111 avalanche paths, a combination of four main terrain parameters were identified as the best for predicting maximum avalanche runout or α, the angle between the maximum runout and the top of the slide (Figure 13). One of these predictors, β, is the angle from the point in the avalanche path where the slope declines to 10˚ (the β-point). This was originally thought to be the approximate point at which large avalanches begin to slow and deposition occurs, but is now simply considered a reference point. β can be easily measured in the field and provides a simple description of the main inclination of the avalanche track. Lied and Bakkehoi (1980) selected 10˚ as the β-point because it seemed to correspond to the lowest value of the dynamic friction coefficient (μ) in avalanche snow or a point that is identified by a low ratio of friction between the two surfaces. The β-point is subject to some judgement as small benches higher up on the avalanche path may decline to 10˚ or less. In Toppe (1987) the β-point is confined to the β-field (Figure

13) which is defined as the portion of the profile limited by points where the angle between the tangent of the parabola and the horizontal plane is between 5˚ and 15˚. The other parameters include the average inclination of the starting zone (θ) within the top 100 vertical metres of the avalanche path, the total vertical fall (H) as measured on the best fitted parabola from the top of the parabola to the minima point on the curve and the curvature of the slope (y″) that is represented by the orange dashed line in Figure 13. Bakkehoi et al. (1983) increased the sample size of avalanches studied from 111 to 206 to derive Equation 2.1. Because the correlation between angles α and β was so dominant a simplified expressed was developed using only β as a predictor (Equation 2.2). The three predictor model only improves the prediction to a minor degree (Lied, 1998). As a result, Equation 2.2 is more commonly used to predict possible runout and does so with fairly high accuracy. R^2 is the coefficient of determination, S is the standard error of the estimate and N is the sample size.

Equation 2.1 represents a three predictor model:

$$\alpha = 0.92\beta - 7.9 \times 10^{-4} H + 2.4 \times 10^{-2} Hy''\theta + 0.04 \quad (2.1)$$

($R^2 = 0.85$, $S = 2.28^{\circ}$, $N = 206$)

Equation 2.2 represents a simplified one predictor (β-only) model:

$$\alpha = 0.96\beta - 1.4^{\circ} \quad (2.2)$$

($R^2 = 0.85$, $S = 2.30^{\circ}$, $N = 206$)

A concern with the three predictor model is that the independent variables may correlate strongly with one another which would lead to an issue of multicollinearity. However, with the small change in R value in dropping the H and Hy″θ from the three predictor model to the one predictor model and the relatively small discrepancy in the regression coefficient for β between the two equations, it may be that there is no relationship between Hy″θ and H or that the relationships are reasonably stable.

In the Norwegian example, the procedure for mapping runout in a GIS begins with the identification of all starting zones by using digital elevation model data (30 x 30 m resolution) and digital forest cover data. All areas on a map with a slope of 30˚-55˚ and not covered by dense forest were identified as starting zones. Avalanche runout zones were essentially classified as those areas below the starting zones with the maximum runout being determined by Equation 2.1. For each avalanche path, a GIS operator physically entered the avalanche path as identified from the top of the starting zone. A profile of the path is computed by the GIS and maximum runout distance is plotted on the profile. The resulting information is transferred as a continuous zone over the map surface (Lied and Toppe, 1989; Toppe, 1987). Verification was completed by comparison to air photos and field observations. Maps were then edited based on subsequent field work.

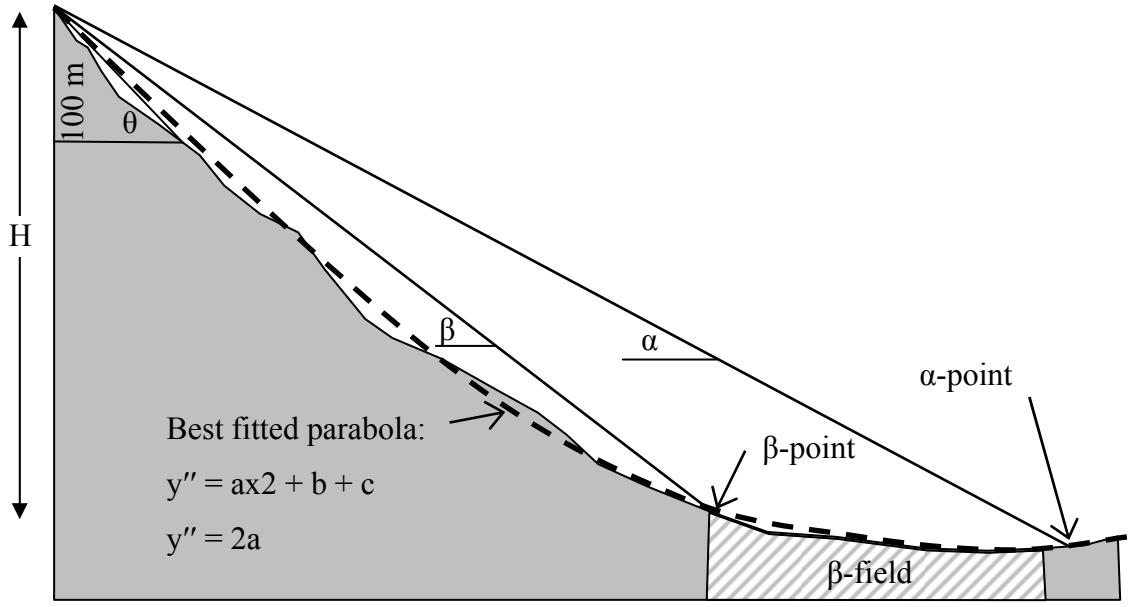

Figure 13. Alpha-Beta runout model. Adapted from (Toppe, 1987)

The Norwegian method has been adapted for several different countries in order to represent their mountain ranges (Table 8). R^2 is the coefficient of determination, *S* is the

standard error of the estimate and *N* is the sample size. Differences in runout distances, and thus alpha-beta runout regression models, are typical for different climatic and mountain regions as identified in subsequent work on statistical prediction of avalanche runout from other mountain ranges (McClung et al., 1989; Mears, 1989).

Table 8. Comparison of alpha-beta regression models from different mountain regions. (^ indicates predicted value)

Country	Relation	R^2	S	N	Reference
Norway	$\hat{\alpha} = 0.96\beta - 1.4^{\circ}$	0.85	2.3˚	206	(Bakkehoi et al., 1983)
Norway *	$\hat{\alpha} = 0.93\beta$	0.86	2.1˚	192	(Johannesson, 1998)
Austria	$\hat{\alpha} = 0.946\beta - 0.83^{\circ}$	0.92	1.5˚	80	(Lied et al., 1995)
Iceland	$\hat{\alpha} = 0.85\beta$	0.52	2.2˚	44	(Johannesson, 1998)
Canada:					
Rockies/Purcells	$\hat{\alpha} = 0.93\beta$	0.75	1.75˚	126	(McClung and Mears, 1991)
Coast Mountains	$\hat{\alpha} = 0.90\beta$	0.74	1.70˚	31	(Nixon and McClung, 1993)
Catalan Pyrenees	$\hat{\alpha} = 0.86\beta + 1.05^{\circ}$	0.75	1.98˚	64	(Furdada and Vilaplana, 1998)
Alaska	$\hat{\alpha} = 0.86\beta$	0.58	n/a	52	(McClung and Mears, 1991)
Colorado	$\hat{\alpha} = 0.80\beta$	0.50	n/a	130	
Sierra Nevada	$\hat{\alpha} = 0.76\beta$	0.60	n/a	90	
Western Norway	$\hat{\alpha} = 0.90\beta$	0.87	n/a	127	

* Norway runout equation derived from a dataset that has been trimmed to omit some of the most extreme avalanches (Johannesson, 1998)

As there are no published alpha-beta parameters for the Selkirk/Columbia Mountains, this thesis builds upon this body of knowledge by contributing an alpha-beta model specific to the Rogers Pass area. As well, the approach of utilizing a high resolution GIS to extract the terrain parameters for this calculation is a new approach for Canada. Normally statistical models are not used to predict avalanche width; however, Keylock et al. (1999) attempted to estimate derive widths for different sizes of avalanche and use a size-frequency distribution to simulate widths. For this thesis avalanche width is estimated based in part upon vegetative cover.

2.4 GIS applications related to snow avalanche modeling and visualization from Europe and North America

GIS is a powerful tool because its visualization capacity can aid recreationists in understanding and assessing risks in avalanche terrain. Maps produced with GIS have the capability to summarize visually complex information, which can help recreationists and professionals make better decisions. Recreational providers are also beginning to integrate the capacity of visualization into management practices by using GIS mapping to convey information on avalanche terrain to the recreational user. It is important to note that in many cases GIS is used in research to produce avalanche hazard maps, but this information is not typically made available to the public and is mainly an aid for the avalanche forecaster or a hazard mapper. New technologies and software are emerging as a means to integrate sophisticated modeling techniques into GIS as well as wireless capabilities which hold promise as an aid to recreationists as an innovative tool that can be used in the backcountry. The following review highlights some of the GIS applications related to avalanche mapping and modelling from Europe and North America.

2.4.1 European GIS applications

The production of GIS maps to visualize risks in avalanche terrain and information pertaining to avalanche formation has been particularly well developed in European

countries. Europeans have been leaders in utilizing GIS not only for mapping but more recently for integrating advanced modeling techniques with GIS at both regional and local scales. The following discussion provides selected examples of GIS related mapping initiatives, GIS hazard mapping, integration of new wireless technologies with GIS to aid recreationists in real time in the backcountry as well as emerging innovative software that integrates GIS with sophisticated snow avalanche models.

2.4.1.1 GIS applications at the Swiss Federal Institute of Snow and Avalanche Research (http://www.slf.ch/avalanche/avalanche-en.html)

At the Swiss Federal Institute for Snow and Avalanche Research in Davos the approach of combining the results of numerical and expert analysis with the strength of GIS visualization has led to the production of a series of maps that are accessible to the public. Since 1996, through the Avalanche Warning Switzerland 2000 project, data from automatic snow and weather stations, weather forecasts, feedback from avalanche forecasters and data from models such as NXD-REG (Brabec and Meister, 2001) and SNOWPACK (Lehning et al., 1999) are compiled to provide daily national, regional and local avalanche maps and bulletins using GIS applications (Russi et al., 1998; Stoffel et al., 2001; Stucki et al., 1998)

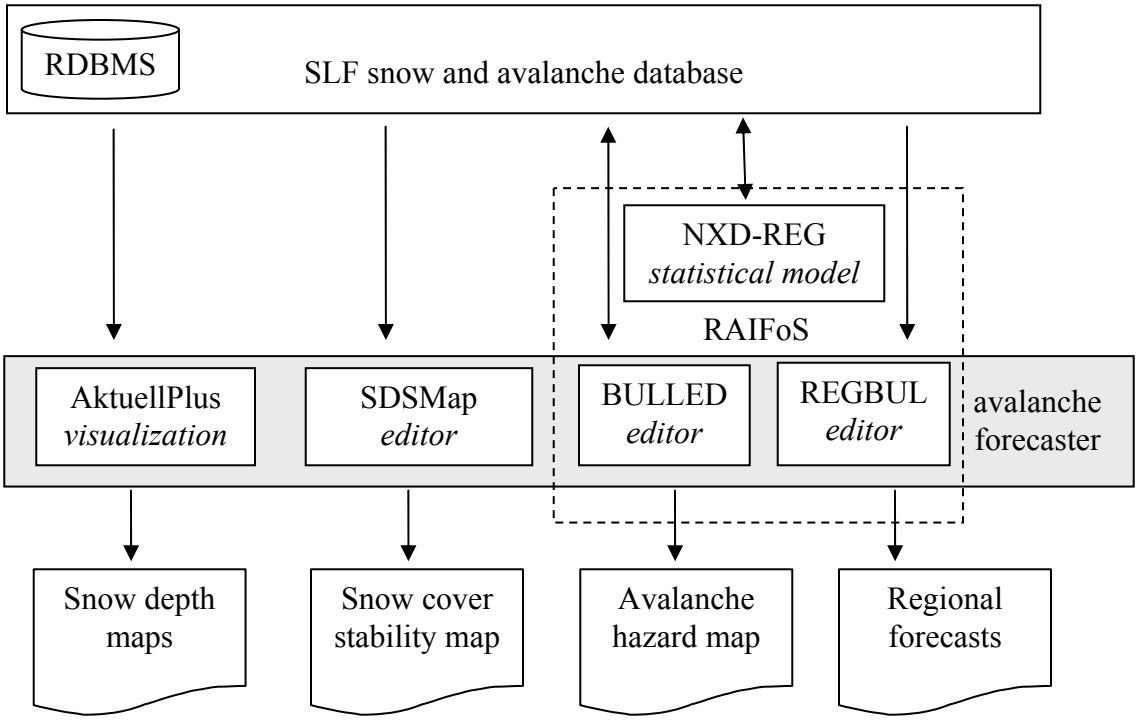

Figure 14. GIS Applications at the Swiss Federal Institute of Snow and Avalanche Research (Stoffel et al., 2001)

Figure 14 illustrates how GIS applications of AktuellPlus, RAIFoS and SDSMap utilize a database of weather, snowpack and avalanche records to produce map products of snow cover depth, stability, avalanche hazard and regional forecast. This database, stored using Oracle software, contains data gathered from manual and automatic networks, snow profiles, avalanche observations, as well as results from calculated models (Stoffel et al., 2001). All GIS applications are developed in ArcView using Avenue scripts. To visualize the database information, AktuellPlus is used to support the forecaster in viewing current or past weather, snow and avalanche conditions in the Swiss Alps. As with all map products produced at the Swiss Federal Institute of Snow and Avalanche Research, the results from AktuellPlus can be printed, published to the Internet (Figure 15), and sent to a fax delivery system or InfoBOX. InfoBOX is a software package that allows the downloading and display of all SFISAR products and data from automatic stations and observers to local avalanche centres (Stucki et al., 1998).

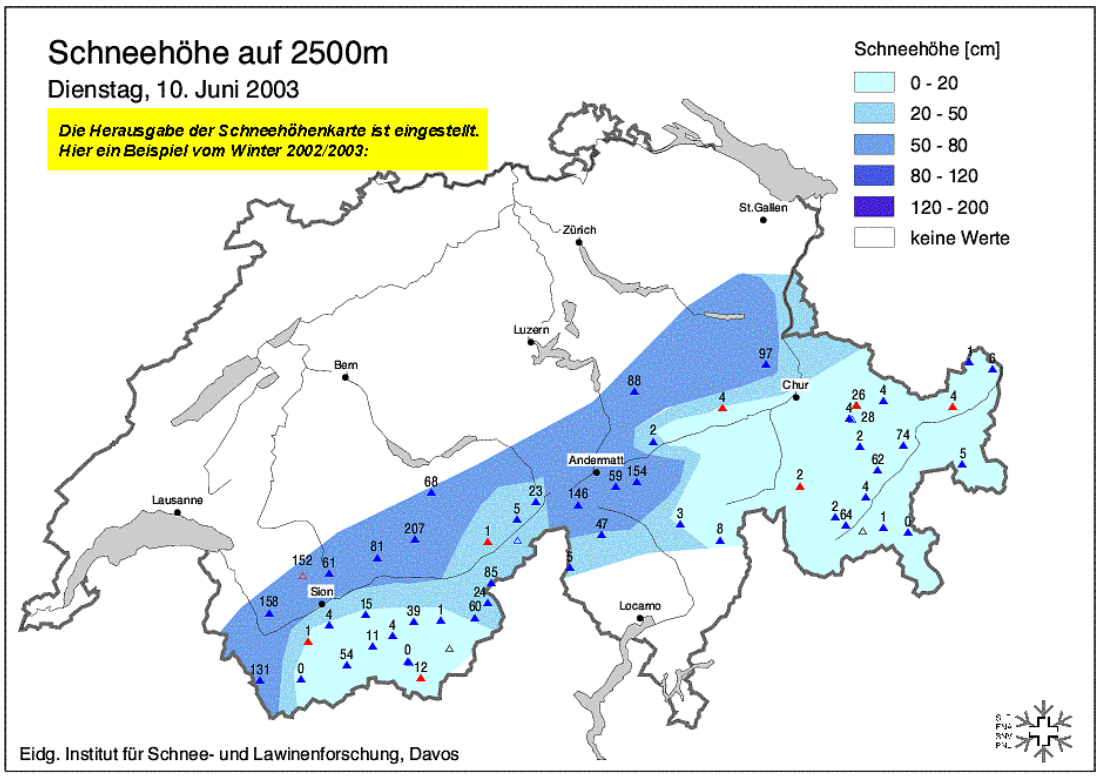

Figure 15. Snow Depth

The Regional Avalanche Information and Forecasting System (RAIFoS) is a computer-aided system that consists of three applications: a statistical model using a nearest neighbour approach (NXD-REG) to forecast hazard for Switzerland, a GIS based editor for building maps that show the estimated avalanche hazard for the regional level (BULLED), and a text editor (REGBUL) that provides a written forecast for each region (Brabec et al., 2001). NXD-REG (Next-X-Days-Regional) uses a nearest neighbours calculation (using S-Plus statistical software) to estimate avalanche hazard from 60 stations throughout the Swiss Alps based on over ten years of historical observations. The observations from the stations are then interpolated in ArcView GIS using an inverse distance-weighted interpolation to determine a spatial map of estimated avalanche hazard (Brabec et al., 2001). BULLED uses ArcView as the interface for map production and Oracle for storing all hazard estimates in a database. The hazard estimates derived from NXD-REG are published to the Internet (Figure 16), or made available through the means described for AktuellPlus, based on the European avalanche hazard scale.

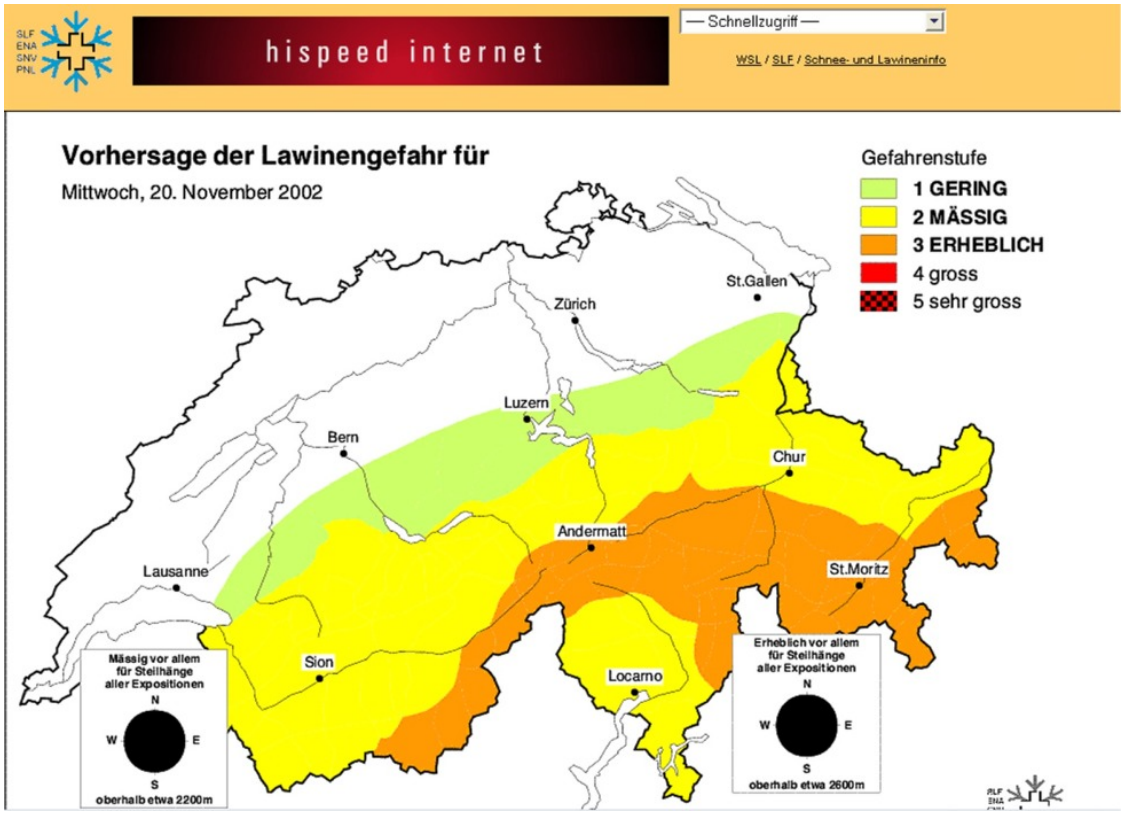

Figure 16. The Swiss Avalanche Bulletin

SDSMap is a GIS application that analyses current and past snow profile data to derive a snow cover stability map (Stoffel et al., 2001). Snow profile data is collected by digging pits and examining the exposed snow layers. Data regarding layering, snow crystal type and size, snow hardness, density, and temperature are recorded along with the results of stability tests (i.e. rutschblock test) performed on isolated blocks of snow. Data collected from 50 snow profile sites across the Swiss Alps, twice monthly, are used to derive stability based on a 5 class system ranging from very poor to very good. Figure 17 represents a map with point locations that indicate snow cover stability and is available to users via the Internet.

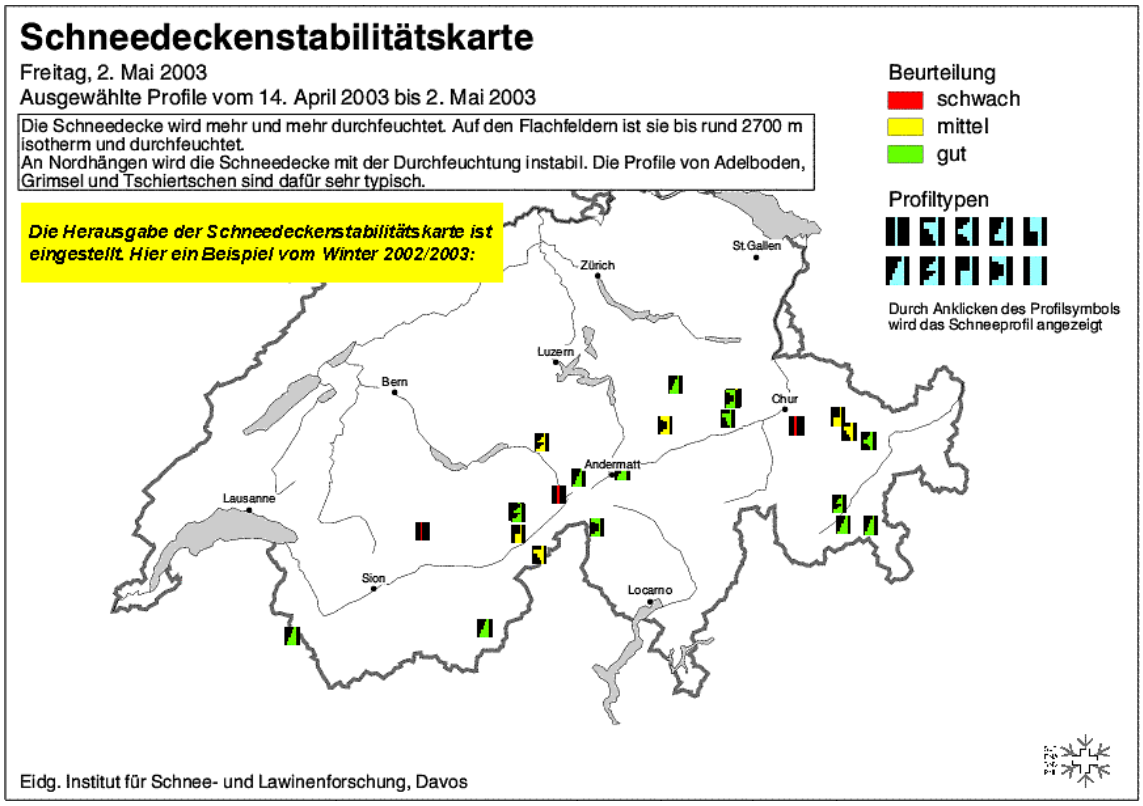

Figure 17. Snow Stability Map

The success of the distribution of the map products from the SLF is revealed in the approximately 2,000,000 requests by Internet, fax, InfoBOX or telephone during the winter 2000/2001 season, with 80% of the requests coming from the SLF website (Stoffel et al., 2001).

2.4.1.2 SAMOS (Snow Avalanche Modelling and Simulation)

SAMOS is a numerical modeling tool developed by the Austrian Institute for Avalanche and Torrent Research to create scenario hazard maps. SAMOS is based on a numerical calculation of avalanche flow for dense and powder snow component layers of an avalanche (Sailer et al., 2002; Sampl and Zwinger, 2004). A 2-D granular flow model is used for the dense snow flow layer together with a 3-D turbulent flow model for the powder snow layer and a simple transition model. SAMOS provides additional information on velocity, deposit depth and impact pressures for each avalanche site. GIS

is used to interpret and visualize the results of the SAMOS numerical simulation to generate hazard maps (Buckley et al., 2004).

2.4.1.3 Norway

A collaborative association of Norwegian government organizations that includes agencies such as the Norwegian Mapping Authority, the Norwegian Geotechnical Institute (NGI), the Norwegian University of Technology, and the Norwegian Foundation for Scientific and Industrial Research has set up a National Avalanche Database to provide digital avalanche maps through an Internet Gateway (http://www.skrednett.no/). The Internet Gateway provides an interactive and dynamic web mapping interface for the public to access map information depicting avalanche events and avalanche hazards. The map service is geared to the public by providing maps along with avalanche information written in a format that is for the non-expert. Online map functions allow a user to zoom in and out of a map that covers the entire country as well as facilitating the printing of areas of interest.

The intention of these maps is to protect structures, settlements and recreation users from avalanche danger. These maps were originally produced for the Norwegian Army. Starting and runout zones (includes track) were mapped at a 1:50, 000 scale by the NGI to provide the army with hazard maps to reduce risk during winter military exercises. Starting zones are identified in a GIS based upon slope and areas above tree line or with sparse forest cover; maximum and minimum runout zones are calculated with a regression equation based upon terrain parameters derived from the DEM (Bakkehoi et al., 1983; Lied and Bakkehoi, 1980; Lied et al., 1989).

2.4.1.4 PARAMOUNT project (Public SAfety and CommeRcial Info-Mobility Applications and Services in the MOUNTains)

The PARAMOUNT project was an EU funded program jointly operated by IfEN GmbH (Neubiberg, Germany), AGIS, (University of the Bundeswehr München), Institut Cartogràfic de Catalunya (Barcelona, Spain), and the Search And Rescue (SAR)services from Germany and Austria represented by BRK Bergwacht Bayern (Munich, Germany) and Oesterreichischer Bergrettungsdienst (Klagenfurt; Austria) (González et al., 2003). The consortium developed a Location Based Service (LBS) prototype to aid backcountry travellers equipped with Pocket-PCs. GPS, mobile cell phone technology and GIS were combined to provide tourists with guidance in the mountains (Löhnert et al., 2001). The project was implemented in two pilot test areas in the German Alps (30x30 km^2 study area) and Spanish Pyrenees. The user-friendly services included geographic maps with information pertaining to terrain and helpful services such as points of interest including locations of the nearest restaurant, avalanche and weather forecasts, a search and rescue alarm to allow users to call for help and route search and research to their location and a utility to track the users' movements to aid in updating trail networks (Löhnert et al., 2004). These services also included maps showing avalanche hazard or Cartographic Avalanche Forecasting (CAF). CAF refers to a spatial interpretation of the avalanche hazard bulletin, a means of taking the text format bulletin and providing a cartographic representation, showing the distribution of the avalanche hazard (Moner et al., 2004).

2.4.1.5 Avalanche Hazard Mapping System (AHMS) and Rapid Mass Movements (RAMMS)

For avalanche modeling and hazard mapping, the Swiss Federal Institute for Snow and Avalanche Research (SLF) has developed an integrated system using avalanche numerical simulation models with GIS (Gruber, 2001; Haeberli et al., 2004). Figure 18 provides an overview of the system. Data inputs of digital elevation data and land cover as well as information pertaining to parameters required for the numerical flow models are incorporated into a GIS to both model and visualize hazard of high, moderate, low and no hazard areas. The numerical models are based on a progressive development of

dynamic runout modelling that has been integrated with GIS (Bartelt et al., 1999; Gruber and Bartelt, 2007; Gruber et al., 1998). From the DEM, terrain considerations of slope, aspect and curvature are input into the numerical model as well as being used to automatically identify potential release zones. The user interface allows the operator to identify input parameters concerning flow parameters and conditions of fracture depth and snow density in to any location on the map. GIS software (Arc/Info) in combination with C programs and IDL and Xlib applications power the computer processing. The main purpose of the hazard map is for land use planning to determine the potential impact of avalanches on human infrastructure.

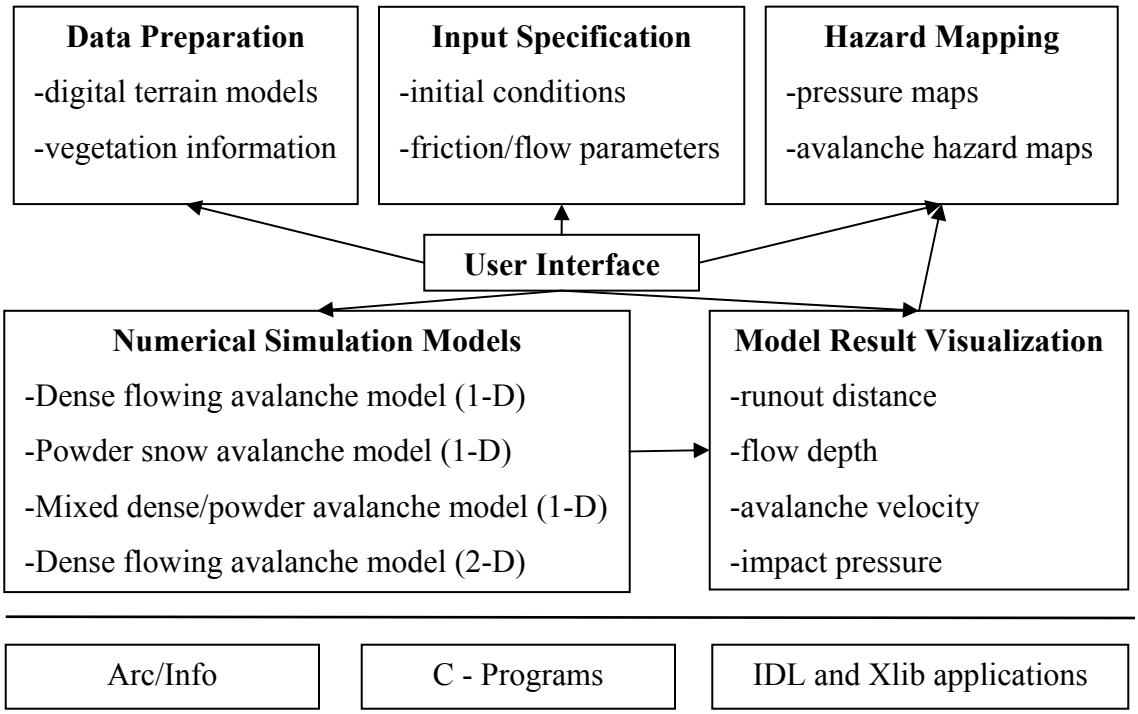

Figure 18. GIS-based Avalanche Hazard Mapping System (AHMS) (Haeberli et al., 2004)

RAAMS is emerging as a new software system that uses GIS tools to model natural hazards of snow cover and avalanches, debris flows and rock fall (Christen et al., 2007). Initiated in 2005, the program also operates under the Swiss Federal Institute for Snow and Avalanche Research. RAAMS facilitates dynamic modeling of avalanche motion

based on a two dimensional flowing avalanche model (Gruber et al., 1998). The software allows for automatic identification of avalanche starting zones, based on work by Maggioni and Gruber (2003), and sophisticated 3D visualization. The system relies upon the use of digital terrain models. RAAMS is a new initiative and is still in the development phase.

2.4.1.6 NivoLog

NivoLog is an avalanche forecasting software system that combines nearest neighbour calculations and expert systems for analysis of avalanche hazard. NivoLog consists of three modules; NivoLog Data, (database) for storing information pertaining to weather, snowpack and avalanche activity, NivoLog View for the purposes of visualization using GIS software (ArcView), and NivoLog Graph, which displays graphs to summarize information and highlight trends (Bolognesi, 1998). To facilitate the spatial representation of the model, GIS is used to determine several categories of avalanche starting zones based on terrain characteristics such as slope, aspect and elevation (Bolognesi et al., 1996). Avalanche hazard is assigned from the model results to each avalanche area based upon similar terrain characteristics. The final representation of the results in map format is to aid forecasters and avalanche control workers with improved visualization of areas of high avalanche potential. Further developments as indicated in Figure 19 involve the linking of NivoLog to automatic sensors such as Flowcapt (measures snowdrift) and automatic weather stations as a step towards an automatic prediction system (Chritin et al., 1998). Validation exercises have indicated 80% success in correctly making avalanche predictions (Bolognesi et al., 1994). Although this application is not available online to the public, it represents a unique combination of GIS with expert systems and automatic sensors. This application is a research and development project of METEORISK (http://www.meteorisk.com/).

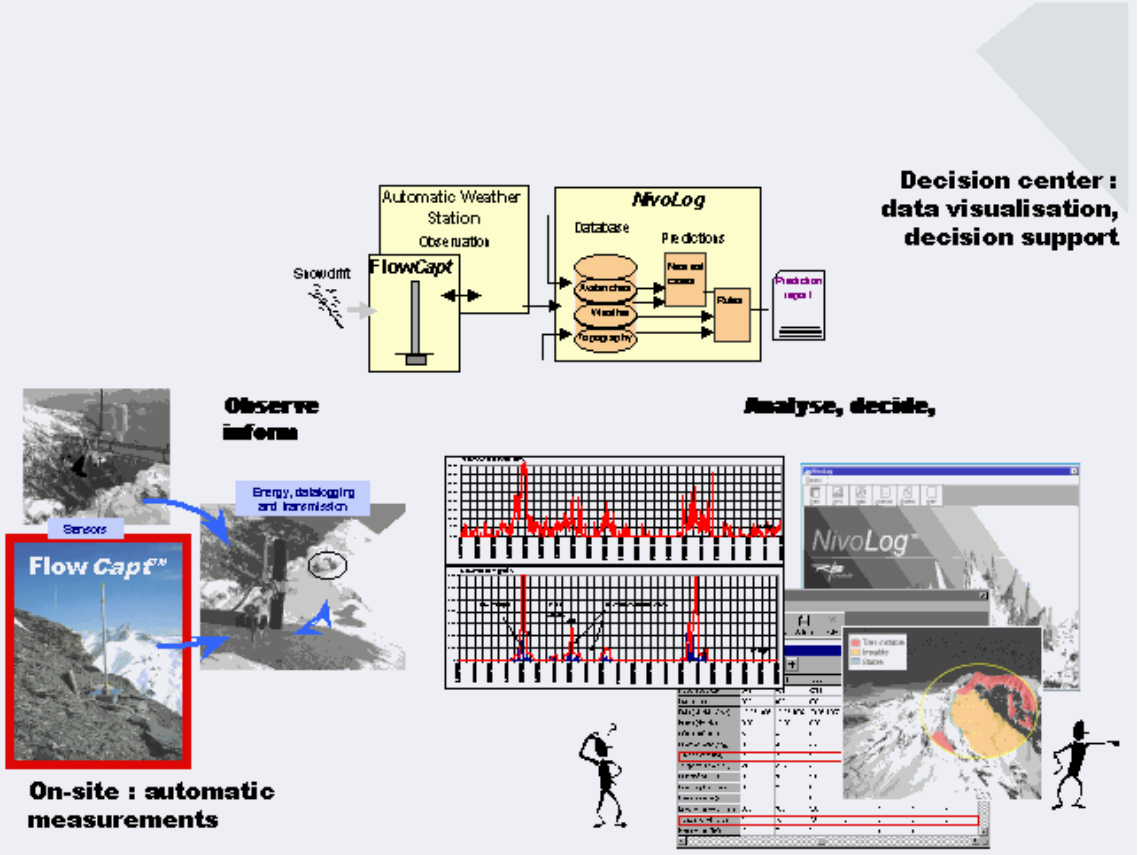

Figure 19. NivoLog integrated with automatic sensors (Chritin et al., 1998).

2.4.2 GIS applications in North America

The majority of avalanche mapping using GIS in North America is typically done by consultants for the forest industry (Kelly and Stevens, 1997), transportation sector (Scott, 2006), ski areas, industrial, residential or as projects for various GIS programs at universities and colleges (McLaren, 2000; Royer and Lemieux, 2006). In most cases, potential starting zones are identified automatically in GIS based upon slope angle, aspect with respect to wind, forest cover and then refined with expert interpolation. In some instances, GIS is used as a cartographic tool to visualize historical records or provides a means to record expert delineated or surveyed avalanche data in order to build an avalanche database or atlas. For recreational purposes, the helicopter ski industry in Canada uses GIS for run mapping. Few of these applications transition to the online

environment. One of the main limitations to GIS development in Canada is the lack of high resolution DEMs and imagery to conduct studies at a slope scale, something that is addressed in this thesis.

The Canadian Avalanche Association has recently recognized the potential of GIS to contribute to the needs of the avalanche community. As a result, the CAA is initiating a project to develop a GIS data management system. CADS, (Canadian Avalanche Data System), is proposed to capture weather, avalanche, snowpack and terrain information to aid avalanche related operations in Canada. This system will be geographically based and take advantage of GIS technologies.

An example of online GIS avalanche mapping services developed for avalanche areas in the United States (http://www.avalanchemapping.org/index.htm) highlights maps of avalanche paths, commonly referred to as avalanche atlases, and offers services to produce maps displaying potential avalanche areas. Selected maps are available to the public for purchase or online viewing. These avalanche path maps are based on slope, aspect and forest cover with further refinements made based on expert interpolation using supplementary imagery (Scott, 2006). Advanced runout modeling is not being incorporated into the mapping. Users can download maps and use a free GIS viewer to view and print their own maps. Further capabilities allow users to download maps and snowpit data collection software to their personal handheld devices equipped with Global Positioning Systems (GPS). The user can then enter their own snowpit data that is displayed on a map which adheres to guidelines established by the American Avalanche Association and the National Avalanche Centre (Scott, 2004).

An advanced application, initiated in North America, that used the power of GIS visualization in combination with an extensive avalanche database is Gvis, Geographic Visualization (Maceachren et al., 1999; McCollister et al., 2002) integrated with results generated from Knowledge Discovery in Databases (KDD). Gvis revealed regional spatial patterns of avalanche activity at various scales. A correlation between weather and

a spatial pattern of avalanche activity was analyzed to gain a better understanding for avalanche forecasting. The approach facilitated the handling of large archived weather and avalanche activity datasets to incorporate geography at different scales. Nearest Neighbours is used in the KDD to search the archived datasets for the most similar historical days of avalanche activity for geographically mapped slide paths in the GVis. An example of this technique was conducted at Jackson Hole Ski Area, Wyoming (McCollister et al., 2002). Slide path probabilities were calculated for each slide path. Aspect and elevation were related to the associated weather parameters. This method permitted the user to run numerous scenarios and visualize the probability patterns of slide paths. Weather variables considered include; new snowfall, wind speed and wind direction.

2.5 Discussion

Digital elevation data at increasingly higher resolutions offers the potential of modeling avalanche terrain at a scale that is of great interest to backcountry users who are interested in individual slopes. Avalanche terrain maps that are generated from DEM data are essentially time-independent, static maps that based on primary topographic attributes can model slopes that are susceptible to avalanche formation and runout. Avalanche forecasting maps which would attempt to map snow stability are time dependent, dynamic maps that are reliant upon constantly changing weather and snowpack information. At a regional scale, avalanche forecasting maps provide a general overview of predicted conditions based upon current and forecasted weather and snowpack information. However, as discussed previously, attempts to model climatic factors such as the impacts of wind and solar radiation on snowpack stability at a slope scale have been extremely difficult to accomplish in mountainous terrain and require input parameters of a high resolution. In order to better estimate snow stability at a slope scale the density of weather stations and snowpack data at varying elevations and proximity would need to be greater than anything currently available in the Columbia Mountains. Due to a fundamental lack of understanding of all the physical relationships related to

snow stability it would be impossible to accurately map or model snow stability at this scale even with ideal meteorological data.

The study area benefits from a 40 year historical record of avalanche path statistics that provides the raw data for GIS analysis. The process of modelling avalanche runout potential, both dynamically and statistically, has been pioneered in several European countries, namely Norway, Switzerland and France. This thesis uses a statistical approach, that is based on the pioneering work of Bakkehoi and Lied undertaken in Norway, and uses the same alpha-beta runout model that has been successfully applied worldwide to predict maximum avalanche runout in Rogers Pass. The alpha-beta runout model has not been applied to the Columbia mountain region, so the potential exists to create a made-in-Canada model that is built upon a tested and proven body of research.

GIS has also been used to help recreationists improve their risk assessment and management in avalanche terrain by collecting and distributing pertinent data in a user-friendly visual format. Online database collections and interactive maps and newly emerging avalanche modeling software such as RAMMS lead the way in innovative initiatives making full use of the capabilities of GIS. North America lags behind in terms of public access to online avalanche mapping data, as most of the current mapping has been for the forestry, transportation or research sectors and little has been done to integrate advanced snow models into a GIS environment. Recent efforts in the United States are providing publicly accessible online maps, which is following the general trend already established in Europe.

GIS is a powerful tool for visualizing avalanche terrain and modelling runout potential. It can provide insights to both researchers and backcountry recreationists as it can improve avalanche hazard prediction and decision-making when travelling in avalanche terrain. It is vital that GIS visualizations and representations of avalanche hazard are validly backed by science and it is in this regard that GIS can be abused in terms of creating attractive cartographic visualizations without sufficient scientific data or understanding. GIS is

reliant upon the availability of high quality digital elevation data for visualization and modeling. The next chapter will outline the process of creating a DEM for the Rogers Pass study area.

Chapter Three: DEM Generation and Stereo Vector Capture

3.1 Introduction

Terrain is a fundamental factor influencing avalanche phenomena and digital elevation models are a vital component for analysis and modeling of terrain using GIS. Most digital elevation data is generated with photogrammetric data capture using stereoscopic interpretation of aerial photographs and frequently supplemented with additional elevation data collected with Global Positioning Systems (GPS) (Li et al., 2005; Wilson and Gallant, 2000). Using a digital photogrammetric workstation, a higher resolution DEM for selected portions of the Rogers Pass study area was created. In addition, vector data representing expert knowledge of highway corridor avalanche paths relating to avalanche starting zones, maximum runout extent, start of runout and the centreline of the avalanche profile along with vegetation were digitized in stereo 3D.

This chapter highlights the softcopy photogrammetry process of air photo capture, geo-correction and the related tasks of building a digital elevation model, extracting DEM values and the process of vector data capture based upon expert knowledge (Figure 20). The higher resolution DEM was created to provide a detailed representation of terrain to aid in building models which incorporate the complexity of terrain features that contribute to avalanche formation. Better than conventionally available DEM data from government sources, the higher resolution DEM provides a superior surface for image overlay and enhanced computer visualization as well as the increased potential for terrain analysis.

3.2 Building a Digital Elevation Model (DEM)

The procedure for building and extracting data from a DEM is outlined in Figure 20. Once data specifications of scale, resolution and coverage area are identified, the flight can commence and the imagery will be acquired. In order to extract 3D data from aerial

photographs, stereo models or stereo image pairs are created using photogrammetric methods and then 3D coordinates of terrain objects are measured on the stereo model (Li et al., 2005). This process involves accurately geocoding each image through a process of aerial triangulation and subsequently each data model is built for the stereo pair images. Once the imagery has been processed, feature extraction can occur in stereo to extract 3D elevation values as well as vector data. Orthophoto mosaics mesh the stereo images together with respect to elevation to provide an overview of the area covered by the imagery.

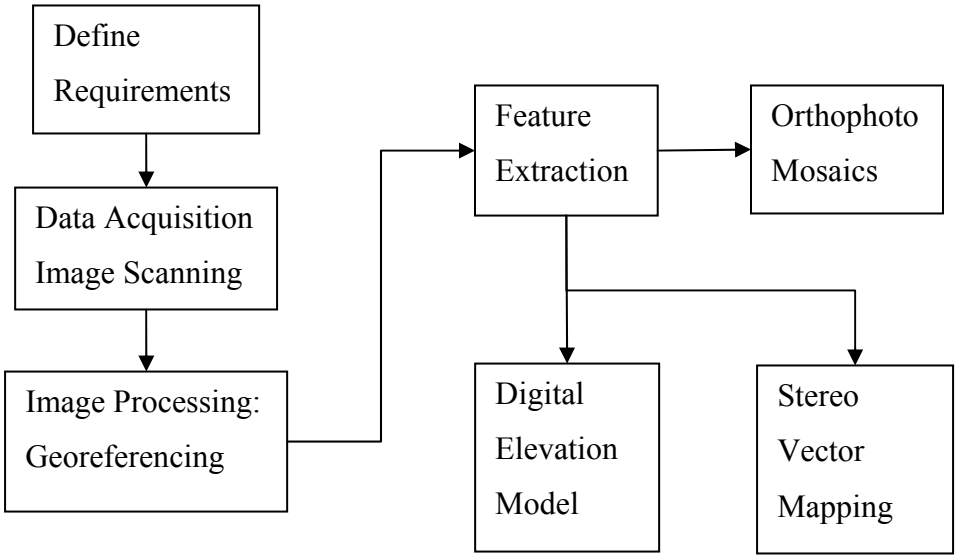

Figure 20. Workflow for generating a Digital Elevation Model and preparing aerial photos for mapping of vector features

3.2.1 Data acquisition and image scanning

In the fall of 2004, Parks Canada contracted the Calgary, Alberta, Canada company Geodesy Remote Sensing Inc. to capture air photo data for several mountain parks. The flights for Glacier National Park took place on September 27 and October 1, capturing color air photos at a 1:30,000 scale. These photos were subsequently scanned at a resolution of 25 microns which results in a raw ground pixel size of 0.75 metres (25 µm x

30,000). Realistically, at least 4 pixels are required to identify a feature in the image indicating a ground space of 3 m (4 x .75μm) and is required for subsequent softcopy photogrammetry interpretation. The coverage of air photos along with flight lines, air photo centres and control points are displayed in Figure 21. Typically an overlap of 60% exists between photo pairs in the same flight line and a 30% overlap between the flight strips. The flight report is included in Appendix A.

The camera used for the flight survey is a potential source of error when capturing air photographs. In February 2003, the National Research Council of Canada prepared a calibration report of the camera used (Ziess Jena LMK 15) by Geodesy Remote Sensing Inc. for the flights over Glacier National Park. This calibration report provides data on any potential errors in the camera and the parameters identified were input into the photogrammetry software during image processing in order to mitigate any errors generated by the camera. The report confirms that the camera met required standards for aerial photograph surveys and details specific attributes that include measured parameters on image illumination, shutter speeds, focal length, radial measured distortion, asymmetry and measures of any distortion (Cai, 2003).

3.2.2 Image processing: georeferencing aerial photographs to build stereo-models

To georeference aerial photographs properly to a ground location a procedure known as aerial triangulation (AT) is required. Aerial triangulation is the process that involves matching known ground control points to identifiable pixels on the image in order to reference the image with real-world coordinates. AT also corrects for lens distortion, camera tilt, earth curvature and refraction (Welch and Jordan, 1996). In order to obtain the highest possible control with which to geoference the air photographs TRIM ground control points (GCP) were purchased from the Province of British Columbia's Base Mapping and Geomatics Services branch.

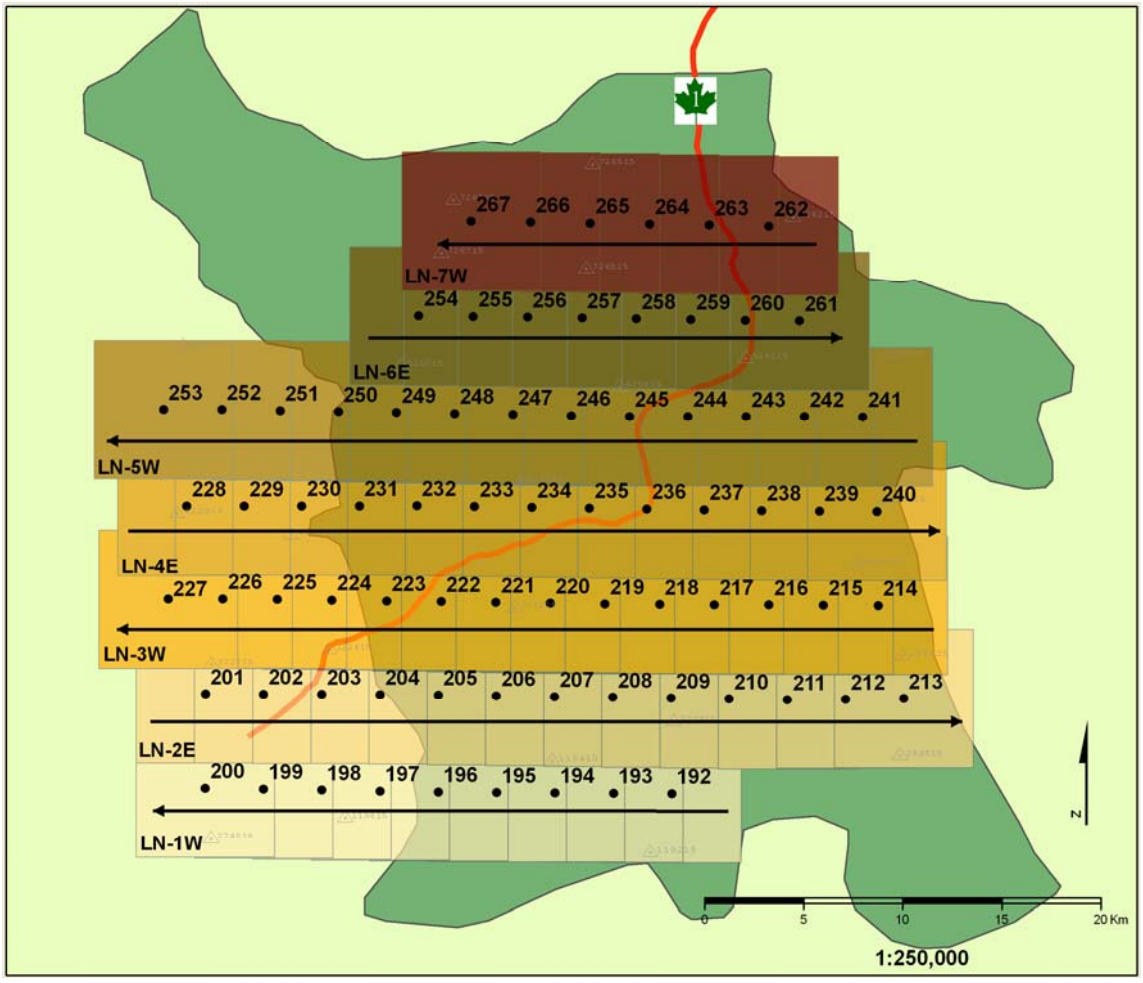

Figure 21. Glacier National Park air photo flight lines. (Data source: Geodesy Remote Sensing Inc., 2004)

The TRIM data represents the best available ground control locations. It has a maximum RMS error in X, Y, Z of +/- 3 m (BMGS, 2007). The aerial triangulation is a semi-automated process whereby an operator is in control of selecting the ground control targets and the software program calculates the final coordinates through a least squares algorithm. To perform the aerial triangulation of the Parks Canada air photos, Integrated Mapping Technologies (IMT) of Vancouver, BC was contracted to perform the correction procedure using a DiAP digital photogrammetric workstation.

IMT generated 69 stereo models for the air photo dataset. Their report (Appendix B) indicated that vertically (Z), the control used fits the models to within 1.4 m; while

horizontally (X/Y) the control fits to within 1.75 m. Overall the statistical results show a relative accuracy of less than .2m. The absolute accuracy of obtaining the best mean fit with the control points and photo centre coordinates is in the order of 1.5 metres.

3.2.3 Feature extraction- building a Digital Elevation Model

Once the image processing is complete, feature extraction can commence using the digital photogrammetric workstation. As outlined in the literature review, there are three main methods of extracting a DEM; manually capturing elevation points, automatic collection of data elevation points using correlation algorithms or a hybrid approach which utilizes a combination of manual and automated processes. For this thesis, a different approach was utilized to generate a high resolution DEM that relied heavily upon manual data entry by an operator. DEM points from TRIM data were used as a base at 25 m x 25 m horizontal resolution. These data points were supplemented using a selective sampling procedure that mimics field surveying whereby a skilled operator added Very Important Points (VIP) (Li et al., 2005). In some cases the BC TRIM DEM data points were completely removed. VIP points are irregularly placed points that best represent terrain features. In addition, breaklines were added to represent changes in terrain surface such as ridges, streams, roads, cliffs, and other abrupt changes in elevation.

The advantage of a manual based procedure is that a skilled operator can place fewer points than automated methods yet maintain a comprehensive coverage that represents the surface with high accuracy. For example, in an automated process the computer may place elevation points on either side of a ridgeline completely missing the highest point along the ridgetop, whereas, a skilled operator will place points on the tops of ridges and other representative points on terrain features to best represent the shape of the feature.

Manually creating a DEM is a time consuming process and thus only selected areas were chosen for creating a higher resolution DEM (Figure 22). Yellow boundary lines indicate

those areas selected for DEM generation. These areas include two popular backcountry skiing areas of Connaught Creek and the Asulkan drainage, outlined in dashed blue with a combined surface area of 4,400 ha, as well as an additional 230 ha from the 45 avalanche paths along the highway corridor, highlighted in pink.

A drawback of this method is that it is time consuming and requires considerable interpretation skills of the stereo model. Geodesy Digital Mapping Inc., Calgary, AB was contracted to provide this service using a SOCET SET v. 5.2 digital photogrammetric workstation and the work required approximately 2 weeks to complete. This method of irregularly placed points can not be reproduced by computer algorithms and is regarded as a highly accurate method data capture of elevation data (Molander, 2001).

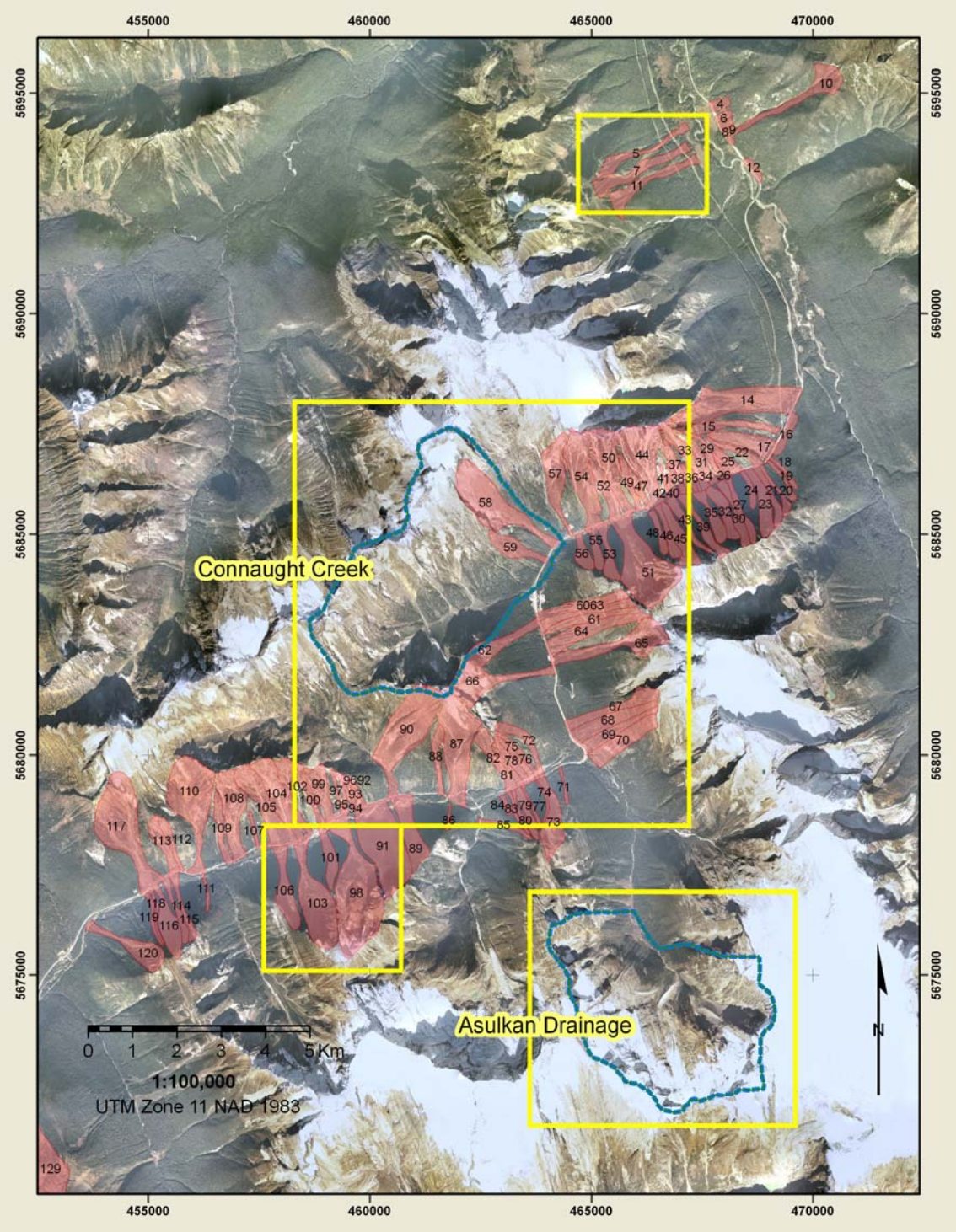

Figure 22. Rogers Pass with selected areas for DEM generation highlighted in yellow outlines. Pink shaded areas indicate avalanche paths. Blue dashed lines represent the two popular backcountry skiing areas of Connaught Creek and Asulkan drainage.

3.2.4 Interpolation of a gridded DEM surface

Once the breaklines and elevation points have been manually captured using digital stereo photogrammetry, a gridded DEM surface can be interpolated. Figure 23 provides a generalized example of the interpolation process from taking the manually entered data to build a DEM to the interpolation of a final gridded DEM product. From the source elevation data as described in section 3.2.3, a Triangulated Irregular Network (TIN) was created using ArcGIS®. The Delaunay method of triangulation is the most commonly used method and is the method used by the ArcGIS® software. Delaunay triangulation involves constructing triangles by connecting three neighbouring points consisting of a line vertex or elevation point. Each triangle is linked but is unique, does not overlap and is as equilateral as possible (Li et al., 2005). Information on slope, aspect and elevation is available for each triangle. Once the TIN was generated, a gridded DEM was produced using a linear interpolation method. Linear interpolation regards the TIN triangles as planes and assigns each grid cell a value based upon which triangle it falls within as well as taking into consideration the position of the cell centre relative to the position on the triangle plane (ESRI, 2006a). This procedure mirrors the approach used by the Province of British Columbia and was selected in order to compare the DEM models to each other. A gridded DEM of 5 m was produced from the TIN and was used to extract the high resolution terrain parameters and perform analysis.

a.

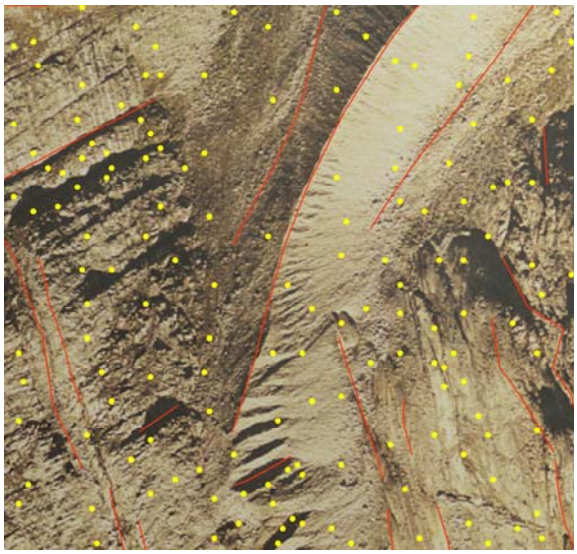

b.

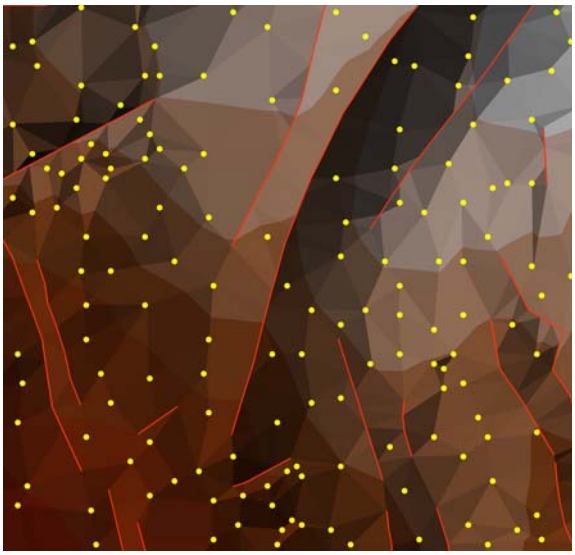

c.

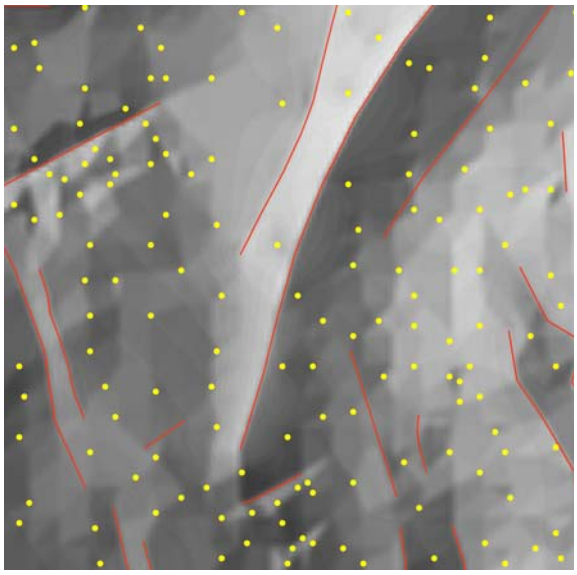

Figure 23. Process for interpolating a gridded DEM. a. Manually entered breaklines and spot elevation points from air photographs. b. Triangulated-irregular-network (TIN) generated from breaklines and elevation points. c. Gridded DEM interpolated from the TIN at a specified resolution.

3.2.5 Digital orthophoto mosaic

Once the airphotos have been subjected to image processing and a DEM has been created, an air photo mosaic or digital orthophotography is only one additional step to the photogrammetric workflow. An operator controls the image mosaicking process whereby the geocorrected images are matched and attached to each other and positioned to the DEM surface. The orthophoto then provides not only compensation for tilt or positional displacement but relief displacement as well. In mountainous areas, remotely sensed images are susceptible to the shadowing effects cast by surrounding mountains. North facing slopes and valley bottoms are particularly prone to this effect. To minimize the effect of shadowing in the valley bottoms for the purpose of geographic 3D visualization, the valley bottoms in the orthophoto mosaic were brightened in Photoshop® (Figure 24).

3.3 Province of British Columbia TRIM DEM data

The low resolution DEM was obtained from the Base Mapping and Geomatic Services branch, Province of British Columbia. The DEM product is also generated using a stereo compilation based on 1: 70,000 scale aerial photography. For the consultants producing the DEM data for the Province, there are two acceptable methods for data capture – gridded and random data capture. For random DEM capture, an operator is required to capture data points at a minimum of every 100 m and every 75 m in terrain with an average slope greater than 25˚. Using a gridded pattern to collect points, the operator must record points every 75 m unless the terrain exceeds 25˚, which then requires capture at 50 m spacing (MELP, 1992). Supplementary breaklines to increase representation of the topography are collected subject to not exceeding a resolution of 25 m in the final DEM.

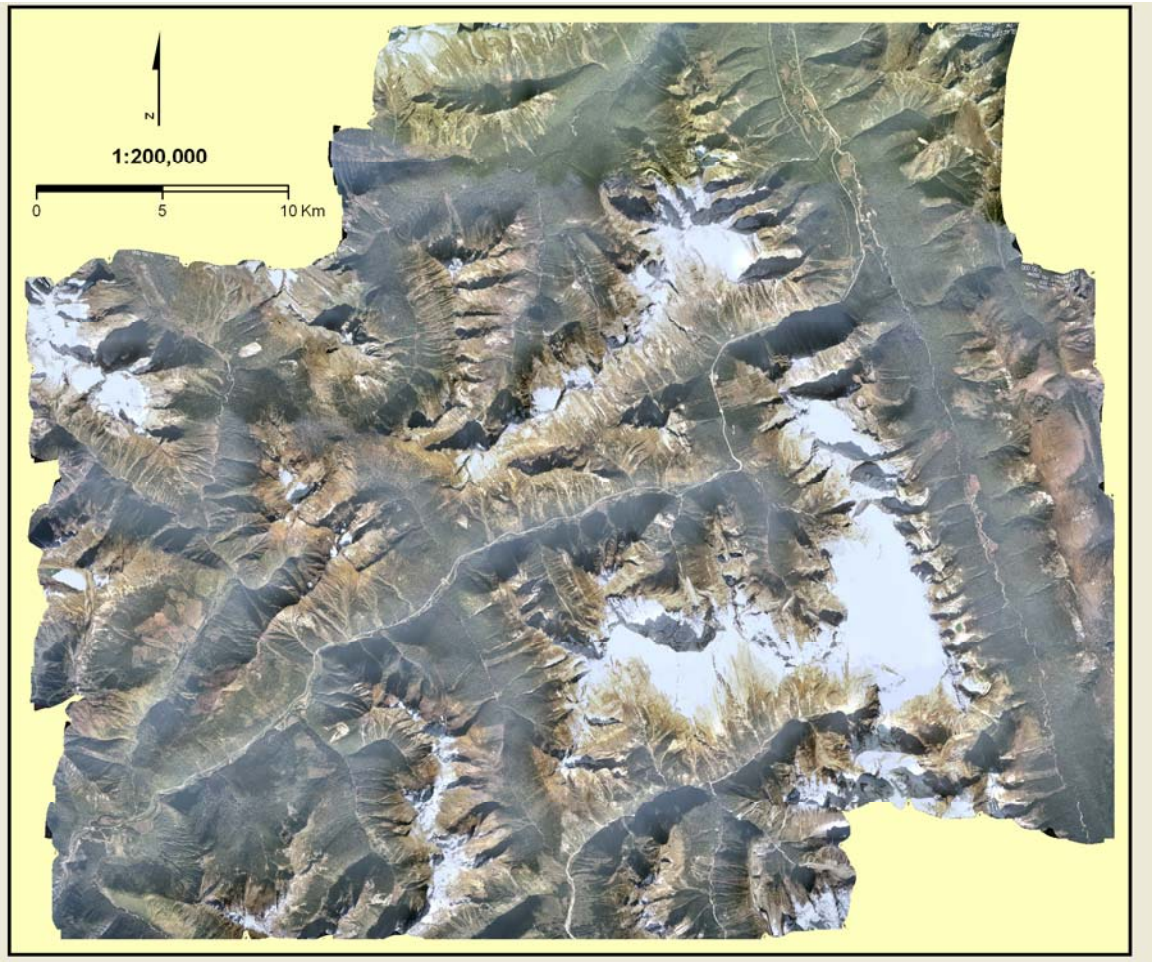

Figure 24. Orthophoto mosaic compiled from the 76 aerial photographs taken for Glacier National Park. Valley corridors have been lightened in Photoshop® in order to compensate for the effects of shadowing

The DEM product is created from a sampling of a TIN (built from the elevation data points and breaklines) at 25 m intervals using a linear interpolation and written to a raster file of elevation data (BMGS, 2002). Linear interpolation is a transformation of the TIN to a raster DEM whereby each output cell for the DEM grid is assigned an elevation value by determining which triangle in 2-D space it falls into and then assessing the grid cell centre relative to the triangle plane (ESRI, 2006a). British Columbia specifications require that 90% of all discrete DEM points be accurate to within 5 m of their true elevation while 90% of interpolated points are accurate to within 10 m of their true

elevation (BMGS, 1996). The coverage of the low resolution DEM includes the entire study area.

3.4 DEM verification

There are several methods to check the accuracy of DEMs generated by photogrammetric means. These include (Daniel and Tennant, 2001; Hutchinson and Gallant, 2000):

- Generation of contours or shaded relief to allow for a visual inspection of anomalous terrain
- Inspection of frequency histograms of primary terrain attributes
- Measures of residuals during AT
- Comparison of elevation values from the DEM to surveyed elevation points on the ground

Two methods of visually inspecting a DEM are to generate a shaded relief and to derive elevation contours (Hutchinson and Gallant, 2000). A shaded relief allows an inspection of any anomalous bright or dark spots. Derived contours are sensitive to elevation errors in source data and with contour labels added, they allow inspection of spurious contour lines along with incorrect contour values. In Figure 25, below, a shaded relief map has been generated for both the high and low resolution DEMs. The area selected is the Asulkan drainage, a popular backcountry skiing area. Upon inspection of the shaded relief for the area no anomalous bright or dark spots are appearing; however, the high resolution DEM shows more details in the terrain. Note that the high resolution DEM was only generated for the terrain inside the Asulkan valley. There is some evidence of a "corn row" or striping effect in the low resolution image that is removed within the valley in the high resolution image.

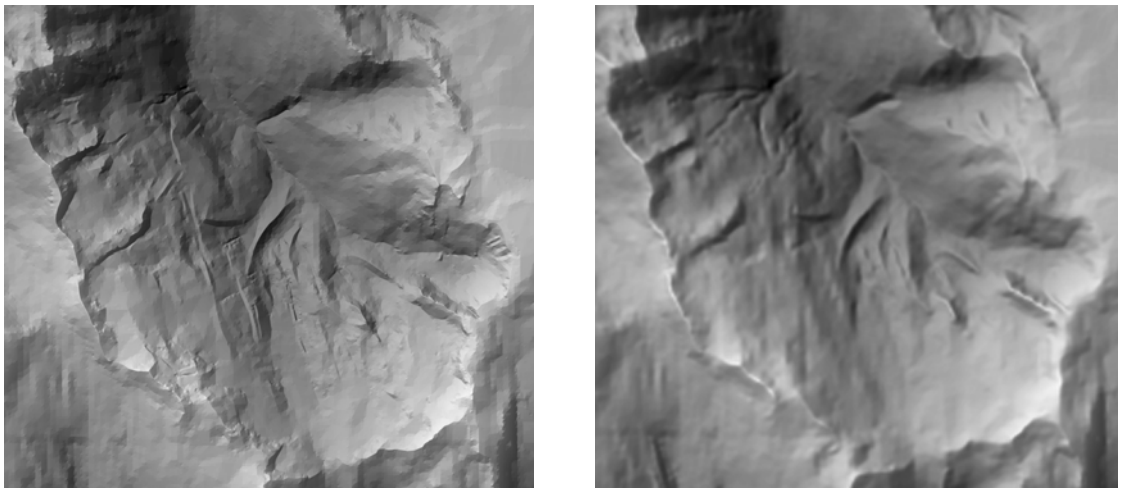

Figure 25. Shaded relief of high (left image) and low (right image) resolution DEMs for the Asulkan drainage

Another method of evaluating DEMs is to examine frequency histograms of primary terrain attributes such as elevation and aspect (Hutchinson and Gallant, 2000). In Figure 26 and Figure 27, for both elevation and aspect, the low resolution DEM displays sharper peaks and pits as compared to the smoother high resolution DEM. For the high resolution DEM, values from only within the Asulkan drainage were plotted on the graphs below as the high resolution DEM does not extend beyond the watershed boundary.

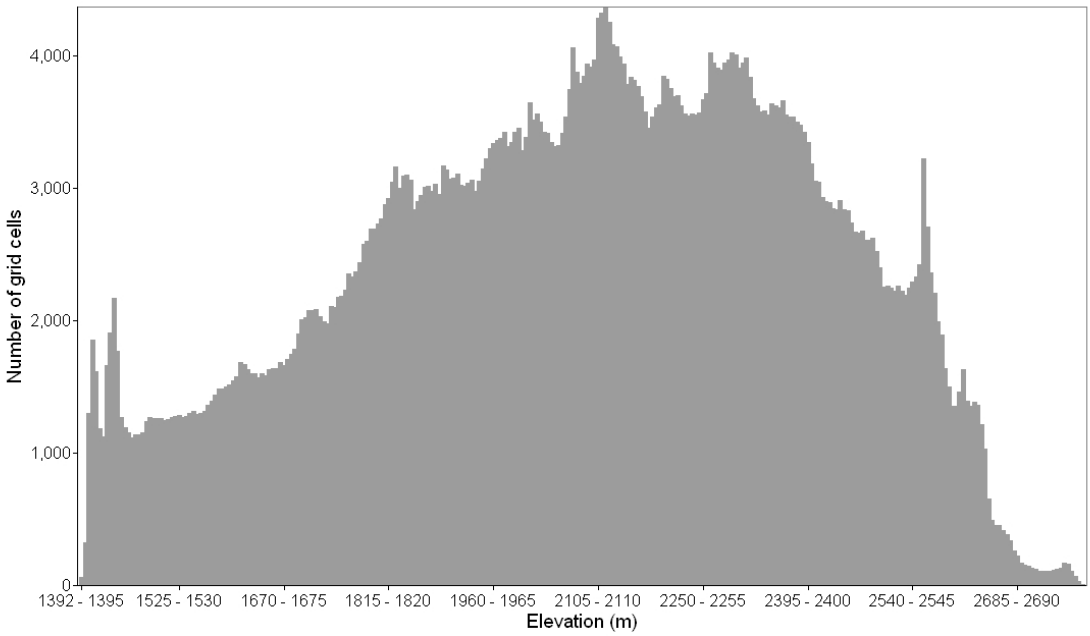

Frequency histogram of elevation values for the high resolution digital elevation model in the Asulkan Drainage

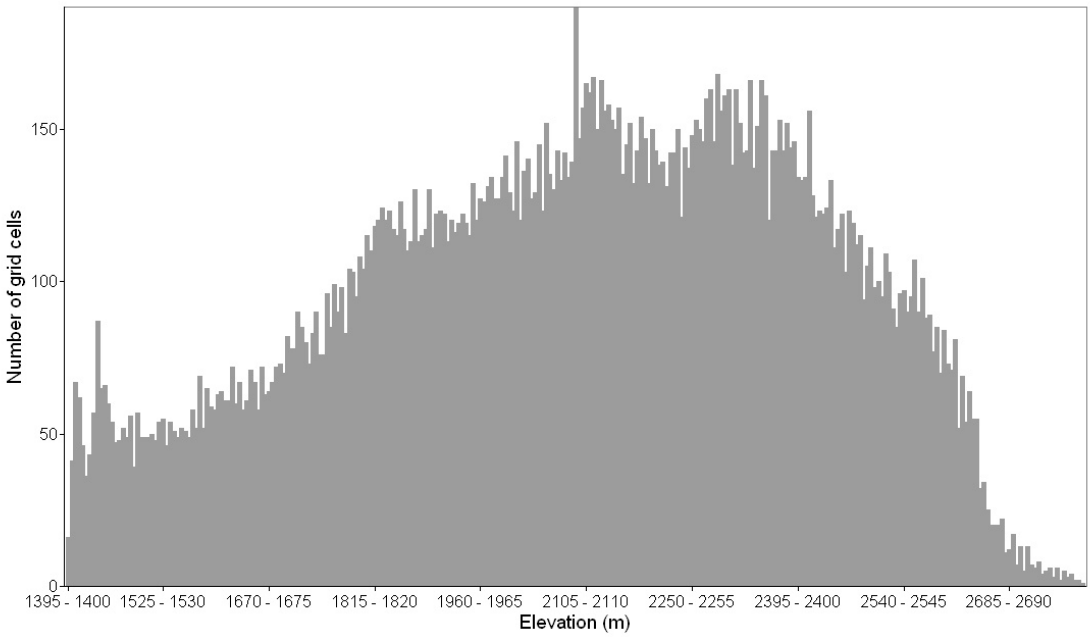

Frequency histogram of elevation values for the low resolution digital elevation model in the Asulkan Drainage

Figure 26. Frequency histograms of elevation values for high and low resolution digital elevation models in the Asulkan drainage

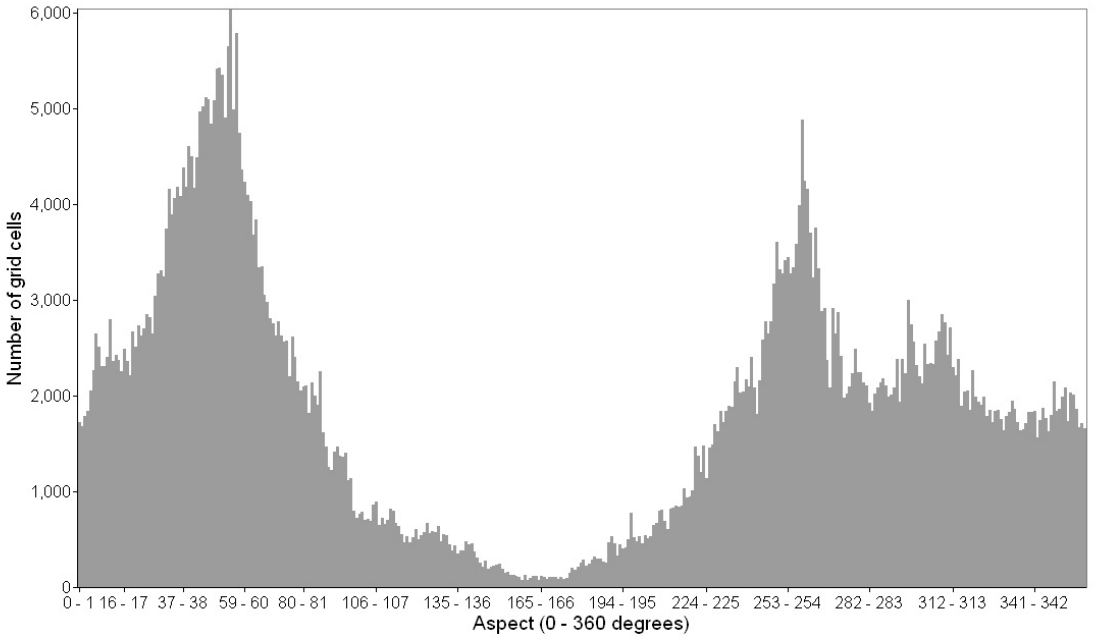

Frequency histogram of aspect values for the high resolution digital elevation model in the Asulkan Drainage

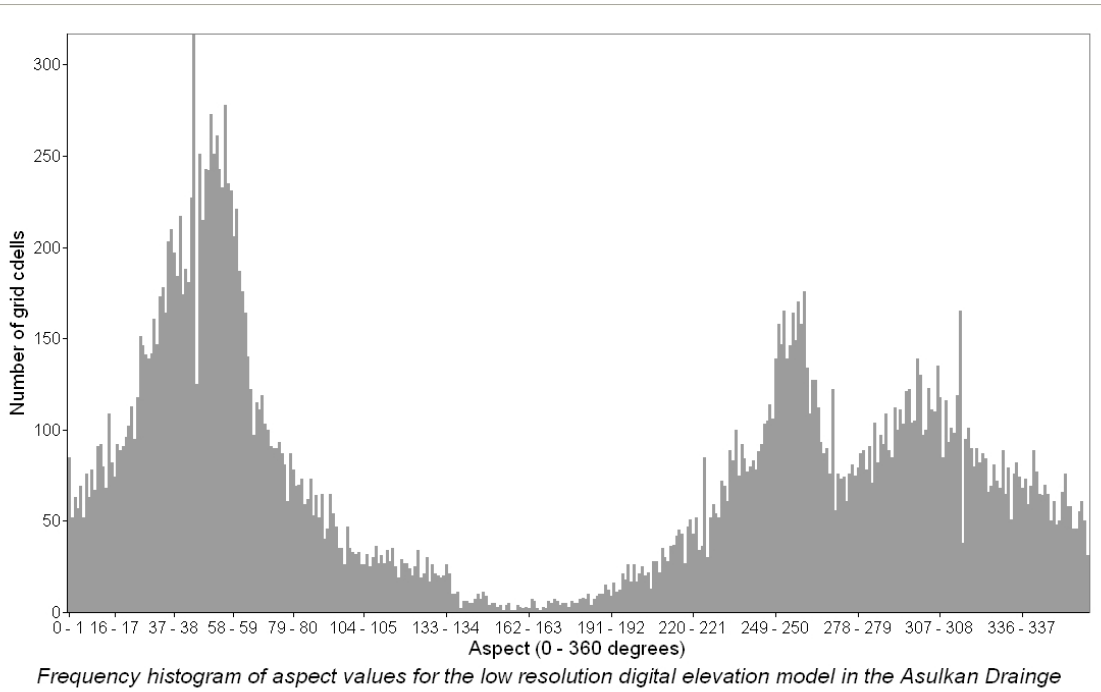

Frequency histogram of aspect values for the low resolution digital elevation model in the Asulkan Drainge

Figure 27. Frequency histograms of aspect values for high and low resolution digital elevation models in the Asulkan drainage

Table 9. Descriptive statistics of the frequency histograms for elevation and aspect models for the Asulkan drainage

Dataset	Min	Max	Mean	Std. Dev.	Sample Size	T-test (means)
High Resolution – Elevation	1393	2779	2085.449	311.370	673216	*t*-value = 1015.922
Low Resolution – Elevation	1395	2790	2095.982	315.558	26938	*p*-value = <0.0001
High Resolution – Aspect	0.002	359.999	168.617	119.400	673216	*t*-value = -55.665
Low Resolution – Aspect	0	359.813	166.330	119.353	26938	*p*-value = <.0001

The descriptive statistics in Table 9 of primary terrain variables indicates that the minimum, maximum, mean and standard deviation for the high and low resolution data are similar; however, there is a significant difference between the means of elevation and aspect between the high and low resolution datasets as indicated by the T-test results.

The measures of the residuals for low resolution DEM are required to meet the specifications set out by the Province of British Columbia. For the higher resolution DEM, the image processing was conducted to minimize residual values as much as possible. The results of the original correction process were checked and verified by Geodesy Remote Sensing Inc.

The purpose of utilizing digital stereo photogrammetry for feature extraction of DEM values is to minimize the costs of collecting survey points in the field. For this thesis, field data points from which to compare the results of the DEM produced were not obtained due to cost and time constraints. In order to collect suitable data points, a GPS base station would need to be set up in the study area at a surveyed location and used to correct collected points by a roaming GPS unit in the field. These points would have to be selected based upon locations that are readily identifiable in the field and on the aerial

photography. Unfortunately, existing survey points with a suitable spread and accuracy in the area were not available.

3.5 Vector capture

Vector capture refers to the process of digitzing information from the air photo imagery into a GIS, such as forest cover, avalanche paths, avalanche centrelines and start zone features. Using photogrammetry software, the data is captured in a 3D 'etch-a-sketch' method. A SOCET SET® photogrammetry workstation was used to digitize vector information relevant to avalanche activity in the study area. The author wore stereoscopic eyewear to view imagery in stereo and trace the features as directed by the avalanche expert. For this thesis, the data captured were based on expert input from Bruce McMahon, Senior Avalanche Officer at the Parks Canada Rogers Pass headquarters.

At several times during the vector capture process, the expert was consulted and shown the vector linework to confirm the data entered. Edits and revisions were made based on his input. Much of this work was done in Rogers Pass at the Avalanche Control Centre in order to have access to the original databases and field notes upon which the linework was based. The avalanche control program at Rogers Pass has a set of avalanche and meteorological observations dating back to 1959 and a consistently reliable database back to 1965. The Senior Avalanche Officer at Mount Revelstoke and Glacier National Parks (Bruce McMahon) has over 20 years of operational experience. This first hand knowledge was essential as he was able to remember back to observations made. In addition, his detailed knowledge of terrain and the avalanche activity tied to the avalanche paths along the highway is not available in any database. Bringing this wealth of information out and inputting it into the GIS was a critical component of the mapping work undertaken in this thesis. The linework digitized (Figure 28) for each highway avalanche path based on expert input included: the start zone (yellow), the avalanche path centreline (blue), the estimated start of runout (green), the avalanche path outline

(red) and the observed maximum extent of the avalanche path. The estimated start of the runout reflects the expert defined point at which avalanche deposition first occurs.

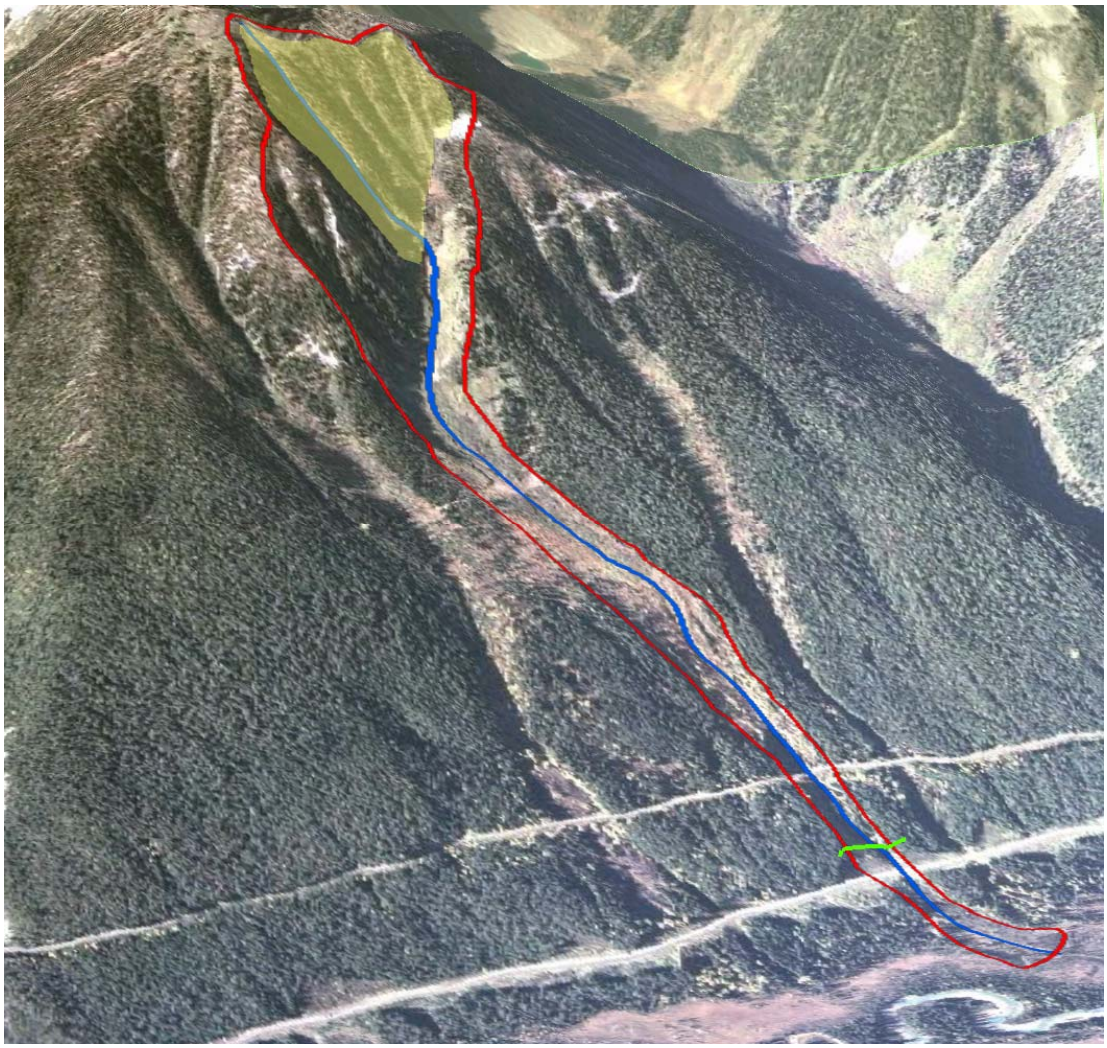

Figure 28. Digitized linework based on expert knowledge. Yellow shaded area at the top of the path represents the starting zone. The blue line is the centreline of the avalanche path and the red outline is the avalanche path outline. The green line estimates the location of where the avalanche begins to retard and deposition occurs.

3.6 Discussion

The factors influencing accuracy of the photogrammetric DEM are a result of the instruments (camera, scanner) used in the process, the ground control data for AT, scale of the photo taken and the methods used to extract the DEM (Daniel and Tennant, 2001). Other sources of error include: vegetation interference, personal bias of operator and image matching algorithms. Everything possible was done to minimize these factors in the generation of the higher resolution DEM. Different interpolation algorithms to create a DEM can result in DEM variations even using the same base data (Rasemann et al., 2004). Thus to compare the low and high resolution DEMs, it was necessary to create the higher resolution DEM in a manner comparable to the methods used by the Province of BC to effect the best comparison results. Based on the verification measures the higher resolution DEM was shown to be a better model than the low resolution DEM. The purpose of which is to provide greater detail of the terrain surface in order to enhance the development of avalanche models.

In a similar attempt to achieve the best results possible, the stereo vector data capture involved numerous iterations or ‘back-and-forth’ sessions with the avalanche expert in order to perfect his interpretation of the maximum observed runout, avalanche path centreline, avalanche path outline, start zone areas and estimated location of where avalanche runout typically begins. Once this linework was prepared and verified, the associated topographic values from both high and low resolution DEM were extracted and used to develop the runout models discussed in the next chapter.

Chapter Four: Statistical runout modeling of snow avalanches

4.1 Introduction

Determining maximum snow avalanche runout extent is an important consideration for mapping avalanche hazard for backcountry users, transportation corridors and other human infrastructure. The maximum runout refers to the furthest reach of the deposit expected for a specified return period, which for backcountry recreation is 10 years (Canadian Avalanche Association, 2002a). Runout zones can be identified through a combination of field observations, historical records, meteorological data and analysis of aerial photos and topographic maps for vegetative and geomorphic evidence (Canadian Avalanche Association, 2002a; Mears, 1992; Weir, 2002). In areas where historical observations and field evidence are lacking, estimating avalanche extent may be difficult and runout models provide an option for estimating maximum runout. Snow avalanche runout modeling is generally accomplished with statistical models, physically based models or a combination of the two approaches. The statistical models, which are used in this thesis, provide an estimate for maximum runout along the centreline of the avalanche path and are limited in that they do not indicate the lateral extent of avalanches.

Dynamic models are adept at indicating velocity and impact pressures along with avalanche runout and are especially suited for analysis where defence structures would be situated or impacts to forest resources or infrastructure are concerned; however, they require estimates of friction coefficients and release mass which may be unavailable or difficult to estimate in remote areas or areas with varying terrain cover and unknown slab thickness. Small variations in these parameters can lead to great discrepancies in estimating runout distance (Lied, 1998).

Statistical models using regression equations with simple topographic inputs, first introduced by Bovis and Mears (1976), are able to predict maximum runout but do not

provide estimates of avalanche size, speed, force or lateral extent. For the purposes of hazard mapping for recreational users, the maximum runout predicted by statistical models is sufficient to identify the extent of avalanche paths to a backcountry user. The alpha-beta regression runout model (Bakkehoi et al., 1983; Lied and Bakkehoi, 1980; Lied et al., 1989), initially applied in Norway by the Norwegian Geotechnical Institute (NGI) and applied in other parts of the world (Fujisawa et al., 1993; Furdada and Vilaplana, 1998; Johannesson, 1998; Jones and Jamieson, 2004; Lied et al., 1995) is well suited to topographic mapping. A modified version of the Norwegian model, the runout-ratio model, has been developed for extreme value distributions. The main assumption is that avalanche runout distances follow a Gumbel distribution as opposed to an assumed normal distribution of the residuals from a regression model (McClung, 2000; McClung and Lied, 1987; McClung and Mears, 1991; McClung and Mears, 1995; McClung et al., 1989). Comparisons between the runout-ratio model and the regression model have been made using different data sets. In Iceland, runout ratio models did not show an improvement over regression models (Johannesson, 1998). For short path avalanche data in Canada, the runout ratio model often predicted longer runout distances than the alpha-beta model for large non-exceedence probabilities (Jones and Jamieson, 2004). For this chapter, the alpha-beta approach is used for predicting avalanche runout.

The terrain inputs required for the regression runout model are typically taken from topographic maps and field survey measurements; however, in Europe, Geographic Information Systems and digital elevation model (DEM) data (based on data with contour intervals of 20 m) have been used to extract these parameters (Furdada and Vilaplana, 1998; Lied et al., 1989; Lied and Toppe, 1989; Toppe, 1987), with the assumption that better or higher resolution DEM data would improve the models. One part of this chapter examines the assumption that higher resolution DEM data improves regression runout models by running a comparison between the results obtained in an alpha-beta regression analysis between 25 m resolution DEM data and 5 m resolution DEM data.

Variations of the alpha-beta regression model equation have been produced for diverse mountain ranges (McClung and Mears, 1991; McClung et al., 1989). This study focuses on developing a regression model specifically for the Columbia Mountains, Glacier National Park, British Columbia, Canada. An extensive historical database of over 40 years of records is supplemented with expert knowledge along the Trans Canada Highway corridor to develop an alpha-beta regression equation using both high and low resolution DEM data. The model is cross-validated. Two examples demonstrate the model's applicability; one of a highway path outside the dataset used to derive the model and the second on an avalanche path in the backcountry. Although backcountry areas are not exposed to explosive-controlled avalanches, in contrast to the highway corridor, it is assumed that the regression equation will provide a reasonable estimate of maximum runout extent for these backcountry areas. In Jones and Jamieson (2004), the β reference point, that is normally defined as the point at which the slope angle of the avalanche path decreases to 10˚, was modified to 24˚ to accommodate short slopes of less than 600 m. For avalanche mapping, recreationists are often concerned with the runout from shorter slopes. In the backcountry where the regression model is applied, the valley bottom is less broad than the valley through which both the CPR and TCH run, thus exploring the option of applying the regression formula with a β angle of 24˚ was desirable to facilitate runout mapping for backcountry reaches and is examined here.

4.2 Review of data sources

This study is based on extracting topographic parameters from expert defined avalanche paths, starting zones and path centrelines (profiles) to estimate maximum runout from both a high and low resolution digital elevation model. To accurately map the expert defined avalanche path outlines, starting zones and centrelines of avalanche paths with maximum observed runout indicated by the farthest reach of the line, digital stereo vector mapping with a photogrammetry workstation using SOCET SET® accommodated the digitising of the data. In each case, the farthest reach of the line represents the maximum observed extent reached by an avalanche event in the recorded historical database of

approximately 40 years. The digitized data was subsequently verified for accuracy by expert knowledge. To counteract the impact of avalanche runout on the highway and exposed sections of the rail line, additional defensive structures including snow sheds, diversion dams, mounds and other barriers have been constructed. Despite these measures, there are avalanche paths that reach the highway in the valley bottom and in some cases will cross the valley floor and run-up the opposite slope. To control avalanche paths that impact the transportation corridor, weather, snowpack and avalanche observations are evaluated by avalanche forecasters and, if necessary, the TCH and CPR are closed while avalanches are triggered artificially using artillery. Road crews then clear snow and debris from the highway. Closures total about 100 hours per winter and have significant economic impacts.

As discussed in chapter three, the high resolution DEM was created using a process of digital photogrammetry whereby air photos that were taken in the fall of 2004, at a scale of 1:30,000, were scanned, geo-corrected and manually processed to develop a higher resolution DEM of 5 m. Due to the time consuming nature of building a DEM with this method, only a portion of the terrain covered by the avalanche paths along the highway corridor was processed, along with two popular backcountry touring areas the Connaught Creek and Asulkan Drainages (Figure 29). The Asulkan and Connaught drainages are popular ski touring areas where the regression model derived from the highway corridor was applied to predict maximum runout in these lesser-known areas. Figure 29 also highlights the avalanche paths along the highway corridor that were utilized for this study and includes a graduated shading of their average annual frequency. The low resolution DEM with a horizontal resolution of 25 m was obtained from the Base Mapping and Geomatic Services branch of the Province of British Columbia. The low resolution DEM covers the entire study area.

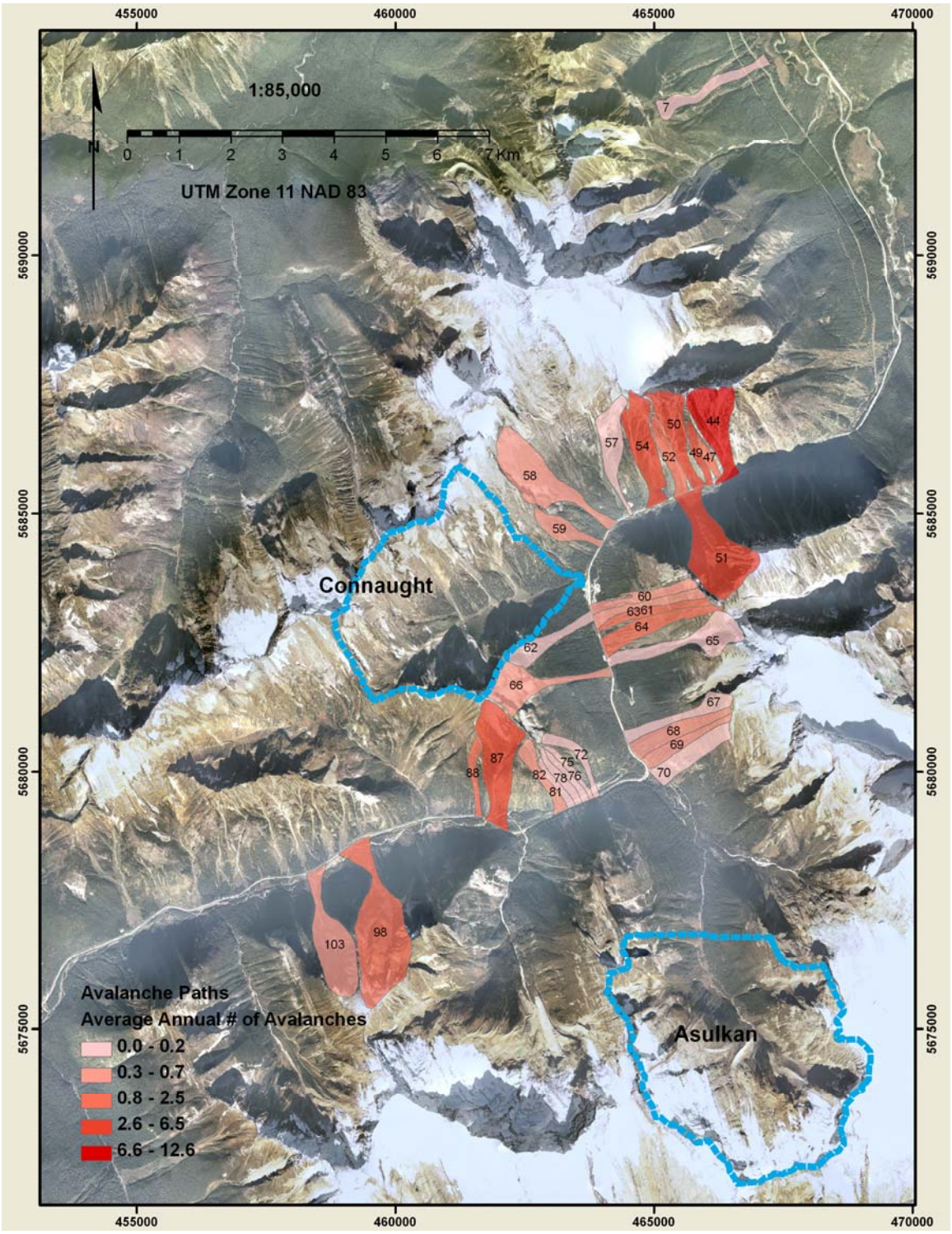

Figure 29. Avalanche frequency of paths used for the regression analysis along the highway corridor. Blue dashed lines indicate backcountry areas with a high resolution DEM.

4.3 The alpha-beta runout model

The following topographic parameters were extracted based on the success of previously cited alpha-beta studies in estimating maximum runout. These parameters (H, β and Hy″θ) have proven useful in regression models for estimating runout maximums (α) in mountainous regions around the world and are illustrated in Figure 30.

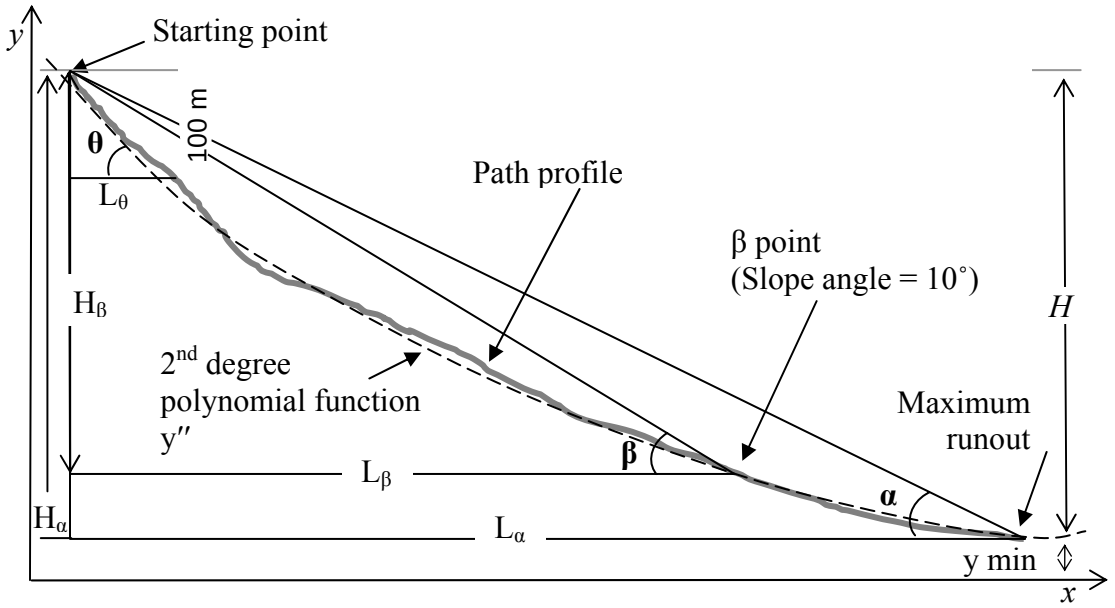

Figure 30. Alpha-Beta runout model. The solid grey line represents the centreline of the avalanche path profile from the DEM. The dashed line is the 2nd degree polynomial derived from the avalanche profile coordinate points. θ is the average inclination of the starting zone in the top 100 vertical meters (arctan(100/L_θ)) of the avalanche path. *H* represents vertical drop as measured on the 2nd degree polynomial from the polynomial's intersection with the y axis at the top of the avalanche path to the minimum point measure on the curve of the polynomial function. β is the average angle (arctan(H_β/L_β)) from the top of the avalanche path to a point at which the slope angle reaches 10˚ (the β point) on the DEM profile. α measures the average angle (arctan(H_α/L_α))from the top of the avalanche path to the maximum observed runout position.

α (alpha): The average gradient of avalanche path from the top of the avalanche path to the end of the maximum observed runout position where $\alpha = \arctan(H_\alpha / L_\alpha)$. Coordinates were extracted from the highest and lowest points from the actual DEM (high and low resolution) on DEM avalanche profile line to yield vertical drop (H_α) and the total

horizontal distance (L_α). α (observed) is calculated based upon where the expert positioned the maximum observed runout position in the GIS.

β (beta): The average gradient (where $\beta = \arctan(H_\beta/L_\beta)$) of the avalanche profile from the top of the path to the point on the avalanche profile within the runout zone where slope reaches 10º (beta point). All slopes of 10˚ and less were mapped in the GIS and the intersection of the DEM avalanche profile and the down slope point at which it crossed the 10º slope threshold in the runout zone was recorded as the beta point.

θ (theta): The average inclination of starting zone in the top 100 meters of the release zone where $\theta = \arctan(100/L_\theta)$. On the high and low resolution DEM, a point was created using GIS within the top vertical 100 m (+/- 5 m) of the avalanche profile. The coordinates were extracted at this 100 m elevation point along with the coordinates from the top of the path line to yield exact vertical height and horizontal length to provide a measure of average inclination of the starting zone.

y″ (curvature): The topographic profile of the avalanche path from the 2nd degree polynomial function. All horizontal distance and elevation data points were collected from along the avalanche profile from the top of the expert identified avalanche path to the expert identified maximum observed runout point. The file was imported into a statistical package (SPSS, 2006) and the 2nd degree polynomial equation line of best fit was determined. The coefficient of x^2 was taken from the equation and multiplied by 2 in order to produce the second derivative constant (y″) that provided a value for the curvature. The procedure was performed for both the high and low resolution datasets.

***H* (vertical displacement)**: is the total vertical displacement as measured on the 2nd degree polynomial function. Vertical displacement is measured as the difference between the top of the avalanche path at the y intercept to the minimum point on the 2nd degree polynomial function, where $y' = 0$.

The full regression equation as expressed in (Bakkehoi et al., 1983; Lied and Bakkehoi, 1980; Lied et al., 1989) takes the form of Equation 4.1 while the simplified β only model takes the form of Equation 4.2.

$$\hat{\alpha} = b_1\beta + b_2 H + b_3 H y''\theta + b_0 \text{(constant)} \quad (4.1)$$

$$\hat{\alpha} = b_1\beta + b_0 \text{(constant)} \quad (4.2)$$

Where $\hat{\alpha}$ is the predicted value of α.

4.4 Description of the dataset

Prior to conducting a full regression analysis, the dataset was explored with diagnostic plots and graphs based on the form of the regression equation (4.1) to identify any potential outlier data points, test for normal distribution of residuals and to examine the distribution of the remaining topographic parameters to be used in the analysis. The dataset consists of 40 avalanche profiles for both 5 m and 25 m DEM resolutions. This was reduced to 35 profiles for each high and low resolution DEMs after outliers were removed. Removal of these outliers allowed atypical and dubious data points to be removed from the regression models.

4.4.1 Identification of outliers

Of the 144 avalanche paths along the highway corridor, 40 paths fall into the area where the high resolution DEM was captured. Only avalanches with a maximum observed runout extent that involved a run up the opposing slope of less than 25 vertical metres, from the valley bottom to the recorded maximum stopping point, are used in the analysis. The alpha-beta regression model is not intended to include run up. Of those avalanche paths that do run- up the opposing slope of less than 25 vertical metres, they are somewhat mitigated by the deposition of snow over the winter that often fills in this discrepancy and reduces the run- up amount. Of the 40 avalanche paths, two exceeded the run-up threshold and were excluded from the data analysis (cases 20 and 22). Cases 20

and 22 stand out as outliers in Figure 31 c, d and particularly in Figure 31 a as the magnitude of studentized deleted residuals of greater than +/-2 are generally worth examining (Norušis, 2006).

Three outliers were also removed leaving 35 paths for the regression analysis. One outlier

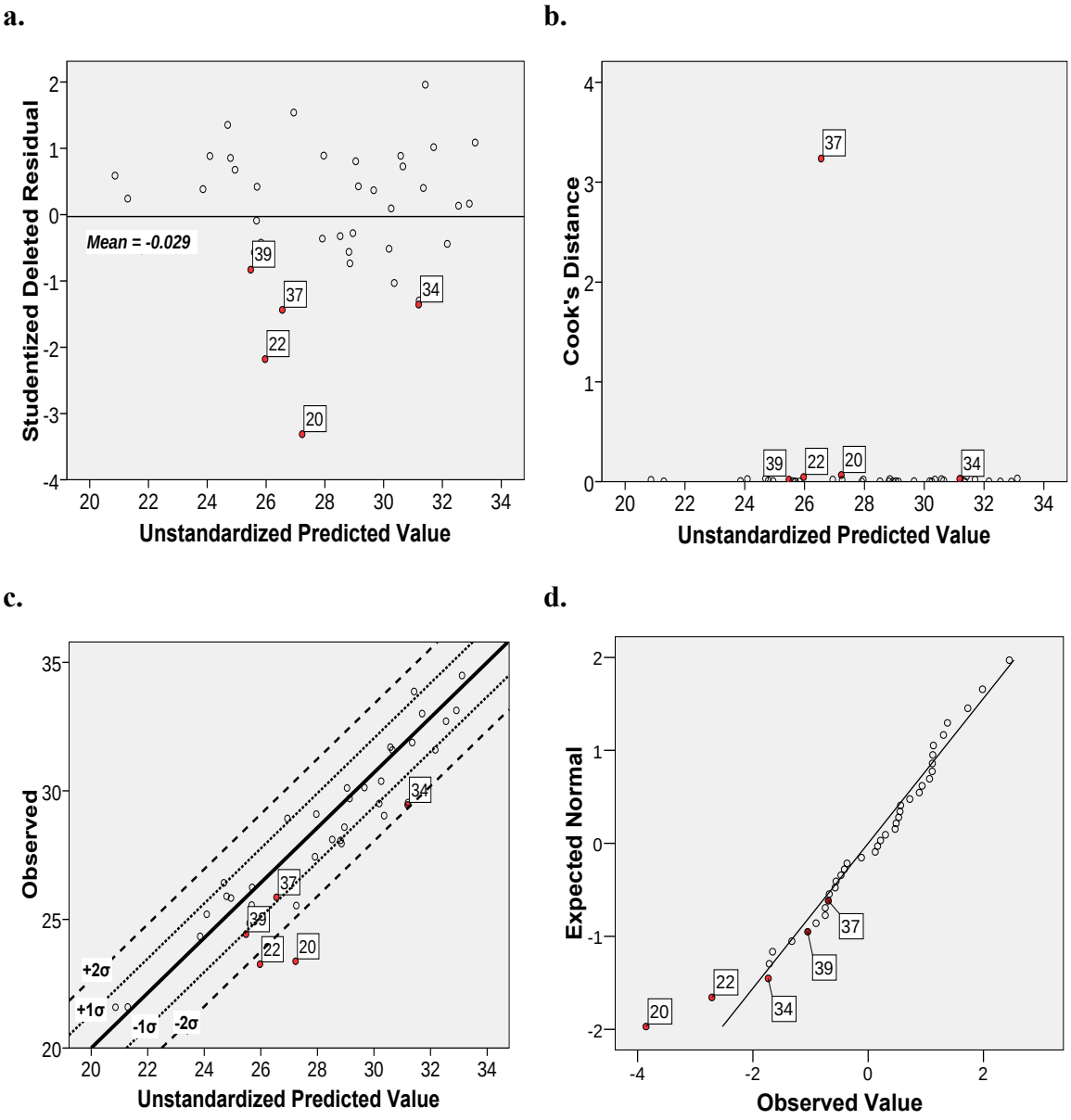

Figure 31. Plots highlighting outliers (in red) for the high resolution dataset of 40 avalanche profiles based on the regression Equation 4.1: (a) plot of studentized deleted residual; (b) scatter plot of Cook's distance and predicted values; (c) observed vs. predicted values; (d) Normal Q-Q plot of unstandardized residual

(case 39) had by far the largest vertical drop (1536.0 m) and longest surface length (3757.2 m). The second outlier (case 37) was also a long slope with the third largest surface length (3005.5 m) and possessed an unusual shape with a significant bend or dogleg in the middle of the avalanche path. The plot with Cook's distance in Figure 31b, demonstrates the measure of change that case 37 would have had on the regression coefficients if the case was omitted from the analysis. The last outlier (case 34) was a short slope avalanche path of 463.6 m vertical drop, but unlike other short slopes in the dataset which had no run-up; this slope had a vertical run-up of 20 m. In Figure 31 c, case 34 lies the furthest away from the regression line after cases 20 and 22. The median run-up of the 35 avalanche paths used for the analysis was 1.1 m. In summary, the outliers that were removed either possessed an exceptionally long vertical drop, involved a run-up or had a lateral bend halfway down the avalanche path. The removal of the outliers resulted in a reduced standard deviation and an improved R^2 value. Diagnostic plots and graphs from the low resolution dataset were the similar to the high resolution dataset with only slight variations in data values.

4.4.2 Tests of normal distribution of the residuals

The alpha-beta regression model assumes a normal distribution of the dataset. The plots and histograms in Figure 32 illustrate the distribution characteristics of the full dataset and reduced dataset for the high resolution DEM data based upon the regression model in Equation 4.1. The plots show that the dataset both before (Figure 32 a, c) and after the outliers were removed (Figure 32 b, d) has normally distributed residuals. The histograms follow a normal distributed with the reduced dataset having a slightly improved normal distribution. The QQ plots indicate normal distribution of residuals. In addition, a 1-sample Kolmogorov-Smirnov test was run on both datasets of n = 35 (p = 0.969) and n = 40 (p = 0.887) and the test distributions for both were normal as indicated by the p-values. Tests from the low resolution DEM dataset were similar to the above with only slight variations in data values.

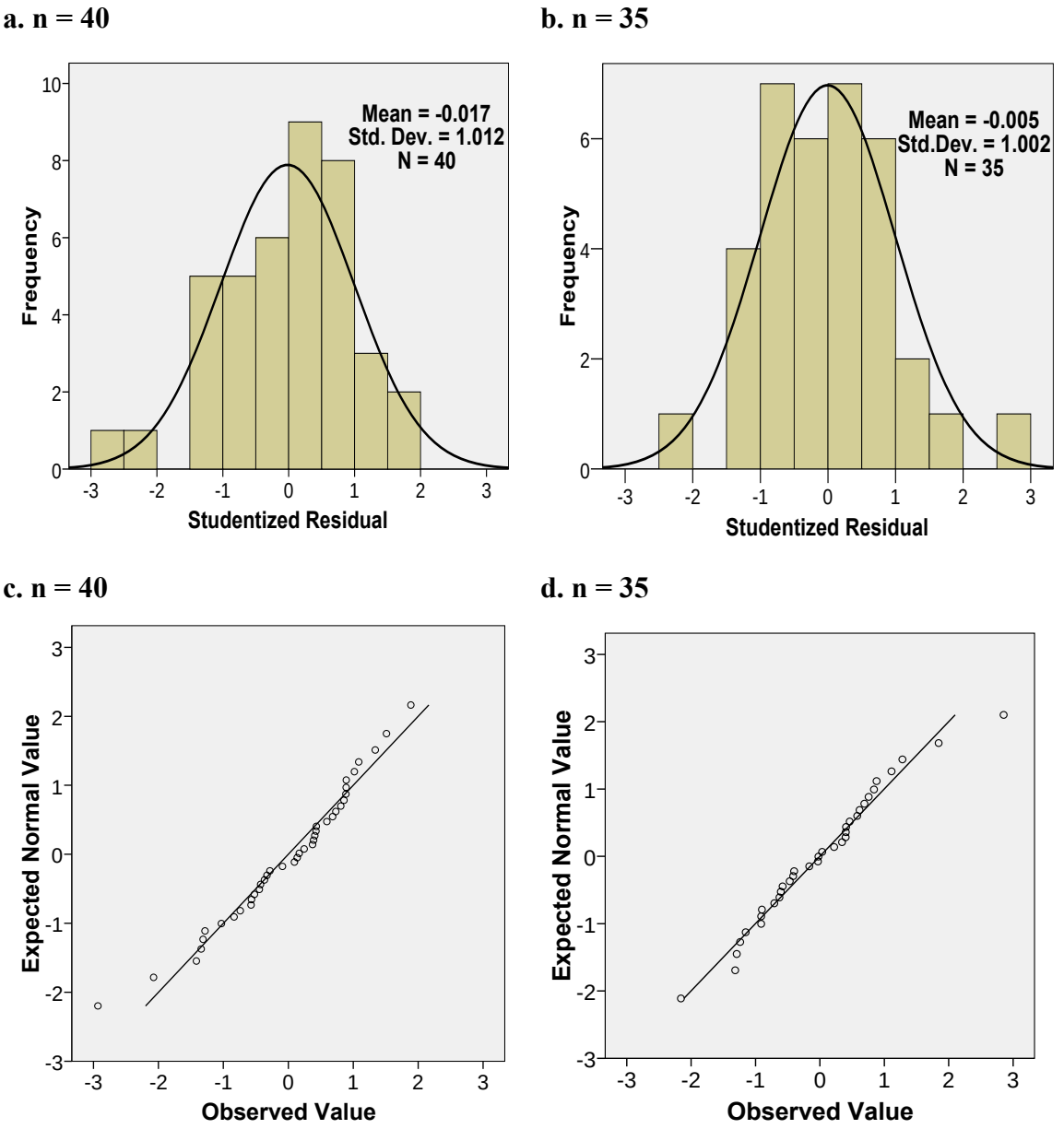

Figure 32. (a) and (b) Histogram of studentized residuals; (c) and (d) QQ plot of studentized residuals

4.4.3 Descriptive statistics of the dataset used for the regression analysis

Table 10 summarizes the mean, standard deviation, median and range of the variables required for the regression analysis for both high and low resolution datasets. In addition

the measured vertical drop and profile surface lengths are included to aid in describing the dataset. Note that the alpha and beta angles for the low resolution dataset slightly underestimate values compared to the high resolution dataset. Theta angles for a shorter slope length appear to be slightly overestimated for the low resolution dataset. The average vertical drop for the avalanche paths is around 940 m with a range of approximately 360 m for the shortest vertical drop to 1375 m for the largest avalanche path. The measure of H, which indicates vertical drop based on the best fitted parabola, has a higher value than the measured vertical drop which is an indicator of the noted elevation difference in the runout zone between the 2^{nd} degree polynomial and the actual ground profile. H values also display greater discrepancy between high and low resolution datasets. Surface lengths range from 740 m to 3115 m for the paths in the dataset. There is little marked difference between the mean high and low resolution values for the y'' topographic parameter. Differences in the $Hy''\theta$ topographic parameter are most likely a result of the difference in H between the high and low resolution datasets. Overall the differences between the values of the topographic parameters for the high and low resolution are minimal and as indicated by the test of means in Table 10 are not showing a significant difference.

Table 10. Descriptive statistics of the topographic parameters used in the regression analysis from both high and low resolution avalanche path datasets

Topographic Parameters	n	Mean		Standard Deviation		Range of Values		2 sample T-test (df = 73, two-tail)	
		Low Res.	High Res.	Low Res.	High Res.	Low Res.	High Res.	*t* - test	*p*-value
α (˚)	35	28.5	28.7	3.2	3.3	21.6 – 34.3	21.7 – 34.5	-0.257	0.798
β (˚)	35	30.4	30.6	3.2	3.3	22.7 – 35.3	22.9 – 35.4	-0.257	0.798
θ (˚)	35	40.1	41.0	5.7	6.0	29.9 – 56.0	31.6 – 58.1	-0.643	0.522
H (m)	35	1165.0	1187.0	357.1	381.3	400.0 – 1760.8	398.2 – 2040.0	-0.249	0.804
y″ (m^{-1})	35	$3.6x10^{-5}$	$3.6x10^{-5}$	$2.4x10^{-5}$	$2.5x10^{-5}$	$6.0x10^{-5}$ – $1.2x10^{-3}$	$5.0x10^{-5}$ – $1.3x10^{-3}$	0	0
H y″ θ (˚)	35	13.9	14.4	4.8	5.1	4.4 – 24.3	4.2 – 24.6	-0.422	0.674
Vertical Drop (m)	35	938.9	941.3	260.6	260.4	359.9 – 1365.4	356.3 – 1375.7	-0.039	0.969
Surface Length (m)	35	2035.5	2044.3	615.4	615.4	740.1 – 3107.9	739.7 – 3117.5	-0.060	0.952

4.4.4 Correlations between the regression model variables

Table 11 and Table 12 below show the correlations between the dependent and independent variables for the high and low resolution datasets. α is the dependent variable while β, H and H y″ θ are the topographic variables used to determine a predicted α angle that indicates the maximum runout extent. As found in the other alpha-beta runout studies previously referenced, β has the strongest correlation with α. For the high and low resolution datasets along the Rogers Pass highway corridor, Hy″θ is also showing a strong correlation with α as well as with β. H does not appear to be strongly correlated with any variable in the model. It is interesting to note that the β and H correlation is significant for the high resolution dataset but not for the low resolution dataset. A concern arising from the cross correlation tables is the strong relationship between β and Hy″θ which may indicate a problem of multicollinearity for the regression model. Multicollinearity impacts the standard errors of the regression coefficients.

Additional topographic variables such as surface length, vertical drop, etc. were not included in the regression analysis due to the small size of the dataset and the desire to develop an alpha-beta regression model that was similar and comparable to that developed in other mountain locations in the world, yet represents the first to be calculated specifically for the Columbia Mountains.

Table 11. Cross correlations for regression parameters from high resolution DEM

		β	H	H y″ θ
α	Pearson Correlation	0.943	-0.210	0.844
	Sig. (2-tailed)	2.6×10^{-17}	0.231	1.9×10^{-10}
	N	35	35	35
β	Pearson Correlation		-0.337	0.828
	Sig. (2-tailed)		0.048	8.6×10^{-10}
	N		35	35
H	Pearson Correlation			-0.408
	Sig. (2-tailed)			0.015
	N			35

Table 12. Cross correlations for regression parameters from low resolution DEM

		β	H	H y″ θ
α	Pearson Correlation	0.944	-0.167	0.834
	Sig. (2-tailed)	1.8×10^{-17}	0.336	4.71×10^{-10}
	N	35	35	35
β	Pearson Correlation		-0.286	0.817
	Sig. (2-tailed)		0.096	2.2×10^{-9}
	N		35	35
H	Pearson Correlation			-0.318
	Sig. (2-tailed)			0.062
	N			35

To determine if there was a significant difference between the *r* values for the high and low resolution datasets, a significance test was performed between the regression parameters. A Fisher's Z transformation (Eq. 4.3) of the correlation coefficient was used to compute a $z(HR)$ and $z(LR)$ for each of the correlation values for both high and low

resolution datasets (Table 13). A z-statistic (Eq. 4.4) was used to test for the difference between the correlation values.

$$z(r) = 0.5 \times \ln\left|\frac{1+r}{1-r}\right| \tag{4.3}$$

Where $z(r)$ is the Fisher's Z transformation, r is the correlation coefficient value from Tables 11 and 12 and ln is the natural logarithm.

$$Z = \frac{z(HR) - z(LR)}{\sqrt{\frac{1}{n_{HR} - 3} + \frac{1}{n_{LR} - 3}}} \tag{4.4}$$

Where Z is the z-statistic, $z(HR)$ and $z(LR)$ are the Fisher's Z transformation values and n is the sample size for high ($_{HR}$) and low resolution ($_{LR}$) datasets.

Table 13. Significance test of cross correlations between high and low resolution datasets (from Table 11 and 12) for the alpha-beta runout regression parameters

Test (H_o:)	$z(HR)$	$z(LR)$	Z	p-value	Decision
$\alpha_{HR}/H_{HR} = \alpha_{LR}/H_{LR}$	-0.213	-0.169	0.178	0.859	Accept
$\alpha_{HR}/\beta_{HR} = \alpha_{LR}/\beta_{LR}$	1.764	1.774	0.036	0.971	Accept
$\alpha_{HR}/Hy''\theta_{HR} = \alpha_{LR}/Hy''\theta_{LR}$	1.235	1.201	0.135	0.893	Accept
$\beta_{HR}/Hy''\theta_{HR} = \beta_{LR}/Hy''\theta_{LR}$	1.182	1.148	0.136	0.892	Accept
$H_{HR}/\beta_{HR} = H_{LR}/\beta_{LR}$	-0.351	-0.294	0.226	0.821	Accept
$H_{HR}/Hy''\theta_{HR} = H_{LR}/Hy''\theta_{LR}$	-0.433	-0.329	0.415	0.678	Accept

Table 13 provides a summary of the tests conducted to determine if there was a significant difference between the high and low resolution correlations. In all cases there was no significant difference detected.

Although there is no test that provides irrefutable evidence that multicollinearity is a problem, there are tests that provide information for making a judgement about the

degree of multicollinearity (Berry and Feldman, 1990). From Tables 11 and 12, high bivariate correlations (typically > 0.80) may not always reflect a multicollinearity problem, thus collinearity statistics were generated for regression parameters from both the 35 and 40 sample datasets that included calculating tolerance ($1 - R^2$) and variance-inflation factor (VIF) values (Table 14). The tolerance value is determined whereby the variable being considered is the dependent variable in the regression analysis and all other variables are used as independent variables (Miles and Shevlin, 2001). If tolerance is < 0.2 a problem with multicollinearity is indicated. SPSS uses a tolerance value of ≤ 0.0001 to cutoff variables for regression analysis. VIF is the reciprocal of tolerance and if it is high it indicates high multicollinearity. Values above 4 are generally used as an arbitrary cutoff to suggest a multicollinearity problem (Miles and Shevlin, 2001). In Table 14, the tolerance and VIF values are both indicating that multicollinearity is not a severe problem for the datasets. Increasing sample size or dropping variables are possible options to offset the impact of multicollinearity (Berry and Feldman, 1990).

Table 14. Collinearity statistics for the regression parameters

	Dataset (n = 40)		Dataset (n = 35)	
Parameter	Tolerance	VIF	Tolerance	VIF
H y″ θ	0.265	3.771	0.296	3.376
H	0.779	1.284	0.834	1.199
β	0.306	3.272	0.315	3.176

4.5 Methods

Avalanche centrelines and maximum runout positions were digitized based upon expert knowledge from the top of the starting zone to the maximum observed runout position based on the 40 year historical record. Digitized linework was referenced to both the high and low resolution DEM data. ArcGIS® v 9.2 was used to extract relevant coordinate points into a spreadsheet to perform the calculations required for the regression model.

4.5.1 Avalanche profiles and determining the model of best fit

Determining the model of best fit for each of the avalanche profiles was essential for determining the curvature and vertical displacement variables for the alpha-beta runout model. Figure 33 highlights the DEM avalanche profiles used for the regression model calculations. Many of the profiles exhibit a "hockey-stick" shape as discussed in Jones and Jamieson (2004) where there is an abrupt slope change in the runout zone as the slope reaches the alluvium in the valley bottom.

Each topographic avalanche profile was fitted with 2nd and 4th degree polynomial functions to derive a profile of best fit (Figure 34). Both functions have high R^2 values and small coefficients. The 2nd degree function resulted in high R^2 values of at least 0.993 for the profiles; however, when the 2nd degree function was plotted on a graph it was apparent that the 2nd degree function did not accurately represent the lower portion of the DEM avalanche profile. For example, in Figure 34, the avalanche profile for path A is represented with a solid black line. The 2nd and 4th degree polynomial functions are indicated respectively in dashed and dotted lines. It was apparent that the second degree function, although it had a high R^2 value, did not represent the bottom of the avalanche profile as well as the 4th degree function. The same issue was observed for the low resolution set of avalanche profiles. These findings correspond to those in Furdada and Vilaplana (1998), who found a similar problem fitting a 2nd degree function in the lower portion of the runout for some of their DEM profile dataset in the western Catalan Pyrenees in Spain. Despite the high R^2 value for the 2nd degree function, the 4th degree polynomial function provided a statistically significant better fit than the 2nd degree polynomial function. Due to this finding, the author decided to test H and $Hy''\theta$ variables calculated on the 2nd degree polynomial as well as H and $Hy''\theta$ from the better fitting 4th degree polynomial in the regression model. Originally, Lied and Bakkehoi (1980) used a 4th degree function to describe the terrain profile of the avalanche path but dropped it in favour of using a 2nd degree function as it appeared to fit their data just as well as the 4th degree function. The difference in fit between the 2nd and 4th degree polynomials is further analyzed in Appendix C.

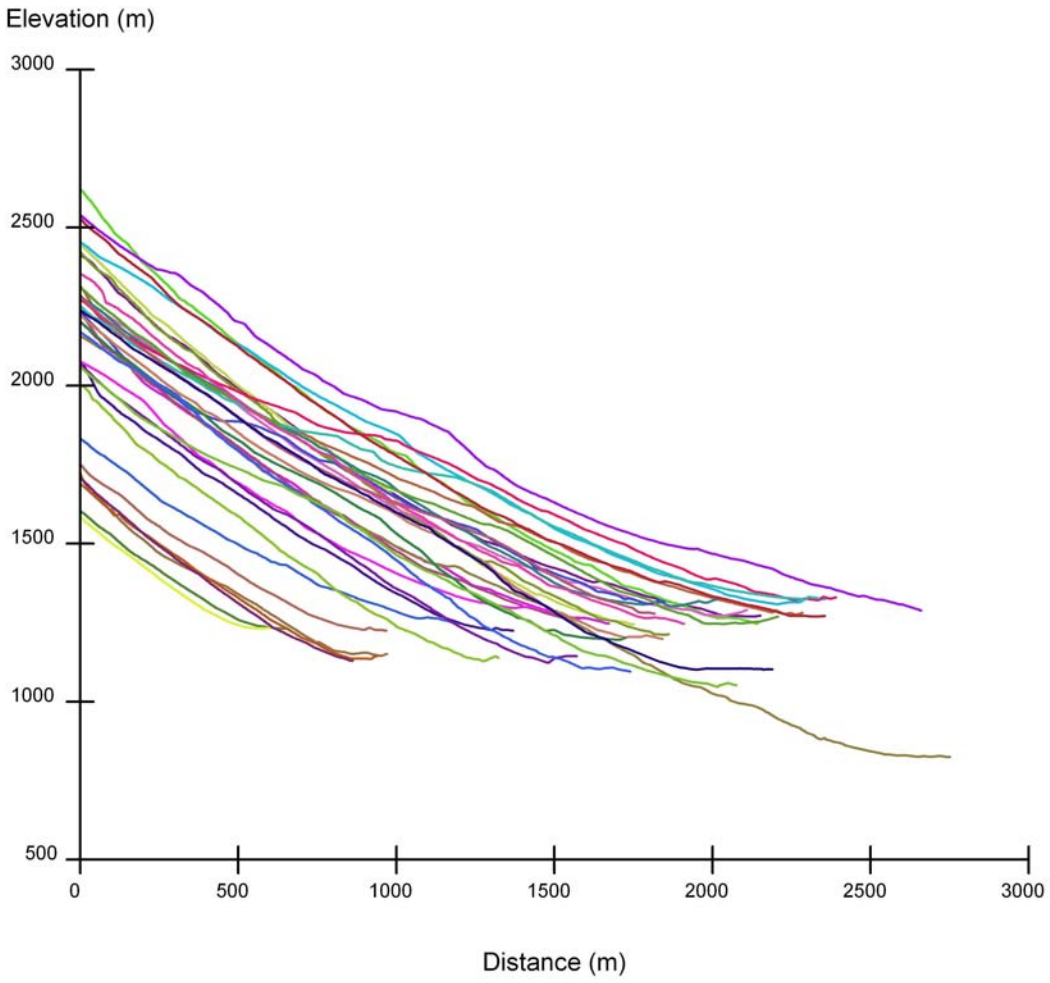

Figure 33. Snow avalanche profiles of the 35 paths used to develop the alpha-beta runout model for Glacier National Park. Each coloured line indicates the elevation of the expert identified avalanche path from starting point to the maximum observed runout distance in the valley bottom.

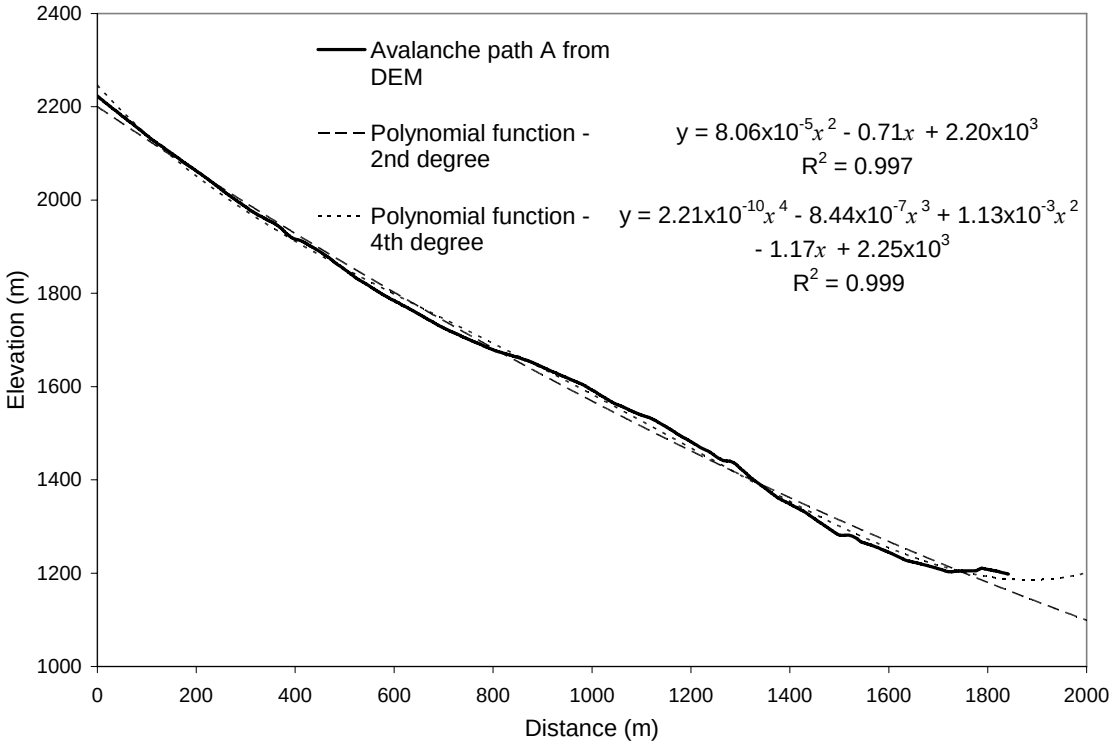

Figure 34. Avalanche profile for path A with best fitted 2nd and 4th degree polynomials. 4th degree polynomial reveals a better fit than the 2nd degree in the runout zone

4.5.2 Alpha-beta runout model results

The regression model was based on the 35 avalanche profiles for both high and low resolution datasets. The variables of β, H and Hy″θ were used to determine a regression equation for $\hat{\alpha}$. In addition, a simplified formula based on only the β parameter was developed as has been common practice in other studies. Further significance tests were performed to determine if there was any difference between the equations derived from the high and low resolution datasets. This included a modification of the β point variable where the definition was changed to indicate a point on the avalanche profile where the slope reached 24˚ (instead of 10˚) in the runout zone.

An initial analysis of the dataset through the regression model revealed that the constant value was not significant. This corresponds to findings from some other studies where the constant value for the alpha-beta regression model has been identified as not significant and dropped (Johannesson, 1998; McClung and Mears, 1991; McClung et al., 1989). Thus the model was run again, forcing the intercept through the origin and these results are presented below. The final step was to validate the model results using a statistical procedure known as leave-one-out (LOO) cross-validation.

The results for the three predictor model forced through the origin for high and low resolution datasets are as follows (where R^2 is the coefficient of determination and s is the standard error of estimation):

<u>High Resolution:</u>

$$\hat{\alpha} = 0.800\beta + 0.00142H + 0.165Hy''\theta \quad (4.5)$$

$R^2 = 0.923$, s = 0.941°, n = 35

where the *p*-values for each parameter are:

β: $p = 3.7\text{x}10^{-21}$, H: $p = 0.002$, Hy″θ: $p = 0.002$

<u>Low Resolution:</u>

$$\hat{\alpha} = 0.826\beta + 0.00127H + 0.131\ Hy''\theta \quad (4.6)$$

$R^2 = 0.919$, s = 0.939°, n = 35

where the *p*-values for each parameter are:

β: $p = 3.8\text{x}10^{-22}$, H: $p = 0.007$, Hy″θ: $p = 0.011$

The three predictor regression models as expressed in the equations above indicate a strong predictive ability of the topographic parameters used as evidenced by the high R^2 values. Figure 35 shows a plot of the predicted vs. observed α values for the high resolution dataset (Eq. 4.5).

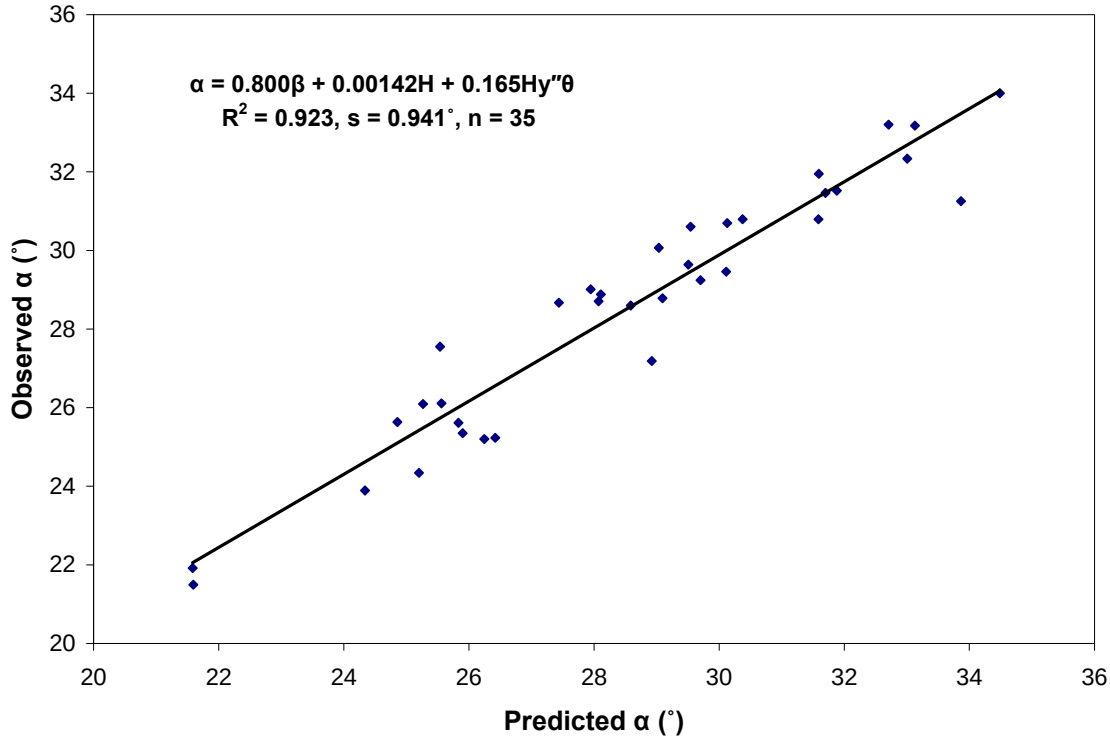

Figure 35. Regression analysis of the high resolution dataset using three predictors

The 3 predictor alpha-beta runout model has been simplified in other countries based on the strength of the relationship between alpha and beta. Due to the potential cross-correlation of Hy″θ with β (Table 11 and 12) and only a slight improvement the fit of the model, Hy″θ and H are dropped and a β only model is used for the dataset. As well, a simplified regression equation offers an ease of use in developing GIS applications to automate mapping of runout in the backcountry. The equations follow for the two datasets:

<u>High Resolution:</u>

$\hat{\alpha} = 0.933\beta$ (4.7)

$R^2 = 0.889$, s = 1.098˚, n = 35

Where the significance value for β is: $p = 5.2 \times 10^{-50}$

Low Resolution:

$\hat{\alpha} = 0.934\beta$ (4.8)

$R^2 = 0.891$, s = 1.051˚, n = 35

Where the significance value for β is: $p = 1.5\text{x}10^{-50}$

To test if there was a significant difference between the regression coefficients for the high and low resolution regression models for the study area, Equation 4.9 was used (Paternoster et al., 1998). As indicated by the test of the coefficients in Table 15 and Table 16, there was no significant difference between the coefficients and hence there is no significant difference between the regression equations derived for the high and low resolution datasets where the intercept is forced through the origin.

$$Z = \frac{b_1 - b_2}{\sqrt{SEb_1^2 + SEb_2^2}} \tag{4.9}$$

Where b_1 and b_2 represent the coefficients for the respective high and low resolution regression equations and SEb_1 and SEb_2 represent the standard error measures for the coefficients being tested. If $|Z|_{calc} < Z_{.025}$ accept H_o and if $|Z|_{calc} > Z_{.025}$ reject H_o.

Table 15. Comparison of regression coefficients for high and low resolution DEMs (Eqs. 4.5 and 4.6)

Parameter	High Resolution		Low Resolution		*t*-value	*p*-value
	Coeff.	Std. Err.	Coeff.	Std. Err.		
β	0.800	0.036	0.826	0.034	0.525	0.601
H	0.00142	0.00044	0.00127	0.00044	0.245	0.807
H y˝ θ	0.165	0.049	0.131	0.049	0.491	0.625

Table 16. Comparison of regression coefficients for high and low resolution DEMs (Eqs. 4.7 and 4.8)

Parameter	High Resolution		Low Resolution		*t* -value	*p*-value
	Coeff.	Std. Err.	Coeff.	Std. Err.		
β	0.933	0.00604	0.934	0.00582	0.119	0.906

The equation for the β_{24} only regression model with β at 24˚ and an intercept forced through the origin follows for the two datasets:

<u>High Resolution:</u>

$\hat{\alpha} = 0.878\beta$ (4.10)

$R^2 = 0.865$, s = 1.211˚, n = 35

where the *p*-value for β is: $p = 1.5 \times 10^{-48}$

<u>Low Resolution:</u>

$\hat{\alpha} = 0.881\beta$ (4.11)

$R^2 = 0.870$, s = 1.152˚, n =35

Where the *p*-value for β is: $p = 3.3 \times 10^{-49}$

The regressions using β_{10} show a higher R^2 and lower standard error of estimation than the regressions using $\beta_{24,}$ which are not analyzed further.

Table 17 presents an analysis of the MSE (mean square error) values comparing the average squared difference between observed alpha values to the predicted values for the 35 avalanche paths in the high resolution dataset. The 3 predictor regression equation (4.5) provides a slightly better fit than the beta only regression Equation 4.7. However, Equation 4.5 is problematic due to the potential of multicollinearity. The least amount of measured difference is found in elevation from the different regression equations.

Table 17. Analysis of MSE values for the predicted alpha from the regression model equations and average horizontal and elevation distance from the observed alpha as measured on the DEM profile.

Equation	MSE	Average distance from observed (m)	Average elevation distance from observed (m)
3 predictor model (Equation 4.5)	0.8˚	51.4	7.6
Beta only model (Equation 4.7)	1.2˚	57.9	8.0
β_{24} model (Equation 4.10)	1.4˚	79.0	8.9

The average difference between the beta only regression (Eq. 4.7) and 3 predictor model (Eq. 4.5) alpha values is less than 0.5˚. With an average path height of 950 m and average alpha of 28.5, a 0.5˚ difference results in a distance of just under 40 m.

4.6 Validation

In order to validate the alpha-beta regression models, a procedure of leave-one-out (LOO) cross-validation, was used to test the high resolution dataset regression equations with β, H and Hy″θ as predictors and the β-only regression models. The "Leave-One-Out" (LOO) cross-validation method involves calculating the regression model without one of the observations and repeating for each subsequent observation. A Mean Squared Error (MSE) was computed by determining the average of all squared differences between the original regression model and each of the LOO observations (Wilks, 1995).

Software from Schenley Park Research Inc., Vizier, was used to facilitate the LOO analysis (Schneider et al., 1997). The error estimations for the regression equations are in Table 18. The three sets of error estimations indicate that in all instances the regression model with the least amount of error is full three predictor model (Eq. 4.5).

Table 18. Leave-one-out cross-validation error estimations for the alpha-beta runout model equations

	3 predictor (Eq. 4.5)	Beta only (Eq. 4.7)	β_{24} (Eq. 4.10)
MSE	1.201	1.294	1.576
Mean Absolute LOO-error	0.890	0.945	1.029
RMS LOO-error	1.096	1.138	1.255

With the process of validation completed using the LOO cross-validation method, two examples show the application of the equations to an avalanche path in the highway corridor and an avalanche path in the backcountry.

4.7 Example of applying the three predictor (Equation 4.6) to a highway avalanche path

The next step was to apply the regression model to a selected avalanche path in the highway corridor (referred to as avalanche path B) that had not been used to generate the equations to compare the model's prediction with an observed maximum runout. This path was selected based on a known maximum runout point from the historical database. Avalanche path B is located on the west side of Rogers Pass.

In order to determine the location of the predicted runout maximum ($\hat{\alpha}$) on an avalanche profile, the intersection must be determined between the line starting at the top of the avalanche profile and traveling downwards at the predicted alpha angle ($y = mx + b$) to the point on the DEM profile. Determining this maximum runout point represents a special challenge as the angle is not a simple straight line shot down from the top of the mountain (such as could be solved in GIS with a simple line-of-sight function) but rather the avalanche profile curves and bends laterally down the slope. Determining the predicted maximum runout was accomplished on profile graphs where the differing alpha predicted equation lines, as derived from the previous regression model equations, were plotted and intersected with the DEM profile. The intersection points of these lines were

determined using the calculus functions in Advanced Grapher software (Alentum Software Inc., 2005) and then transferred to GIS to be mapped.

Using the low resolution data (as no high resolution data was captured for this area) the α observed for avalanche path B, based on the historical database and verified by the avalanche expert, is 23.7˚. In Figure 36, avalanche path B is shown with the starting zone highlighted at the top of the path, the avalanche path outline and the centreline of the avalanche profile. The observed maximum runout has a horizontal distance of 2936.0 m and elevation of 939.1 m. As presented in Table 19, the $\hat{\alpha}$ predicted (23.4˚), using the 3 predictor equation (4.6), intersected with the DEM profile resulting in a horizontal distance of 2979.3 m and elevation of 935.8 m. The difference between this alpha predicted and the observed alpha is 0.3˚ and within the standard deviation of 0.941˚. This leaves an overestimate of a 43.3 m horizontal distance and a 3.3 m elevation drop as measured on the DEM profile. At the bottom of the image in Figure 36, in the runout zone, the profile centreline slightly extends the 43.3 m past the expert identified runout maximum. It is important to recognize that this particular path has an avalanche defence mechanism of piled up mounds that act to shorten the length of the avalanche debris runout.

Table 19. Predicted alpha and maximum runout ground positions (horizontal distance and elevation) for avalanche path B

Equation	$\hat{\alpha}$ Predicted (˚)	Distance (m)	Elevation (m)
3 predictor model (Equation 4.6)	23.38	2979.3	935.8
Beta only model (Equation 4.8)	23.15	3049.4	922.4
β_{24} model (Equation 4.11)	22.68	3140.8	913.8
Alpha observed	23.68	2936.0	939.1

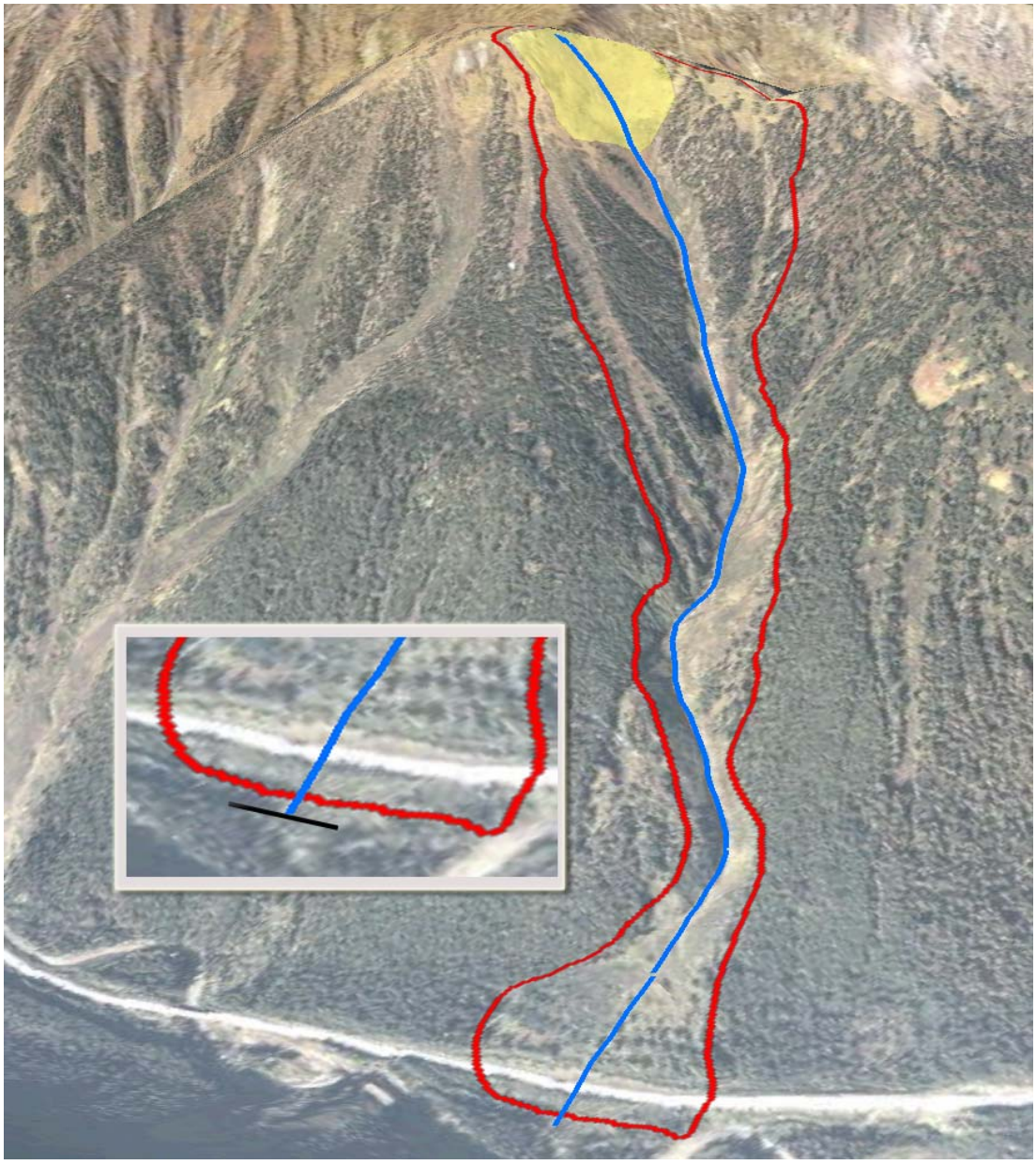

Figure 36. Avalanche path B along the Trans Canada highway corridor. Dark centreline highlights the path profile. Starting zone is identified at the top of the path with light grey shading. The bottom portion of the profile centreline extends slightly past the expert identified maximum runout showing the predicted maximum runout from the alpha-beta regression model (inset)

4.8 Example applying the beta only (Equation 4.7) in the backcountry

The alpha-beta regression equation was also applied to an avalanche path in the backcountry. In Figure 37, the avalanche path is delineated including a profile centreline. The beta point is shown along the avalanche centreline and the calculated maximum runout is marked by an X at the furthest reach of the avalanche centreline. The avalanche path outline is based on vegetation to estimate the avalanche path lateral extents. For ease of calculation in the backcountry the simplified equation (4.7) using beta as the only predictor was used to calculate maximum runout distance.

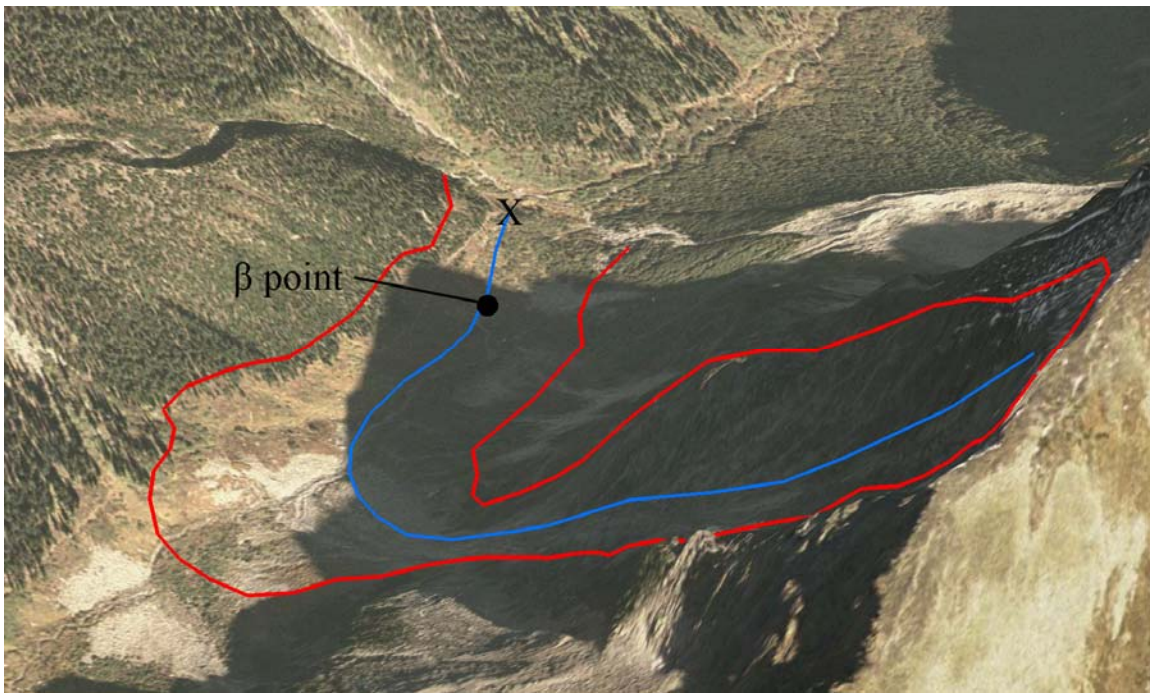

Figure 37. Avalanche path in the Connaught Creek backcountry skiing area. The β point is identified by the dot along the centreline profile where the slope declines to 10˚. Maximum runout is represented by the furthest reach of the avalanche centreline and marked with an X.

4.9 Discussion

One contribution of this study is the development of an alpha-beta regression model that is not only specific to the Columbia Mountains but also is appropriate for avalanche paths

controlled by explosives. Other avalanche controlled transportation corridors in the region may be able to utilize the equations developed to predict runout maximums relevant to their operations. The derived equation need not be limited to transportation corridors as runout maximums can also be estimated for the backcountry. However, for recreational purposes in mapping backcountry runout a 10 year return period is acceptable as the exposure risk for recreationists (Canadian Avalanche Association, 2002a), especially if recreationists heed avalanche bulletins and practice safe backcountry travel. The distance between the 10 and 40 year estimates may not physically involve that much difference on the ground and be even less evident on a map. Alternatively, confidence levels or standard deviations could be used to indicate varying levels of non-exceedence along an extended runout as has been attempted in Europe (Barbolini and Keylock, 2002).

The two compared DEM resolutions did not significantly affect the alpha-beta regression equations. This could be a combined result of using the same control data for the two datasets and is likely further impacted by the fact that beta is the strongest predictor in the regression models and represents an average angle (determined from top and bottom coordinate locations) that is not strongly influenced by variations in DEM resolution. Further, H and $Hy''\theta$ based on 4^{th} or 2^{nd} degree polynomial functions derived from the points extracted along the avalanche profiles provides a generalization of the curvature of the avalanche profile which may not reflect small variations in terrain between the DEM datasets.

For traditional alpha-beta regression models developed through field survey, the top of the avalanche path is collected from topographic maps and is typified by a low resolution of data points. In contrast, the runout is more accurately surveyed in the field resulting in a difference of resolution between the upper and lower part of the avalanche profile. This strategy of plotting profiles may result in a 2^{nd} degree polynomial function fitting the dual resolution profiles better than the 4^{th} degree function for the equations developed in using this approach. For this paper, the 2^{nd} degree polynomial function was used for

determining H and Hy″θ parameters as similar parameters from the 4th degree polynomial were not significant for the regression model.

In estimating the position of runout values using a predicted alpha angle, the DEM profile line will yield a more accurate result than a fitted 2nd order polynomial. As discussed in appendix C, the 2nd degree polynomial does not accurately represent the runout portion of the avalanche profiles, an alpha value positioned on the 2nd degree polynomial can result in a placement that is far removed from the actual observed maximum runout extent. If necessary the 4th degree polynomial provides a better estimate of the DEM avalanche profile line and could potentially be used to estimate maximum runout position if the DEM profile coordinates were unavailable.

The simplified runout equation developed for this study provides interesting comparison with equations from other countries. Similar to other alpha-beta runout models derived worldwide, alpha is correlated more strongly to beta than to other predictor variables for this dataset and the 3 predictor formula provides only a slight improvement in the estimation of maximum runout. Table 20 provides a summary of the simplified alpha-beta runout equations in use from around the world (introduced in chapter two) and includes the equation derived for this thesis.

McClung et al. and MClung and Mears, (1991; 1989), indicate that extreme runout from mountain ranges vary depending upon the terrain properties of the different ranges and are irrespective of snow climate. The alpha-beta model from this research matches the model derived for the Rockies/Purcells. The alpha-beta runout models from the Columbia Mountains, the Rockies/Purcells and the runout model from Norway (where extreme runout values have been removed) are virtually identical. The data from Canada and Norway are distinguished by steeper slopes, a greater vertical drop and shorter runout than the other mountain ranges in Table 20. This corresponds to findings from McClung et al., (1989) where a scale effect was noticed where higher vertical drop, *H*, produces shorter runout. To address the scale effects a partitioning of data into elevation categories

to determine distinct runout models may be one possible solution as suggested by Nixon and McClung (1993). The Coast Mountains in Canada, the Catalyn Pyrennes, and the Western Norway dataset stand out as possible exceptions to the scale effect; where large mean vertical displacement results in longer runout than other mountain ranges with similar mean vertical displacement. However, due to the scale effects within the individual datasets, differences in how the data was collected and estimations of return period it is very difficult to compare the runout models from the different mountain ranges. For the runout model produced with the dataset in this research it is recommended to only apply this model in mountain ranges with similar terrain and a similar range of vertical displacement values to achieve runout estimations that are based on a 40 year historical database.

Table 20. Comparison of alpha-beta runout models. Data Sources: (Furdada and Vilaplana, 1998; Johannesson, 1998; Lied et al., 1995; McClung et al., 1989; Mears, 1988; Nixon and McClung, 1993)

Country	Relation	R^2	*S*	*N*	*Mean α*	*Mean H (m)*	*Mean β*
Norway	$\hat{\alpha} = 0.93\beta$	0.86	2.1˚	192	n/a	n/a	n/a
Austria	$\hat{\alpha} = 0.946\beta - 0.83$˚	0.92	1.5˚	80	n/a	n/a	n/a
Iceland	$\hat{\alpha} = 0.85\beta$	0.52	2.2˚	44	n/a	n/a	n/a
Canada:							
Columbia Mountains	$\hat{\alpha} = \mathbf{0.93\beta}$	0.89	1.1˚	35	28.5˚	946	30.6˚
Rockies/Purcells	$\hat{\alpha} = 0.93\beta$	0.75	1.75˚	126	27.8˚	869	29.8˚
Coast Mountains	$\hat{\alpha} = 0.90\beta$	0.74	1.70˚	31	26.8˚	903	29.5˚
Catalan Pyrenees	$\hat{\alpha} = 0.86\beta + 1.05$˚	0.75	1.98˚	64	24.7˚	753	27.3˚
Alaska	$\hat{\alpha} = 0.86\beta$	0.58	n/a	52	25.4˚	765	29.6˚
Colorado	$\hat{\alpha} = 0.80\beta$	0.50	n/a	130	22.6˚	641	27.4˚
Sierra Nevada	$\hat{\alpha} = 0.76\beta$	0.60	n/a	90	20.7˚	590	26.1˚
Western Norway	$\hat{\alpha} = 0.90\beta$	0.87	n/a	127	29.4˚	827	32.6˚

In Canada, the traditional method for determining alpha-beta regression models is to conduct field surveys. GIS offers another strategy for collecting data on those avalanche slopes that may be difficult to survey in the field. In Norway the runout mapping is prepared in the lab first using GIS and supplemented by subsequent ground-truthing in the field combining the strengths of both computer and field methods (Lied et al., 1989). Further work would be to completely automate the process in GIS as well as compare maximum runout results from the alpha-beta model with dynamic models.

4.9.1 Potential sources of error

There are several potential sources of error including: characteristics of the avalanche profiles, avalanche control in the model-building dataset, the historical database and limitations of photogrammetry. The highway corridor dataset that is used to generate the regression models is controlled with explosives and, as a result, may underestimate runout extent when the derived equation is applied to the backcountry. The control activity is likely to encourage more frequent avalanching and thus larger avalanche events with an increased runout are less likely. As well, the historical database of maximum runout captures only 40 years of data, thus avalanche events with longer return periods may not have been recorded.

Certain characteristics of the avalanche profiles need to be recognized such as the presence of avalanche defence structures and, to a limited degree, barriers like the rail and road line. These barriers may reduce the predicted alpha equations. Other characteristics include overlapping runout profiles with the same stopping point whereby an avalanche path may have more than one avalanche profile with different starting zones but a similar runout and recorded maximum extent. In addition, the avalanche paths along the highway corridor are in a larger valley with a broader and flatter valley bottom than the backcountry valleys. This has the potential to reduce the underestimation of backcountry runout maximums.

Two main issues in regards to photogrammetry interpretation and processing are the difficulty in identifying features in areas of shadow in air photos and in regards to the same control data being used to georeference air photos for both the 25 m dataset and the 5 m dataset. Mountains cast shadows, particularly on north facing slopes. Although every attempt was made to capture DEM data from a variety of aspects, the shadowing effect made data capture impossible on some north facing slopes and thus may bias the data used to generate the regression model.

Differences in elevation values are reduced between the 5 m and 25 m datasets since the same control was used to reference the air photos. This British Columbia control data was the best available georeferencing. Yet the point of creating the 5 m DEM was to increase the level of terrain detail from the 25 m dataset. Other resolution issues include the maximum runout extents as recorded in the historical database which was often measured in extent beyond the highway and were not measured to within 5 m accuracy.

The following chapter continues the analysis of topographic parameters to model avalanche terrain in a backcountry area. A GIS algorithm is developed to utilize input DEM and forest cover data to define areas of Simple, Challenging and Complex avalanche terrain. As part of the process, the simplified beta-only runout equation derived from well-known avalanche observations along the highway corridor, is used to indicate maximum runout position.

Chapter Five: Snow avalanche hazard mapping using Geographic Information Systems to determine avalanche terrain exposure

5.1 Introduction

In 2004 Parks Canada developed an Avalanche Terrain Exposure Scale (ATES) based upon terrain and land cover characteristics to identify avalanche susceptible areas in the backcountry (Statham et al., 2006b). Using a defining set of terrain based criteria, avalanche professionals designate Simple, Challenging and Complex avalanche terrain. ATES was developed to aid backcountry users in reducing risk especially for trip planning and to restrict the areas within which custodial groups lead winter trips in National Parks. The exposure scale relies upon terrain and ground cover parameters that are possible to model within a GIS. Currently, avalanche professionals have collectively reviewed over 200 trips within National Parks and applied a rating to each based upon their expert knowledge and familiarity of the areas. ATES is also used as part of the Avaluator trip planner that takes into account the current avalanche bulletin (Haegeli and McCammon, 2006). Varying levels of caution are recommended depending upon the level of avalanche danger and the type of terrain the user is travelling in.

GIS has been used in combination with Digital Elevation Model (DEM) and land cover data for mapping avalanche hazard in mountainous regions around the world. Many hazard mapping techniques use solely terrain-based parameters in GIS to identify avalanche starting zones or potential release areas and for snow avalanche runout calculations. For example, in Switzerland, potential release areas are identified using an automated procedure in an Avalanche Hazard Mapping System (AHMS) that is based primarily on a GIS that integrates DEM and land cover information such as slope, proximity to ridges, plan curvature and area (Gruber, 2001; Haeberli et al., 2004; Maggioni and Gruber, 2003). For runout calculations both one and two dimensional flowing avalanche models have been integrated into the Swiss AHMS to provide information on runout distance, flow velocities and impact pressures of snow avalanches

(Christen et al., 2002; Christen et al., 2007; Gruber and Bartelt, 2007; Gruber et al., 1998). In Iceland, Tracy (2001) similarly uses topographic features in GIS to identify start zones and runout numerical models to generate maps to reveal hazard zones. The Japanese Geological Survey used DEM data in GIS to assess avalanche danger for the starting zones of Mt. Iwaki; the key variables were slope, aspect and vegetative cover. Further numerical analysis using the Swiss flow model aided in the determination of avalanche flow potential (Yamada et al., 2002).

Statistically based snow avalanche runout calculations estimating maximum runout and identifying starting zones with topographic parameters have also been used to facilitate avalanche hazard mapping with GIS (Furdada and Vilaplana, 1998; Lied et al., 1989; Toppe, 1987). In chapter four, a simplified regression model suitable for the Columbia Mountains was derived based upon observations from known avalanches along the Trans Canada Highway corridor. This formula is used to calculate runout in the Asulkan drainage backcountry area for this chapter.

The simplified form of the alpha-beta regression model for Glacier National Park, Canada using high resolution DEM data is (refer to chapter four):

$$\hat{\alpha} = 0.933\beta \tag{5.1}$$

Where $\hat{\alpha}$ is the predicted maximum runout position and β is the angle from the top of the avalanche to a point on the avalanche profile where the slope reaches 10˚ or less.

This chapter describes a process of using a GIS algorithm to create an avalanche terrain hazard map by using a reduced set of topographic parameters from Parks Canada's ATES and statistical runout modeling to determine maximum runout. Statistical snow avalanche runout modeling is used in preference to dynamic runout models as information on impact pressures and avalanche velocities is not required for an ATES based classification and the input parameters required for dynamic models are difficult to estimate, especially for remote areas in the backcountry. A systematic process takes

topographic parameters that include: land cover, slope incline, slope curvature and starting zone characteristics in combination with runout extents to develop a GIS-ATES classified map that shades terrain within the Asulkan drainage backcountry skiing area in Glacier National Park. This is a semi-automated process where most of the procedures are completed in GIS with the exception of the maximum runout calculation. The long term goal is to refine the model and make it a fully automated process. Routing options are demonstrated by using GIS functions to aid in selecting a route to a backcountry hut based on the classified map. Several limitations of the GIS algorithm are that not all ATES terrain based criteria are used and verification is difficult because the scale to which expert ATES is used has not been generally applied to the individual slope level but is taken over a wider context.

5.2 Avalanche Terrain Exposure Scale (ATES)

The Avalanche Terrain Exposure Scale provides a backcountry framework from which to evaluate terrain exposure with the goal of helping recreation users consider avalanche terrain when planning trips. Table 21 represents the technical framework developed for skilled avalanche experts to refer to when considering terrain exposures categories for routes and trips in avalanche terrain. It is a complex task to classify terrain based on the defining factors for the categories of Simple, Challenging and Complex as the criteria for some factors are not mutually exclusive. Criteria which override others for a particular factor are shown in bold italics (Statham et al., 2006b).

Several of the terrain based criteria in Table 21 can be identified in a GIS with a digital elevation model (DEM) and forest cover data. Factors pertaining to: forest density, slope angle, slope shape and runout zone characteristics can be modeled in a GIS. In addition, maximum runout distance can be estimated and mapped based on avalanche path centrelines. The question becomes how systematically to identify these categories in a GIS.

Table 21. Avalanche Terrain Exposure Scale Model v.1/04 (Statham et al., 2006)

	1 - Simple	2 - Challenging	3 - Complex
Slope angle	Angles generally < 30º	***Mostly low angle, isolated slopes >35º***	***Variable with large % >35º***
Slope shape	Uniform	Some convexities	Convoluted
Forest density	Primarily treed with some forest openings	Mixed trees and open terrain	Large expanses of open terrain. Isolated tree bands
Terrain traps	Minimal, some creek slopes or cutbanks	Some depressions, gullies and/or overhead avalanche terrain	***Many depressions, gullies, cliffs, hidden slopes above gullies, cornices***
Avalanche frequency (events:years)	1:30 ≥ size 2	1:1 for < size 2 ***1:3 for ≥ size 2***	1:1 < size 3 ***1:1 ≥ size 3***
Start zone density	Limited open terrain	Some open terrain. Isolated avalanche paths leading to valley bottom	Large expanses of open terrain. Multiple avalanche paths leading to valley bottom
Runout zone characteristics	Solitary, well defined areas, smooth transitions, spread deposits	Abrupt transitions or depressions with deep deposits	Multiple converging runout zones, confined deposition area, steep tracks overhead
Interaction with avalanche paths	Runout zones only	Single path or paths with separation	***Numerous and overlapping paths***
Route options	Numerous, terrain allows multiple choices	A selection of choices of varying exposure, options to avoid avalanche paths	***Limited chances to reduce exposure, avoidance not possible***
Exposure time	None, or limited exposure crossing runouts only	***Isolated exposure to start zones and tracks***	***Frequent exposure to start zones and tracks***
Glaciation	None	***Generally smooth with isolated bands of crevasses***	***Broken or steep sections of crevasses, icefalls or serac exposure***

5.3 Developing a systematic approach for identifying ATES terrain categories in GIS

In a series of interviews with the avalanche experts from Parks Canada who developed the ATES model, the author created the decision tree algorithm in Figure 38 to identify ATES terrain categories in a GIS. The process attempts to reflect the expert thought process in rating avalanche terrain. The interviews were a form of knowledge acquisition with the purpose being to elicit tacit knowledge from the expert and build what is referred to as a decision tree. A reduced set of terrain criteria (slope incline, forest cover, slope curvature and runout zone characteristics) were used to create the algorithm based upon expert prioritization of the most critical terrain factors from the ATES technical model.

Starting with GIS data layers of forest cover and a DEM, slope incline, forest cover, slope curvature and runout zone criteria outlined in Table 21 are successively narrowed down to the Simple, Challenging and Complex terrain categories. Forest cover and slope emerge at the top of the algorithm as key determining factors in identifying avalanche terrain. Slope curvature, runout exposure and avalanche frequency complete the algorithm characteristics used to identify ATES areas. In order to simplify the avalanche terrain mapping in GIS the algorithm integrates similar criteria or omits some of the criteria in the table such as: glaciation, exposure time and route options. For example, start zone density and forest density are somewhat related in that the amount of open terrain is a determining factor. Exposure time and route options are potentially variables that could be added to the algorithm if specified routes were included as a layer of data to be treated in the model using some of the routing and network functions available in GIS. Glaciation is omitted from the algorithm as it is a special consideration for custodial groups. Any travel on glaciers in National Parks by groups under the age of majority requires the presence of a qualified mountain guide and thus by default any glaciated area falls into the “Challenging” ATES category even though it may be flat, have minimal exposure to crevasses and have non-existent exposure to avalanche formation or release. Specific reference to identifying terrain traps, such as gullies and channels was omitted from the algorithm as it was expected that they would be mapped when identifying slope curvature in the GIS.

The choice of the primary parameters of forest cover and slope in the ATES algorithm reflects the key environmental factors that influence avalanche formation. Forest cover inhibits the contributing factors that enhance avalanche formation such as the formation of dry dense snow slabs with underlying weak snow layers that can result in large avalanches. Tree crowns interrupt snowfall in dense forest stands, forest cover reduces snow transport by wind, trees control incoming and outgoing radiation to moderate snow surface temperature and a sufficient density of tree trunks act to stabilize the snowpack (McClung and Schaerer, 2006). Mixed forest cover where trees are more spaced out is not a sufficient deterrent to avalanche formation and release. Slopes in the range of 25˚-60˚ are suitable starting zones for avalanches, with a median value of 39˚for human-triggered avalanches in Canada, whereas, on slopes greater than 60˚ snow releases frequently and spontaneously in small amounts to prevent large avalanche formation. Slopes of less than 25˚ avalanche infrequently (McClung and Schaerer, 2006; Schweizer and Jamieson, 2001).

Slope shape and runout follow forest cover and slope in the ATES algorithm for identifying terrain in GIS. Slope shape can be derived in GIS using a curvature function which identifies plan (cross slope) and profile (down slope) curvature based on DEM data. Curvature is a useful function for recognizing gullies, channels and terrain traps. Runout is distinguished by a slope angle between 0˚ and 25˚ and whether an avalanche path crosses the slope.

Avalanche frequency is the final criterion identified in the algorithm to identify ATES terrain in GIS. In Canada, studies of avalanche frequency related to terrain factors indicate that fracture point incline, avalanche path incline, runout zone incline, vertical drop, path length, starting zone elevation and runout zone elevation are significant contributors (Schaerer, 1977; Smith and McClung, 1997). Avalanche frequency in the GIS algorithm is estimated based upon a combination of runout exposure and upslope contributing area. An assumption is made in regards to avalanche frequency that results

in a default assignment to the avalanche frequency part of the decision tree. The branches that are not used by the algorithm have been greyed-out in Figure 38.

The digital data sets used for the analysis include an enhanced DEM that was created with digital stereo photogrammetry and land cover data that was digitized from an orthophoto mosaic. As described in chapter three, a 5 m resolution gridded DEM was generated by interpolation from stereo digitized breaklines indicating breaks in slope and digitized point data. The enhanced DEM was generated for the popular Asulkan drainage backcountry area in order to produce the GIS-ATES avalanche map. In the fall of 2004, air photos were taken of the study area and subsequently compiled into an orthophoto mosaic. The GIS program ArcGIS® v. 9.2 was primarily used for data input and analysis phases (ESRI, 2006b).

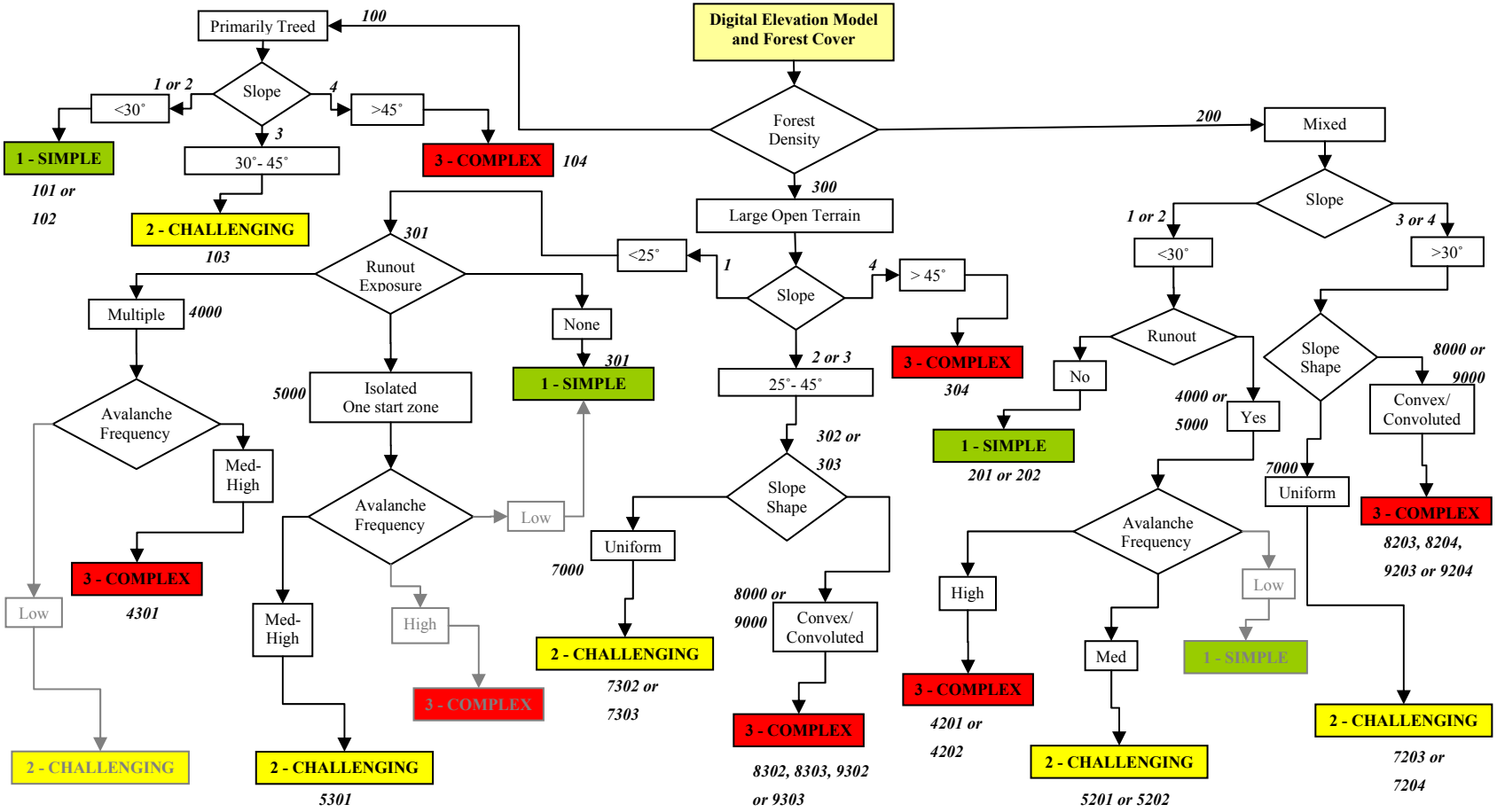

Figure 38. Algorithm for identifying a GIS avalanche terrain exposure based on a reduced set of Avalanche Terrain Exposure Scale topographic criteria. Numbers reflect attribute values for the topographic parameters or a combination of the sum of the attributes from Table 22. Greyed-out portions are where assumptions where made and the path was not followed.

5.4 Applying the algorithm to a backcountry area – the Asulkan drainage

The Asulkan drainage is a popular backcountry skiing area within Glacier National Park that is characterized by a wide valley, avalanche paths, glaciated areas, lower elevation tree cover with bare rock and moraines in the higher elevations. An alpine ski hut attracts overnight ski travelers.

In order to perform the analysis to generate the avalanche terrain map, several data layers needed to be generated using GIS from the source data layers of the orthophoto mosaic and the DEM. The forest cover layer was digitized from an orthophoto mosaic of the Asulkan drainage while topographic information was generated from the DEM. Table 22 details the data layers created from the DEM and orthophoto to isolate the terrain in the Asulkan drainage into ATES categories of Simple, Challenging and Complex. The attribute values are added together for each pixel and are categorized based on the numbers shown in Figure 38.

Table 22. Data dictionary of the layers required for GIS-ATES terrain mapping

Data Source	Data Layer	Attributes	Value
Asulkan Orthophoto	Forest cover	primarily treed	100
		mixed vegetation	200
		open terrain	300
DEM	Slope	0˚- 25˚	1
		25˚- 30˚	2
		30˚- 45˚	3
		>45˚	4
	Planar curvature	≤-3 (gullies)	9000
		-3 to -1.5 (channellized)	8000
		>-1.5 (open slope terrain)	7000
	Runout	multiple paths	4000
		isolated paths	5000

5.4.1 Forest cover

Forest cover information for the Asulkan drainage was digitized into three categories of treed, mixed (less densely treed) and open terrain using aerial photograph imagery flown

in 2004. The categories are defined based upon the criteria indicated in Table 21. Digitizing is a manual process that relies upon the judgement of the operator to classify land cover into designated categories. Government agencies such as the Province of British Columbia use a manual approach for their land inventories. Experienced operators with the BC Ministry of Forests and Range, forest industry and private consultants continually update vegetation cover using digital stereo photogrammetry. Field surveys complement the process to provide a database that contains information on forest cover type, age of the stand and density of the forest canopy as well as many other attributes. Obtaining forest cover information for National Parks and other protected areas in British Columbia can be challenging as the data may not be available. Unfortunately, for this drainage the Provincial forest cover data (Vegetation Resources Inventory) was non-existent. The Asulkan drainage is a relatively small area and much of the higher reaches are bare rock or snow, thus the digitizing of forest cover was not a time consuming process. However for larger areas, computer generated image classifications are an expedient option for categorizing land cover. As an eventual goal of this work is to fully automate the process of identifying ATES terrain in GIS, an automated procedure was explored to classify land cover and compare the results to the manually digitized data layer.

Supervised and unsupervised computer generated image classification techniques are a typical means of identifying land cover. Imagery ranging from satellite data to Simple air photos can be classified automatically by the computer (unsupervised) or with the aid of operator identified “training areas” to produce a supervised classification. The training areas are operator defined samples of the categories of land cover that the operator wants to classify. The results from these classification techniques are hampered by shadowed areas (common in mountainous areas) and problems in distinguishing between land cover with mixed vegetation types. Both supervised and unsupervised classifications were run on the Asulkan drainage image with less than satisfactory results including a misclassification of features in shadowed areas and feature identification problems in areas of mixed or thin forest cover. A different approach was explored for generating an

automated image analysis using hierarchical learning. The purpose of attempting an automatically generated land cover classification for the Askulkan drainage was that if an automated method was derived that produced results matching the manually generated classification, then this automated process could be applied to larger areas with orthophoto coverage that would normally be time consuming to accomplish by digitizing manually.

Hierarchical learning involves the narrowing down of the classification task. Subsequent identification of problems in a previous classification aid in generating a better classification with each following iteration. Figure 39 illustrates the hierarchical learning process developed by using the third party software extension Feature Analyst® that runs in ESRI's ArcGIS® desktop GIS software. Three input training classes were created based on treed, mixed and open terrain categories and combined to form a training data layer. The input image input consisted of three bands: band 1 was the original band 1 from the orthophoto tiff (tagged image file format) image, band 2 consisted of the DEM values, and band 3 was a constant value. By integrating the DEM as an input band in the image (image fusion), shadowed areas were more easily classified into the correct category, such as where the shadowed pixel value from the image failed to represent the correct category. The elevation value was a good indicator to distinguish between open terrain and terrain with vegetation. Foveal representation, a form of visual learning or training for the computer, was used in the hierarchical learning process. Instead of pixel by pixel identification, the foveal representation process takes into account the surrounding composition of the training area as contextual spatial information in order to better classify the image (Visual Learning Systems, 2006). This is particularly helpful in identifying areas with less dense forest cover as bare ground is mixed in with the forest stand. Additional training to add missed features or remove incorrectly classified pixels or false positives refined the classification and post processing cleaned up the results by aggregating together pixels based on size and by smoothing features. The boundary mask layer was a clipping layer that isolated the area of interest within the Asulkan drainage basin.

Figure 40 and Figure 41 display the visual results of the manual digitizing and the hierarchical classification of the orthophoto/DEM image in the Asulkan drainage basin. Based on a visual comparison the results of the classification and digitized data layer are reasonably similar; however, in areas with mixed vegetation of varying height and stand density there is some discrepancy between the automated and digitized classifications. In the area labelled ‘A’ in Figure 40 and Figure 41, the manual operator is identifying a vegetated avalanche path with a forest stand of lesser height and size than the surrounding forest. Regardless of the method of classification used, in order to achieve the best possible forest cover map, field surveys of forest stand heights, widths and species would be required in order to clearly distinguish the mixed vegetation areas. The strength of an automated classification is that it is less subject to operator interpretation and thus may be more consistent over large areas.

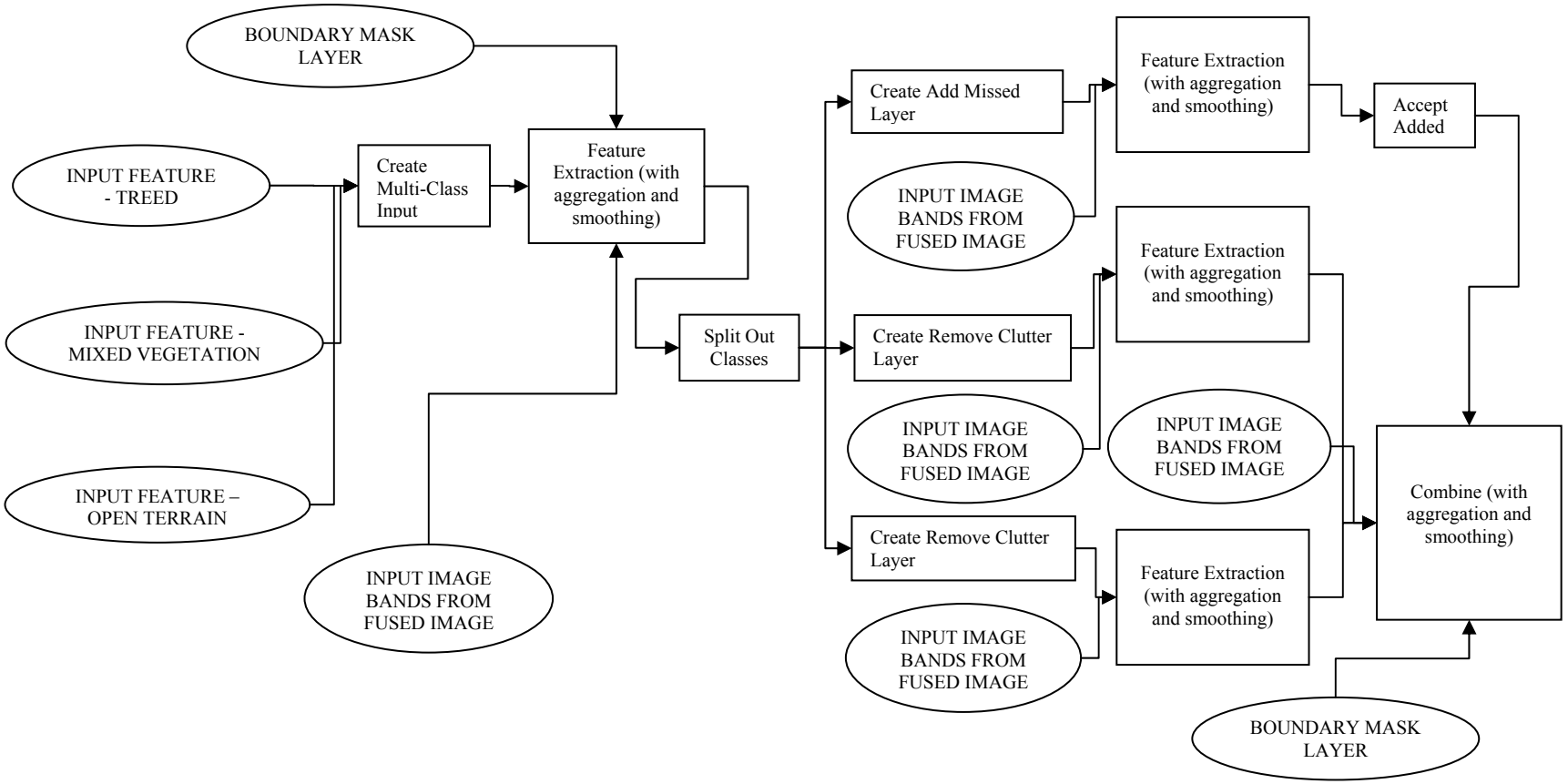

Figure 39. Schematic diagram of hierarchical image classification and methods used to produce a map of land cover

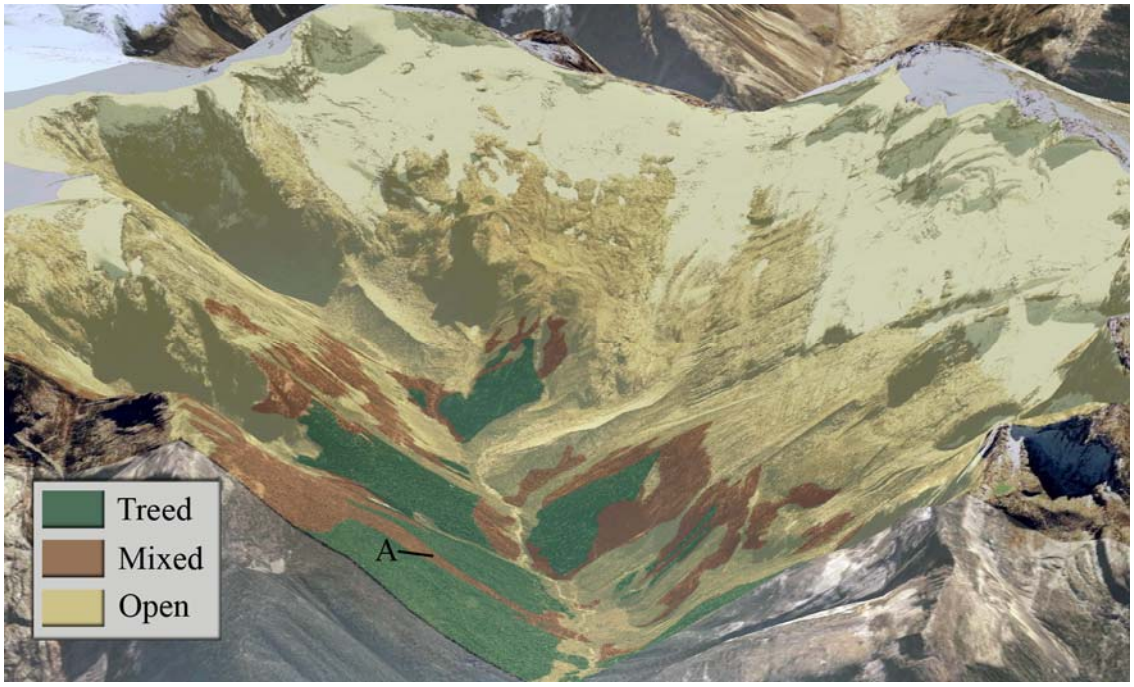

Figure 40. Forest cover digitized. Red shaded areas represent a mixed vegetation land cover, dark green shaded areas are densely treed areas and light yellow indicates open terrain. 'A' indicates a vegetated avalanche path.

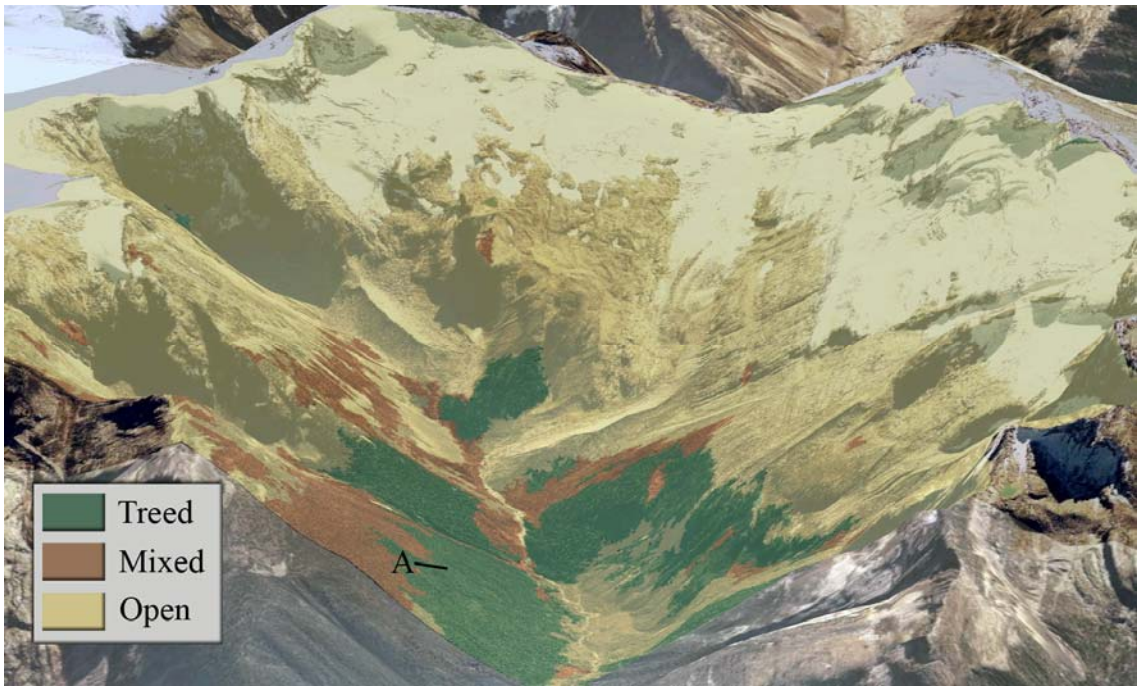

Figure 41. Hierarchical land cover classification. Red shaded areas represent a mixed vegetation land cover, dark green shaded areas are densely treed areas and light yellow indicates open terrain. 'A' indicates the vegetated avalanche path that is not recognized as mixed vegetation in the automated procedure.

5.4.2 Slope incline and slope curvature

From the DEM, slope angle and slope curvature layers can be extracted. For slope categories there is overlap between the categories of Simple, Challenging and Complex as indicated in Table 21. While building the GIS algorithm in Figure 39, the avalanche experts were concerned with four categories of slope; 0˚- 25˚, 25˚- 30˚, 30˚- 45˚ and greater than 45˚. As indicated in the algorithm, slope categories are dependent upon the type of associated land cover as to whether they are categorized into the Simple, Challenging or Complex categories. Slope is calculated in ArcGIS® v. 9.2 using a 3 x 3 cell neighbourhood around a centre cell and then determining the maximum change in elevation value from the centre grid cell (Figure 42).

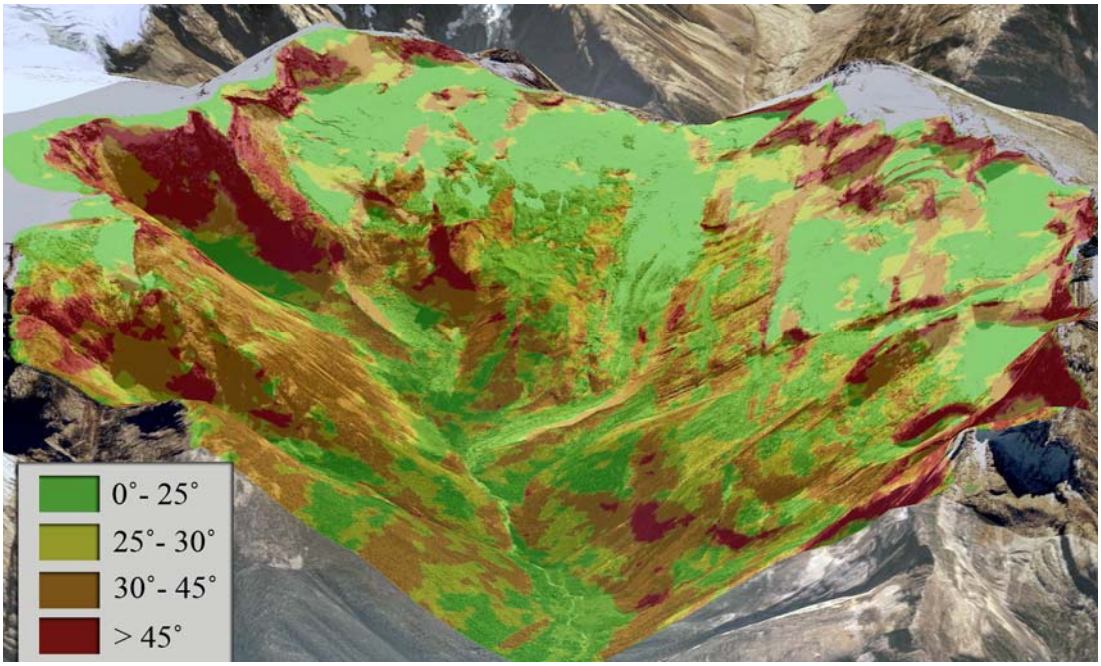

Figure 42. Slope angles within the Asulkan drainage where green shading represents 0˚- 25˚ slopes, yellow shading indicates 25˚- 30˚ slopes, orange shading is 30˚- 45˚ slopes and red shading indicates slopes greater than 45˚

Slope curvature is derived through a procedure that examines the changes in slope between grid cells in the DEM to ascertain convexity or concavity. In the ATES criteria and GIS algorithm, convexities and convoluted slopes yield Challenging or Complex classifications. Using the "curvature" command in ArcGIS®, both planar and profile

curvature can be calculated. In Maggioni and Gruber (2003), planar curvature was used to identify potential release areas whereby the grid cell resolution is reduced to 50 m so as to isolate large curvature features that would be sufficient for large avalanche formation. Gruber and Bartelt (2007), increase the original DEM grid resolution from 25 m to 10 m in order to calculate planar curvature values to identify gullies (planar curvature $C \leq -3$), channelled slopes ($-3 < C < -1.5$) and open slope terrain ($C > -1.5$) for their avalanche flow model.

To identify convex and convoluted terrain for the ATES classification the 5 m DEM grid was analyzed for channelled slopes and gullies using the same planar curvature values as Gruber and Bartelt (2007) with results displayed in Figure 43. Terrain traps such as steep-sided gullies are identified with the curvature parameters utilized.

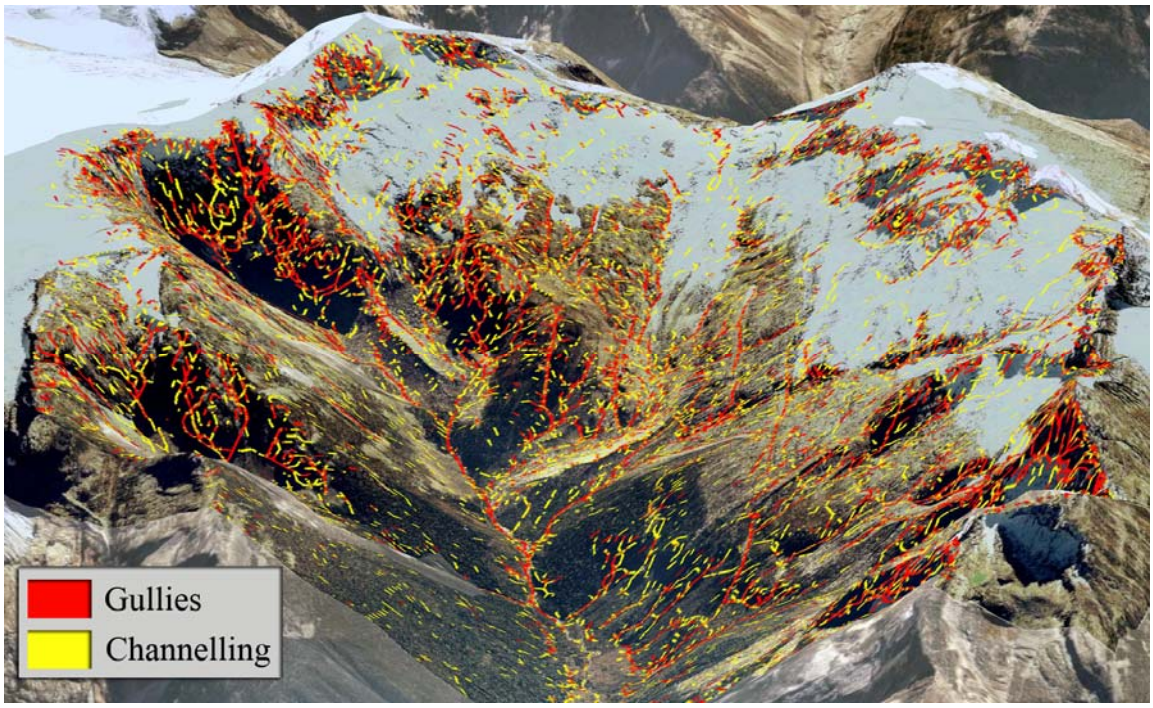

Figure 43. Planar curvature with yellow indicating channelling ($-3 < C < -1.5$) and red illustrating gullies ($C \leq -3$)

5.4.3 Runout zone characteristics

Determining runout exposure is an important consideration for the GIS-ATES system. In referring to the GIS algorithm (Figure 38), runout exposure is the next consideration after partially forested land cover with slopes of less than 30˚ or bare terrain with slopes less than 25˚. For this study, the interest was in identifying the top of the starting zone or avalanche path with a final goal of being able to estimate maximum runout values. In order to estimate the maximum avalanche runout with the alpha-beta runout model, the location of the top of the avalanche path is required. To determine runout an approach was taken to first identify fracture zones from which avalanches were likely to be released and second to model the avalanche flow from these areas down the valley sides.

In identifying potential avalanche release areas, Maggioni and Gruber (2003), use a topographic parameter "distance to ridge" as an important variable in addition to slope and curvature. Distance to ridges is important due to the influence of snow transport. Snow deposition on windward side of the ridge may form cohesive slabs and scoured slopes on the lee side may result in a shallow snowpack. To isolate the fracture area of an avalanche path, all ridgelines within the Asulkan drainage were identified in GIS by using the DEM data to isolate areas with no other points upstream of them. This is typically done by first computing a flow direction grid from the DEM which examines each grid cell and assigns a code value of eight possible directions in which the flow could go from that cell (Maidment, 2002). Next a flow accumulation grid is computed from the flow direction grid which computes a value for each cell based upon how many cells are upstream. Ridgelines are those areas where the flow accumulation is zero.

The tops of the ridges can be relatively flat and are generally considered safe terrain to travel; however, fracture areas are expected on either side of the ridges depending upon climatic conditions. To isolate these areas, the ridgelines were buffered to include areas 100 m from the ridge top and subsequently reduced by only including areas not densely forested and with a slope between 25˚-60˚. These areas do not include the entire potential

avalanche starting zone area, only the top portions where release is expected. Figure 44 shows the potential fracture areas in the Asulkan drainage as shaded yellow.

Once the potential fracture areas were identified, the flow paths from these areas were modeled using the FRho8 multiple flow routing algorithm as described in Wilson and Gallant (2000). This flow routing algorithm is available from the University of Southern California, Department of Geography as a toolbox add-on for ArcGIS® known as TAPES-G. The advantage of multiple flow direction algorithms is that they provide a more realistic flow pattern and eliminate the parallel flow paths common with single flow direction algorithms such as the D8 algorithm that is used by ArcGIS® (Gallant and Wilson, 2000). TAPES-G with the FRho8 algorithm was selected to process the Asulkan drainage DEM to produce a flow routing grid. A least cost path analysis was then run with the potential fracture areas as the input grid and the Asulkan DEM as the cost distance raster that determines the cost surface from most to least cost and the FRho8 grid as the grid to determine the path based upon a cell-by-cell basis with the least accumulative cost. The results are displayed by the grey flow routing lines in Figure 44.

The next step was to determine the maximum avalanche runout location point along the length of the flow paths in Figure 44. The simplified alpha-beta runout equation (5.1) as established for Glacier National Park (chapter four) was employed. In GIS the point at which the flow lines intersect slopes of 10˚ or less is readily identified and the β angle can be determined. The α angle is computed by using Equation 5.1. Unfortunately due to the geomorphometry of the valley, intersect slopes of 10˚ or less (shaded pink in Figure 44) were not always available for determining α angles for all slopes and prohibited a calculation for maximum runout, especially for some of the higher elevation, short slopes.

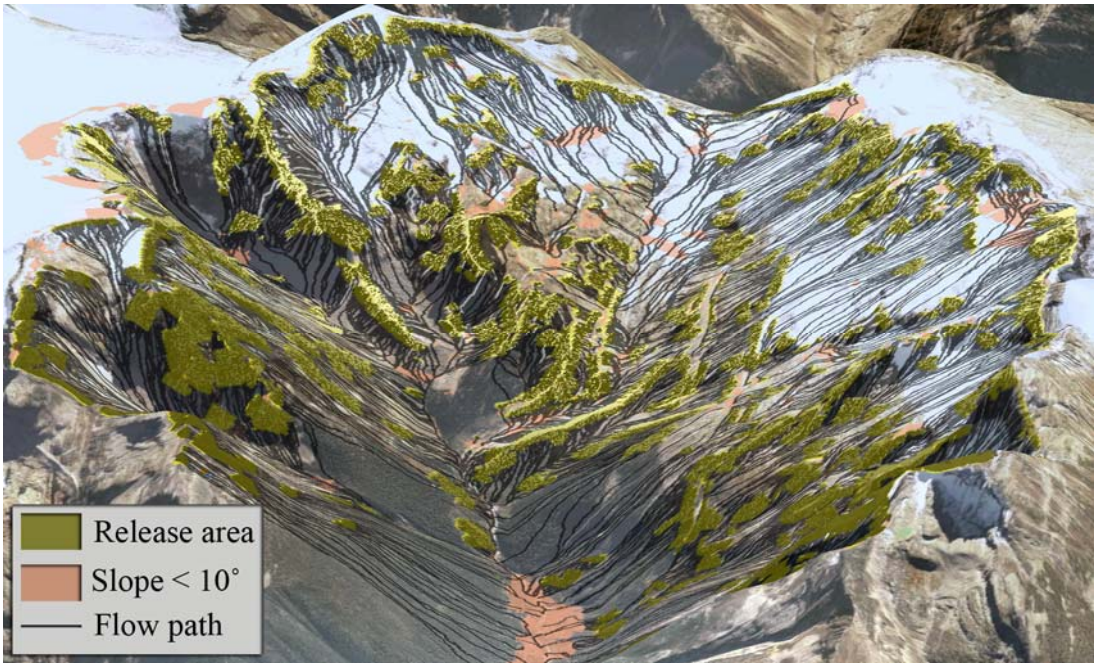

Figure 44. Asulkan drainage. Yellow areas indicate potential avalanche fracture areas. Grey lines illustrate the FRho8 multiple flow routing algorithm showing the flow pattern from the yellow fracture areas. Pink shaded areas indicate slopes of 10˚ or less.

As there are no currently available automated methods for applying the alpha-beta equation to multiple flow lines in GIS, the author manually selected several representative lines in GIS and individually applied the runout model equation to the extracted DEM avalanche profiles, calculated the maximum runout and subsequently mapped the results in GIS. These lines, indicated in red (Figure 45), help to indicate the expected length of the runout zone.

Runout exposure (0˚-25˚) was mapped into categories of multiple (orange) and isolated (light green) based on a combination of the flow lines present on slopes of <25˚and a grid indicating the amount of contributing flow. Flow lines generated from the FRHo8 algorithm were buffered by 25 m to provide a lateral extent and restricted to slopes <25˚. As part of the process of running the TAPES-G FRHo8 algorithm, a grid of contributing area was calculated in addition to the flow grid. Contributing area refers to the area of land upslope of a grid cell and is determined on a slope-weighted basis which allows for a more realistic distribution of upslope contributing areas and causes dispersion of flow in

valleys (Gallant and Wilson, 2000). Runout areas with high values of contributing area (≥3000) were classified as multiple and runout areas with low values of contributing area (<3000) were identified as isolated. This method of identifying runout exposure presented some challenges in estimating the lateral extent of runout zones; however using multiple flow lines, forest cover and slope angle assisted in determining the lateral extents of these areas.

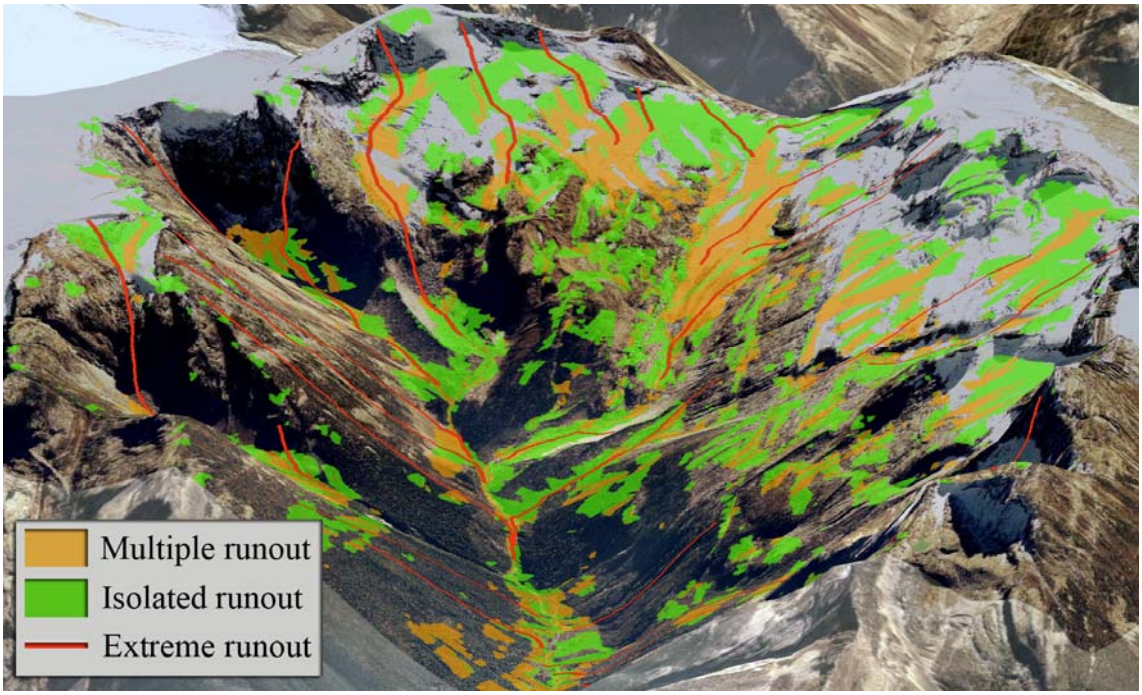

Figure 45. Runout exposure. Red lines represent calculated maximum runout for selected flow paths. Orange areas are multiple runout zones and light green represent isolated runout areas based upon contributing area.

5.4.4 Avalanche frequency

Avalanche frequency is the final component of the algorithm to determine a GIS-ATES map. To establish the topographic factors that contribute to frequency, starting zones in the area were examined for potential relationships with recorded avalanche frequency. Along the Trans Canada Highway, Parks Canada monitors and controls avalanche activity. From the historical database and expert knowledge starting zones were mapped in GIS and topographic parameters were evaluated for a relationship to avalanche

activity. The terrain variables in Table 23 were significantly correlated with avalanche frequency. Explosives are used along the highway corridor to control avalanches and result in inflated avalanche frequency.

Table 23. Topographic variables in the starting zone correlated with avalanche activity

Start zone topographic parameter	*R* value (Pearson correlation coefficient)	*p*-value
Surface area	-0.36	0.037
Surface area ratio	0.60	1.3×10^{-4}
Flat area	-0.37	0.029
Perimeter	-0.46	0.005
Elevation mean (zonal)	0.38	0.026
Elevation min (zonal)	0.45	0.006
Slope mean (zonal)	0.60	1.2×10^{-4}
Slope min (zonal)	0.39	0.021
Start zone end elevation	0.50	0.003
N = 35, 2-tailed pearson correlation		

Attempting to develop a stepwise regression from any combination of the topographic variables in the starting zone resulted in a coefficient of determination (r^2) values of less than 0.55. As well some of the variables exhibit a high level of multicollinearity. Thus these variables were not used to determine avalanche frequency.

5.4.5 GIS-ATES terrain map

In order to complete the GIS algorithm to assign the different categories of Simple, Challenging and Complex to all areas in the Asulkan drainage, an assumption is made that if a runout exposed area has a high contributing area and thus multiple paths it will have high or medium/high avalanche frequency, while an area with low upslope contributing area and generally isolated paths is assumed to have medium or medium/high frequency. Thus from Figure 38, a mixed forest area in an isolated runout zone will have a Challenging terrain classification (5201 or 5202) whereas a mixed forested area with a multiple runout zone will result in a Complex classification (4201 or 4202). For runout in large open areas, multiple paths will have Complex terrain (4301)

and isolated paths Challenging terrain (5301). This last assumption allows the completion of the ATES map (Figure 46) into the requisite categories according to the algorithm outlined in Figure 38.

Finding a suitable route for safe travel in the backcountry can be a challenging prospect for some backcountry users. With the GIS-ATES hazard map a suitable route can be found using the cost distance operations in GIS. The black line in Figure 46 is an example of a computer-generated route from the valley bottom to an alpine ski hut that maximizes the avoidance of Complex terrain. The parameters for selecting the route can be altered to give more weight to different factors such as terrain category, slope angle and land cover. The computer-generated route matches reasonably well with the recommended route from Murray Toft's, Touring at Rogers Pass, 1:50,000 scale topographic map. Both routes cross or skirt complex terrain on the GIS-ATES hazard map. A limitation of the GIS-ATES map is that flow widths in the valley bottom are not adequately represented such as in the "mouse trap" where backcountry users attempt to skirt around or quickly cross through an avalanche runout zone on the way into the cabin. The computer generated route avoids the mouse trap area by taking a higher route in the trees as compared to the normal winter route. The route to the cabin is rated as Complex by Parks Canada.

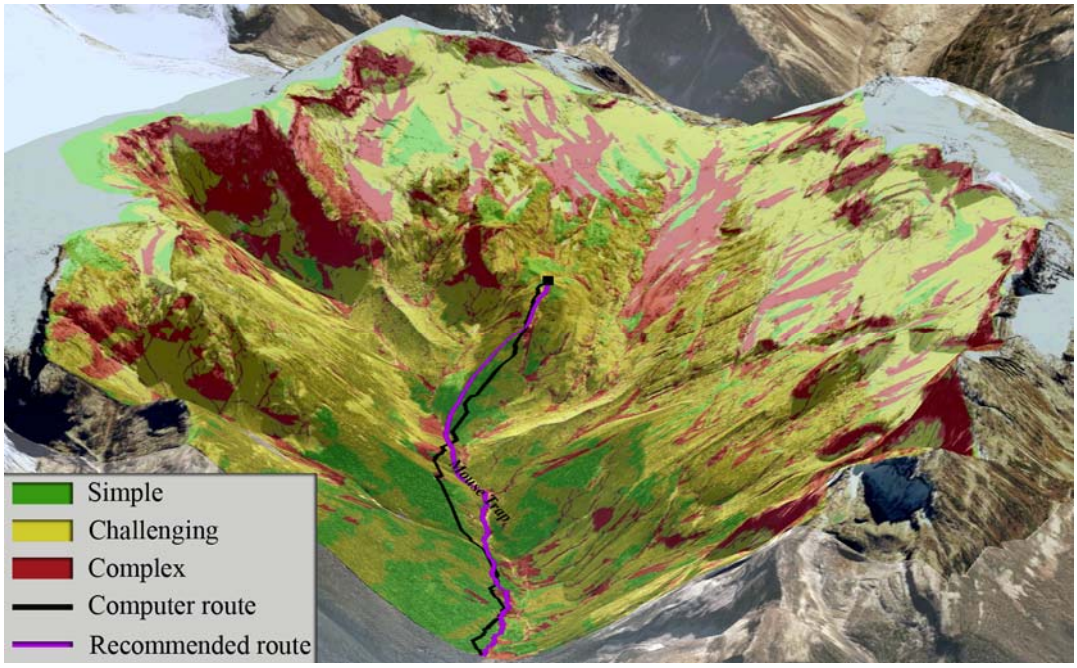

Figure 46. GIS-ATES hazard map. Representing Simple (green), Challenging (yellow) and Complex (red) terrain. The black line indicates a computer-generated route from the valley bottom to an alpine cabin (black box) that maximizes the use of Simple terrain. The purple line represents a generalization of the normal winter route to the cabin.

5.5 Discussion

The expert ATES classification for major backcountry routes in the Asulkan drainage are categorized as "Complex". There are multiple overlapping avalanche paths, steep open terrain, runout exposure and terrain traps that characterize Complex terrain. The GIS-ATES hazard map attempts to reveal the spatial distribution of Simple, Challenging and Complex terrain within the Asulkan drainage. The GIS map of the Asulkan drainage (Figure 46) is not a verified representation of avalanche exposure and no attempt should be made to navigate or make route decisions based on the maps presented in this thesis. Backcountry travel has inherent risks and there is always the potential for avalanches in the terrain described.

Verification of the GIS-ATES algorithm is a difficult task due to scale issues. The GIS generated hazard map can be viewed at the slope scale; whereas, an avalanche expert

takes into consideration their familiarity with the terrain and assessments of the entire route. Although independent verification is challenging, GIS has the potential to assist experts in making decisions on terrain ratings by facilitating the visualization of key topographic parameters as incorporated into GIS-ATES. Further refinements of the GIS algorithm using topographic parameters that are scientifically valid will contribute to a better model and visualization of the factors that play a role in avalanche formation and release.

Terrain parameters that presented problems for modeling within the GIS algorithm were related to avalanche frequency, the flow model and determination of maximum runout. Assumptions were made about avalanche frequency based upon upslope contributing area. From known avalanche paths along the highways corridor neither a strong correlation nor regression model could be found to link frequency to topographic parameters. The flow model used adequately represented flow dispersion in the upper portions of the valley but the flow dispersion was suppressed in the valley bottoms. Further, in determining maximum runout with the alpha-beta runout model, the β angle was difficult to determine as a runout zone of less than 10˚ was not present for some of the shorter slopes from which to calculate a beta angle.

Contrary to findings in other parts of the world, in Canada aspect does not appear to be a conclusive contributing factor to avalanche frequency (Smith and McClung, 1997) or strongly related to skier-triggered accidents. This is evident in the recent development of rule-based decision aids for travel in avalanche terrain which rely upon an analysis of contributing factors from accident records. European decision aids, such as the 3x3 Reduction Method (Munter, 1997) and the SnowCard (Engler and Mersch, 2000), include aspect as a factor to aid backcountry travellers in reducing risk. However the Canadian Avaluator Trip Planner (Haegeli and McCammon, 2006) does not include aspect as a reducing factor. In Canadian datasets, aspect shows a greater circular standard deviation for starting zones than even US datasets (McCammon and Haegeli, 2006). Yet aspect is potentially being considered and generating debate among experts for inclusion in an

ATES v.2., especially in regard to its relevance to climatic effects of solar and wind exposure (Statham et al., 2006b).

For this study, an interpolated DEM of 5 m was utilized. The higher resolution DEM provides enhanced identification for subtle slope scale features such as terrain traps, but a lower resolution DEM would likely be good enough for a terrain classification. The algorithm developed was not specifically created for the Asulkan drainage, thus it has the potential to be used for other areas with different DEM resolutions. A DEM with a lower resolution, such as the more commonly available 25 m DEM grid, would likely also be suitable for using with the GIS-ATES algorithm. The lower DEM resolution would result in a smoothing of the terrain surface; however, snow cover to some extent also smoothes out terrain features. For slope scale terrain evaluation the higher resolution DEM is preferable while lower resolution DEMs may provide a more suitable analysis of terrain features for initiating larger avalanche events. In visualizing a terrain classification developed with a low resolution DEM at a slope scale, a disadvantage would be the coarser grid-like shading and generalization of features that is not as evident with a higher resolution DEM.

Further refinements of the model would be to fully automate all process steps, to refine estimations of avalanche frequency, make improvements to the flow model and to integrate a runout formula that accommodates short slopes. Further research on avalanche frequency and topographic parameters definitively linked to frequency would improve the algorithm. The flow model needs to be modified to turn off the suppression of flow dispersion in the valley bottoms. Incorporating alpha-beta runout calculations currently interrupts the processing flow and with some customization a treatment of the calculations could be accomplished within the system. An analysis of short slope runouts (Jones and Jamieson, 2004) indicates that moving the beta point to an angle along the centreline where the slope incline is 24˚ provides a better estimation of runout for short slopes. Additional research of short slopes in the Columbia Mountains to produce a simplified short slope alpha-beta formula could improve the runout estimations in the

model. The alpha-beta runout equation used for the current model was developed from avalanche slopes with an average vertical drop of approximately 950 m and these slopes were influenced by control measures such as the use of explosives.

There is a temptation to include weather factors in the model and to modify the terrain classifications based upon current weather conditions and future outlook. For estimating snow stability at a slope scale a network of snowpack and weather stations would be required that at present does not exist for this area and if ideal weather data was available only a rough estimate would be attainable due to the lack of understanding of the complex physical variables involved in predicting snow stability. The goal of this study was to solely utilize topographic parameters to identify a terrain classification for slopes that has been previously applied by expert designation for popular ski routes and backcountry destinations in the area. GIS has the potential to visualize terrain classifications to aid experts and backcountry users in assessing avalanche hazards.

Chapter Six: Conclusions and Further Research

6.1 Conclusion

This thesis modeled avalanche terrain in Glacier National Park, Canada using Geographic Information Systems and developed GIS techniques that can be used to recognize avalanche terrain elsewhere. To enhance the capacity for topographic modeling, analysis and visualization using GIS a higher resolution digital elevation model was built for areas along the highway corridor and in two popular backcountry skiing areas. From an intensive digitizing process that integrated expert knowledge and a historical record of over 40 years a digital database of avalanche paths, path profile centrelines, starting zones and maximum runout location was created from which to examine avalanche terrain characteristics. Drawing from this digital database along the Trans Canada Highway corridor, alpha-beta maximum runout models for the Columbia Mountains were derived using GIS based on both high and low resolution DEM datasets. Finally, by utilizing the relationships derived from the well-known avalanche paths along the highway corridor and in combination with an expert aided GIS algorithm, a GIS avalanche terrain exposure map was generated for a popular backcountry skiing area. As outlined in chapter one the specific outcomes and contributions from the objectives of this thesis were as follows:

Objective 1: Build a detailed digital avalanche atlas for the avalanche paths along the Trans Canada Highway within Glacier National Park. A detailed digital avalanche atlas was created for the avalanche paths, profiles, path centrelines and starting zones along the Trans Canada Highway corridor in Glacier National Park. The atlas incorporates both historical records of maximum avalanche runout and expert knowledge. By extracting topographic parameters from digital elevation data based on the digital linework, this digital database acted as the foundation for the analysis of the maximum runout. One of the main contributions of building the digital atlas was to support the analysis of topographic parameters that contribute to avalanche formation and runout. A

limitation of the digital database is that only a portion of the avalanche paths along the highway corridor were captured at a higher DEM resolution thus limiting the number of paths for analysis and comparison.

Objective 2: Construct a high resolution digital elevation model for selected portions of the study area. A high resolution digital elevation model was created for portions of the study area to facilitate GIS analysis, modeling and visualization as well as to allow a comparison between high and low resolution data for avalanche terrain modeling. A Digital Elevation Model (DEM) is the basis for terrain analysis; it provides a representation of the topographic features. To produce an accurate DEM, manual techniques of data input were used to minimize error and an interpolation procedure was used to generate a 5 m elevation grid. Due to the time consuming nature of creating a high resolution DEM through manual means, only a reduced portion of the study area was rendered. This included an area representing 40 avalanche paths along the highway corridor and two backcountry skiing areas. Unfortunately remotely sensed means of data capture such as LiDAR were unavailable. LiDAR would have been a preferable method for high resolution data capture to facilitate a denser grid of elevation points and to offer more reliability in areas with forest cover and areas impacted by shadowing. The higher resolution DEM provided a better basis for GIS visualization and for the identification of subtle terrain features such as terrain traps.

Objective 3: Develop an avalanche runout zone model specific to the Columbia Mountains in Glacier National Park. An alpha-beta maximum runout model was derived that is specific to the Columbia Mountains. Based on the digital database of expert identified maximum runout locations for the Trans Canada Highway corridor, topographic parameters were extracted from high and low resolution DEM datasets. Previous work in Norway, Austria, Japan, Spain and other parts of the world has utilized the alpha-beta runout model for maximum runout estimation. Building upon this body of work, alpha-beta runout equations were derived using high and low resolution datasets that provided excellent goodness-of-fit values with R^2 ranging from 0.889 to 0.923.

Objective 4: Compare high and low resolution DEM runout model equations. Assumptions from previous alpha-beta runout studies that utilized DEM data and GIS indicated that a higher resolution DEM would perhaps result in better runout estimation. For this thesis, based upon a comparison of runout equations from high and low resolution DEMs no significant difference was found between equations derived from the differing DEM resolutions.

Objectives 5, 6 and 7: Verify the runout model and assess sources and margin of error within the model. Use the runout model to determine maximum runout position of avalanche paths along the highway corridor and apply the runout model to selected popular backcountry recreation areas within Glacier National Park. A leave-one-out cross validation procedure was used to provide an indication of the variability of the predictions of the runout models. The error estimations ranged from 0.89˚ to 1.3˚ which on the ground is approximately 50-75 m of error. To demonstrate the application of the runout equations, examples from the highway corridor and backcountry were included in chapter four. To determine maximum runout position it is preferable to use a DEM profile line to position the α point. Otherwise a 4^{th} degree polynomial appears to provide a better representation of the runout portion of the avalanche path rather than a 2^{nd} degree polynomial function.

Objective 8: Identify avalanche terrain according to an ATES classification system that is compatible with GIS to assist recreationists in recognizing avalanche terrain in winter backcountry areas. Avalanche experts have created a description based Avalanche Terrain Exposure Scale for determining recreational classifications of avalanche terrain. As some of the terrain criteria for the expert model are possible to model in GIS, a GIS-ATES algorithm was developed providing a drape of Simple, Challenging and Complex shading on a map for a backcountry area. This contribution of a GIS-ATES map has potential to aid recreational route selection based on topographic parameters from GIS rather than from conjecture and memory of an expert. The model demonstrated a classification of avalanche terrain at the slope scale.

This thesis contributed to the body of knowledge through an original investigation of maximum runout modeling in the Columbia Mountains and by developing a GIS-ATES algorithm for avalanche exposure mapping in the backcountry. The equations derived from the known avalanche paths along the highway corridor for this thesis can be applied to other transportation corridors and backcountry areas in the Columbia Mountains. Additionally, determining the runout calculation in GIS is not dependent on the availability of a high resolution DEM. DEM resolution in the 25-30 m range which is more readily obtainable is sufficient for alpha-beta runout modeling. Ideally a maximum runout position (α angle) will be determined using a DEM generated profile. Attempts to use a 2^{nd} degree polynomial to position maximum runout should be avoided as the 2^{nd} degree polynomial did not accurately represent the shape of the runout. For field surveys where additional points beyond the final survey point may not be available, a 4^{th} degree polynomial is preferable for determining maximum runout position as it provided a better representation of the terrain shape of runout zone.

A limitation of the alpha-beta runout model derived from the avalanche paths along the highway corridor in Glacier National Park is that the maximum runout positions are based on a historical record of observed avalanches that have occurred within the past 40 years, many of which were initiated with explosives. An assumption is made that a runout model derived from these observations is suitable for backcountry recreational mapping which requires a threshold return period of 10 years. Thus the statistical runout models presented in this thesis may be shorter than runouts estimated from other countries that either have a longer observation period or are supplemented with vegetative evidence and are used to aid land use planning. This is supported by a comparison of runout equations in chapter four where a Norwegian runout model based on record of greater than 100 years results in a longer runout than the model from this research; however, when extreme avalanche observations are removed the revised Norwegian model closely matches the runout model derived for this research.

With refinements to overcome some current limitations, the GIS-ATES algorithm for avalanche terrain exposure mapping has the potential to be applied elsewhere to aid in the determination of avalanche terrain exposure especially in remote backcountry areas. The delineation of terrain exposure using GIS would aid avalanche experts in making official terrain classifications and recommendations. As well there is a potential that backcountry users could use the visualizations of terrain to aid in trip planning. Refinements to the algorithm could be made to automate the procedure to allow GIS users to apply the procedure to other areas. A limitation that was discovered in developing the GIS-ATES algorithm was in delineating runout extents. The steep sided valley walls or in some cases the short slopes were not conducive to finding a β point at which the slope declined to 10˚. This made it difficult to determine a maximum runout position. Another limitation was inherent in the flow model used to indicate avalanche flow width. In the upper reaches of the valley, the flow model provided a good estimation of flow dispersion; however, lower in the valley the flow dispersion was suppressed and did not adequately represent avalanche path width in the valley bottoms. A means of determining topographic parameters to estimate avalanche frequency was also problematic. The higher DEM resolution provides better visualization and identification of subtle terrain features. It is likely that lower resolution DEM data in the range of 25 -30 m would result in a smoothing of terrain and would not capture important, but small, terrain features. The model has received limited verification at all elevation bands and further verification is required when some of the current limitations have been addressed.

6.2 Future Research

The body of work from this thesis has opened up numerous paths for future research. These include refinements of the models, automation of computer algorithms and further investigations of topographic factors on avalanche formation. The following section highlights research that work from this thesis could support:

- From the digital avalanche atlas and the low resolution DEM, a greater number of avalanche paths could be used to derive alpha-beta runout equations based upon the vertical drop. The assumption is that shorter slopes may have a significantly different runout equation than longer slopes as has been indicated in other studies. In addition, for development of an alpha-beta equation for the shorter slopes, an investigation into moving the β point could be examined to better estimate maximum avalanche runout in backcountry areas with constricted valley slopes.
- To improve the prediction of avalanche frequency with topographic parameters, analysis of topographic parameters from the digital avalanche atlas and DEM data in combination with temporal data such as aspect related to sun and wind could be examined to determine if there was a significant relationship.
- Refinements to an improved GIS-ATES algorithm could include the automation of the entire process and inclusion of an improved means of estimating avalanche frequency, a refinement to the flow model to adequately capture flow dispersion in the valley bottoms and improvements to runout models to better estimate runout extents for short slopes and constricted valleys.
- The hydrological model used in chapter five to model avalanche flow could be slightly modified to maintain dispersion of flow lower in the valley. Comparisons from known runout extents in the TCH corridor to be used to verify the model modifications.
- Based upon the procedure of identifying avalanche release areas and calculating flow from the algorithm in chapter five, a method of delineating avalanche paths and determining maximum runout position using the alpha-beta equations could be developed and automated for detection of avalanche paths in other areas.
- Field data collection of GPS ground control locations within the study area and supplemented with a base station correction for accuracy could be used to compare the relative accuracies of the DEM data used. Further, a comparison could be made between the DEM data and additional remotely sensed sources if they were to become available.

- Web sensor technology could be integrated into a system with GIS based terrain mapping to aid in developing predictive models with data inputs pertaining to temporal factors that contribute to avalanche formation.

References

Alentum Software Inc., 2005. Advanced Grapher 2.11. Alentum Software Inc.

Alldritt-McDowell, J., 1998. The Ecology of the Englemann Spruce - Subalpine Fir Zone. Province of British Columbia, Ministry of Forests.

Armstrong, R.L. and Armstrong, B.R., 1987. Snow and avalanche climates of the Western United States: a comparison of maritime, intermountain and continental conditions, Proceedings of the Davos Symposium: Avalanche Formation, Movement and Effects. International Association of Scientific Hydrology (IAHS); no. 162, Davos, Switzerland, pp. 281-294.

Bakermans, L. and Jamieson, B., 2006. Measuring near-surface snow temperature change over terrain. In: J.A. Gleason (Editor), International Snow Science Workshop, Telluride, CO, pp. 107-116.

Bakkehoi, S., Domaas, U. and Lied, K., 1983. Calculation of snow avalanche runout distance. Annals of Glaciology, 4: 24-29.

Barbolini, M. and Keylock, C.J., 2002. A new method for avalanche hazard mapping using a combination of statistical and deterministic models. Natural Hazards and Earth Systems Sciences, 2: 239-245.

Bartelt, P., Salm, B. and Gruber, U., 1999. Calculating dense-snow avalanche runout using a Voellmy-fluid model with active/passive longitudinal straining. Journal of Glaciology, 45(150): 242-254.

Berry, W.D. and Feldman, S., 1990. Multiple Regression in Practice. Quantitative Applications in the Social Sciences. Sage Publications, Newbury Park, 95 pp.

BMGS, 1996. British Columbia Specifications and Guidelines for Geomatics: Gridded DEM Specification - Release 1.1, Base Mapping & Geomatic Services Branch, Ministry of Sustainable Resource Management, Province of British Columbia.

BMGS, 2002. British Columbia Specifications and Guidelines for Geomatics: Gridded Digital Elevation Model Product Specifications, Base Mapping and Geomatics Services Branch, Ministry of Sustainable Resource Management, Province of British Columbia, Victoria, BC.

BMGS, 2007. Aerial Triangulation Specifications. Ministry of Agriculture and Lands, Integrated Land Management Bureau (ILMB), Base Mapping and Geomatic Services Branch, Victoria, BC, pp. 50.

Bolognesi, R., 1998. NivoLog™ : An avalanche forecasting support system, International Snow Science Workshop (ISSW), Sunriver, Oregon, pp. 412-418.

Bolognesi, R., Buser, O. and Good, W., 1994. Local Avalanche Forecasting in Switzerland: Strategy and Tools, a New Approach., International Snow Science Workshop, Snowbird, Utah, USA, pp. 463-472.

Bolognesi, R., Denuelle, M. and Dexter, L., 1996. Avalanche forecasting with GIS, International Snow Science Workshop (ISSW), Banff, Canada, pp. 11-13.

Bovis, M.J. and Mears, A.I., 1976. Statistical prediction of snow avalanche runout from terrain variables in Colorado. Arctic and Alpine Research, 8(1): 115-120.

Brabec, B., Meister, R., Stöckli, U., Stoffel, A. and Stucki, T., 2001. RAIFoS: Regional Avalanche Information and Forecasting System. Cold Regions Science and Technology, 33(2-3): 303-311.

Brun, E., David, P., Sudul, M. and Brunot, G., 1992. A numerical model to simulate snow-cover stratigraphy for operational avalanche forecasting. Journal of Glaciology, 38(128): 13-22.

Brun, E., Martin, E., Simon, V., Gendre, C. and Coleou, C., 1989. An energy and mass model of snow cover suitable for operational avalanche forecasting. Journal of Glaciology, 35(121): 333-342.

Buckley, A., Hurni, L., Kriz, K., Patterson, T. and Olsenholler, J., 2004. Cartography and visualization in mountain geomorphology. In: M.P. Bishop and J.F.J. Shroder (Editors), Geographic Information Science and Mountain Geomorphology. Springer-Verlag, Berlin, pp. 253-287.

Buisson, L. and Charlier, C., 1993. Avalanche modelling and integration of expert knowledge in the ELSA system. Annals of Glaciology, 18: 123-128.

Cai, X., 2003. Calibration Report - Calibration of Aerial Survey Camera to the Specification for Aerial Survey Photography. NRC Report No. OP-2003-335, National Research Council Canada.

Campbell, C., Jamieson, B. and Hageli, P., 2004. Small-scale mapping of snow stability: If not, why not? Avalanche News, in press.

Canadian Avalanche Association, 1998. Introduction to Snow Avalanche Hazard Mapping. Course Manual. A Canadian Avalanche Association Continuing Professional Development Course. Canadian Avalanche Association, Revelstoke, BC.

Canadian Avalanche Association, 2002a. Guidelines for Snow Avalanche Risk Determination and Mapping in Canada. Canadian Avalanche Association, Revelstoke, BC, 24 pp.

Canadian Avalanche Association, 2002b. Land Managers Guide to Snow Avalanche Hazards in Canada. Canadian Avalanche Association, Revelstoke, BC, 27 pp.

Canadian Avalanche Association, 2002c. Observation Guidelines and Recording Standards for Weather, Snowpack and Avalanches. Canadian Avalanche Association, 78 pp.

Christen, M., Bartelt, P. and Gruber, U., 2002. AVAL-1D: An avalanche dynamics program for the practice, International Congress Interpraevent 2002 in the Pacific Rim, Matsumoto, Japan, pp. 715-725.

Christen, M., Bartelt, P. and Gruber, U., 2007. Modelling Avalanches. GEOconnexion International Magazine, April 2007: 38-39.

Chritin, V., Bolognesi, R. and Gubler, H., 1998. Flowcapt: A New Acoustic Sensor to Measure Snowdrift and Wind Velocity for Avalanche Forecasting, International Snow Science Workshop (ISSW), Sunriver, OR.

Cloutier, R., 2000. Legal Liability and Risk Management in Adventure Tourism. Bhudak Consultants, Kamloops, BC, 195 pp.

CSA, 1997. (R2002). Risk Management: Guidelines for Decision-Makers. CAN/CSA-Q850-97, Canadian Standards Association.

Daniel, C. and Tennant, K., 2001. DEM Quality Assessment. In: D.F. Maune (Editor), Digital Elevation Model Technologies and Applications: The DEM Users Manual. American Society for Photogrammetry and Remote Sensing (ASPRS), Bethesda, Maryland, pp. 395-440.

Durand, Y., Brun, E., Merindol, L. and Guyomarc'h, G., 1993. A meteorological estimation of relevant parameters for snow models. Annals of Glaciology, 18: 65-71.

Durand, Y., Giraud, G., Brun, E., Merindol, L. and Martin, E., 1999. A computer-based system simulating snowpack structures as a tool for regional avalanche forecasting. Journal of Glaciology, 45(151): 469-484.

Durand, Y., Giraud, G. and Merindol, L., 1998. Short-term numerical avalanche forecast used operationally at Meteo-France over the Alps and Pyrenees. Annals of Glaciology, 26: 357-368.

Egan, B., 1998. The Ecology of the Interior Cedar-Hemlock Zone. Province of British Columbia, Ministry of Forests.

Egilsson, J.G., 1996. Two destructive avalanches in Iceland, International Snow Science Workshop (ISSW), Banff, Canada.

Engler, M. and Mersch, J., 2000. SnowCard: Lawinen - Risiko - Check. Verlag, Sulzberg, Germany.

Environment Canada, 2002. National Climate Data and Information Archive - Online Canadian Climate Normals or Averages 1971-2000. Environment Canada.

ESRI, 2006a. ArcGIS Desktop Help. Environmental Systems Research Institute, Redlands, CA.

ESRI, 2006b. ArcGIS v. 9.2. Environmental Systems Research Institute Inc., Redlands, CA.

Feick, S., Kronholm, K. and Schweizer, J., 2007. Field observations on spatial variability of surface hoar at the basin scale. Journal of Geophysical Research, 112(April): 1-16.

Fowler, R., 2001. Topographic Lidar. In: D.F. Maune (Editor), Digital Elevation Model Technologies and Applications: The DEM Users Manual. American Society for Photogrammetry and Remote Sensing (ASPRS), Bethesda, Maryland, pp. 207-234.

Fredston, J. and Fesler, D., 1994. Snow Sense: A Guide to Evaluating Snow Avalanche Hazard. Alaska Mountain Safety Center, 116 pp.

Fujisawa, K., Tsunaki, R. and Kamiishi, I., 1993. Estimating snow avalanche runout distances from topographic data. Annals of Glaciology, 18: 239-244.

Furdada, G. and Vilaplana, J.M., 1998. Statistical predication of maximum avalanche run-out distances from topographic data in the western Catalan Pyrenees (northeast Spain). Annals of Glaciology, 26: 285-288.

Gallant, J.C. and Wilson, J.P., 2000. Primary Topographic Attributes. In: J.P. Wilson and J.C. Gallant (Editors), Terrain Analysis. Principles and Applications. John Wiley & Sons, Inc., New York, pp. 51-85.

Geodesy Remote Sensing Inc., 2004. Aerial photography flight lines, Calgary, AB.

George, J., 1999. Avalanche strikes Kangiqsualujjuaq: nine dead, 25 injured, Nunatsiaq News, Iqaluit, Nunavut, Canada.

Giraud, G., 1992. MEPRA: an expert system for avalanche risk forecasting., International Snow Science Workshop, Breckenridge, CO, pp. 97-104.

Giraud, G., Brun, E., Durand, Y. and Martin, E., 1994. Validations of objective models to simulate snowcover stratigraphy and avalanche risk for avalanche forecasting., International Snow Science Workshop (ISSW), Snowbird, UT, pp. 509-517.

Giraud, G., Brun, E., Durand, Y. and Martin, E., 1998. Safran/Crocus/Mepra models as an helping tool for avalanche forecasters. In: E. Hestnes (Editor), 25 Years of Snow Avalanche Research. Norges Geotekniske Institutt/Norwegian Geotechnical Institute, Oslo, Norway, pp. 108-112.

Gleason, J.A., 1994. Terrain parameters of avalanche starting zones and their effects on avalanche frequency, International Snow Science Workshop (ISSW), Snowbird, Utah, USA, pp. 393-404.

González, J.C., Moner, I., Marturià, J., Whittmann, E. and Sayda, F., 2003. Information and navigation system for mountaineers: the PARAMOUNT project, 9th EC-GI & GIS Workshops ESDI: Serving the User. European Commission, A Coruña, Spain, pp. 1-12.

Gruber, U., 2001. Using GIS for avalanche hazard mapping in Switzerland, Proceedings of the 2001 ESRI International User Conference, San Diego.

Gruber, U. and Bartelt, P., 2007. Snow avalanche hazard modelling of large areas using shallow water numerical methods and GIS. Enivronmental Modelling & Software, 22: 1472-1481.

Gruber, U., Bartlet, P. and Haefner, H., 1998. Avalanche hazard mapping using numerical Voellmy-Fluid Models. In: E. Hestnes (Editor), 25 Years of Snow Avalanche Research. Norges Geotekniske Institutt, Oslo, Norway, pp. 117-121.

Gruber, U. and Margreth, S., 2001. Winter 1999: a valuable test of the avalanche-hazard mapping procedure in Switzerland. Annals of Glaciology, 32: 328-332.

Gruber, U. and Sardemann, S., 2002. High frequency avalanches: Release area characteristics and runout distances. In: J.R. Stevens (Editor), International Snow Science Workshop (ISSW), Penticton, BC, Canada, pp. 84-89.

Haeberli, W., Benz, C., Gruber, U., Hoelzle, M., Kääb, A. and Schaper, J., 2004. GIS applications for snow and ice in high-mountain areas: Examples from the Swiss Alps. In: M.P. Bishop and J.F.J. Shroder (Editors), Geographic Information Science and Mountain Geomorphology. Springer-Verlag, Berlin, pp. 381-402.

Haegeli, P. and McCammon, I., 2006. Avaluator Avalanche Accident Prevention Card, Canadian Avalanche Association (CAA), Revelstoke, BC, Canada.

Haegeli, P. and McClung, D., 2007. Expanding the snow-climate classification with avalanche-relevant information: initial description of avalanche winter regimes for southwestern Canada. Journal of Glaciology, 53(181): 266-276.

Harbitz, C., Issler, D. and Keylock, C.J., 1998. Conclusions from a recent survey of avalanche computational models. In: E. Hestnes (Editor), Proceedings of the Anniversary Conference 25 Years of Snow Avalanche Research, Voss, 12-16 May 1998. Norwegian Geotechnical Institute, Oslo, pp. 128-135.

Hutchinson, M.F. and Gallant, J.C., 2000. Digital Elevation Models and Representation of Terrain Shape. In: J.P. Wilson and J.C. Gallant (Editors), Terrain Analysis - Principles and Applications. John Wiley and Sons, New York, pp. 29-50.

ISM, 1997. The Fundamentals of Digital Photogrammetry. International Systemap Corp., Vancouver, British Columbia, 72 pp.

Jamieson, B., 2003. Risk management for the spatial variable snowpack. Avalanche News, 66(Fall).

Jamieson, B. and Geldsetzer, T., 1996. Avalanche Accidents in Canada 1984-96, 4. Canadian Avalanche Association, Revelstoke, BC, 203 pp.

Jamieson, J.B. and Johnston, C.D., 1992. Snowpack characteristics associated with avalanche accidents. Canadian Geotechnical Journal, 29(5): 862-866.

Johannesson, T., 1998. Icelandic avalanche runout models compared with topographic models used in other countries. In: E. Hestnes (Editor), Proceedings of the Anniversary Conference 25 Years of Snow Avalanche Research, Voss, 12-16 May 1998. Norwegian Geotechnical Institute, Oslo, pp. 43-52.

Jones, A.S.T. and Jamieson, B., 2004. Statistical avalanche runout estimation for short slopes. Annals of Glaciology, 38: 363-372.

Kelly, D. and Stevens, R., 1997. Avalanche likelihood mapping. TFL 56 (1:20,000), BC Ministry of Forests, Revelstoke, BC, Canada.

Keylock, C.J., McClung, D. and Magnusson, M.M., 1999. Avalanche risk mapping by simulation. Journal of Glaciology, 45(150): 303-314.

Kowalczuk, R., 2007. New tools for avalanche education, Avalanche News. Canadian Avalanche Association, pp. 60-64.

Krajina, V.J., 1972. Ecosystem Perspectives in Forestry. The H.R. MacMillan Lectureship in Forestry, University of British Columbia, Vancouver, British Columbia.

LaChapelle, E.R., 1966. Avalanche forecasting - a modern synthesis, International Symposium on Scientific Aspects of Snow and Ice Avalanches. International Association of Scientific Hydrology (IAHS); no. 69, Davos, Switzerland, pp. 350-356.

Lehning, M., Bartelt, P., Brown, B. and Fierz, C., 2002a. A physical SNOWPACK model for the Swiss avalanche warning Part III: meteorological forcing, thin layer formation and evaluation. Cold Regions Science and Technology, 35: 169-184.

Lehning, M., Bartelt, P., Brown, B., Fierz, C. and Satyawali, P., 2002b. A physical SNOWPACK model for the Swiss avalanche warning Part II: Snow microstructure. Cold Regions Science and Technology, 35: 147-167.

Lehning, M., Bartelt, P., Brown, B., Russi, T., Stoeckli, U. and Zimmerli, M., 1999. SNOWPACK model calculations for avalanche warning based upon a new network of weather and snow stations. Cold Regions Science and Technology, 30: 145-157.

Li, Z., Zhu, Q. and Gold, C., 2005. Digital Terrain Modeling - Principles and Methodology. CRC Press, Boca Raton, Florida, 323 pp.

Lied, K., 1998. Snow avalanche experience through 25 years at NGI. In: E. Hestnes (Editor), Proceedings of the Anniversary Conference 25 Years of Snow Avalanche Research, Voss, 12-16 May 1998. Norwegian Geotechnical Institute, Oslo, pp. 7-14.

Lied, K. and Bakkehoi, S., 1980. Empirical calculation of snow-avalanche run-out distance based on topographic parameters. Journal of Glaciology, 26(94): 165-177.

Lied, K., Sandersen, F. and Toppe, R., 1989. Snow avalanche maps for the Norwegian army. Annals of Glaciology, 13: 170-174.

Lied, K. and Toppe, R., 1989. Calculation of maximum snow-avalanche runout distance by use of digital terrain models. Annals of Glaciology, 13: 164-169.

Lied, K., Weiler, S., Bakkehoi, S. and Hopf, J., 1995. Calculation methods for avalanche run-out distance for the Austrian Alps. The contribution of scientific research to safety with snow, ice and avalanche., ANENA, Grenoble, France, pp. 63-68.

Löhnert, E., Mundle, H., Heinrichs, G. and Wittmann, E., 2004. Wireless in the Alps. GPS World, 15(3): 30-37.

Löhnert, E., Wittmann, E., Pielmeier, J. and Sayda, F., 2001. PARAMOUNT - Public safety and commercial info-mobility appplications and services in the mountains, ION GPS 2001 14th International Technical Meeting of the Satellite Division of the Institute of Navigation. ION Publications, Salt Lake City, Utah.

Maceachren, A.M., Wachowicz, M., Edsall, R., Haug, D. and Masters, R., 1999. Constructing knowledge from multivariate spatiotemporal data: integrating geographic visualization with knowledge discovery in database methods. International Journal of Geographical Information Science, 13(4): 311-334.

Mackenzie, W., 2006. The Ecology of the Alpine Zones. Province of British Columbia, Ministry of Forests and Range.

Maggioni, M. and Gruber, U., 2003. The influence of topographic parameters on avalanche release dimension and frequency. Cold Regions Science and Technology, 37: 407-419.

Maggioni, M., Gruber, U. and Stoffel, A., 2001. Definition and characterisation of potential avalanche release areas, Proceedings of the 2001 ESRI International User Conference, San Diego.

Mah, S., Thomson, S. and Demarchi, D., 1996. An ecological framework for resource management in British Columbia. Environmental Monitoring and Assessment, 39(1-3): 119-125.

Maidment, D.R. (Editor), 2002. ARC Hydro: GIS for Water Resources. ESRI Press, Redlands, CA, 300 pp.

Mases, M., Buisson, L., Frey, W. and Marti, G., 1998. Empirical model for snowdrift distribution in avalanche-starting zones. Annals of Glaciology, 26: 237-241.

Maune, D.F., Kopp, S.M., Crawford, C.A. and Zervas, C.E., 2001a. Introduction. In: D.F. Maune (Editor), Digital Elevation Model Technologies and Applications: The DEM Users Manual. American Society for Photogrammetry and Remote Sensing (ASPRS), Bethesda, Maryland, pp. 1-34.

Maune, D.F., Maitra, J.B. and McKay, E.J., 2001b. Accuracy Standards. In: D.F. Maune (Editor), Digital Elevation Model Technologies and Applications: The DEM Users Manual. American Society for Photogrammetry and Remote Sensing, Bethesda, Maryland, pp. 61-82.

McCammon, I. and Haegeli, P., 2006. Evaluation of a rule-based decision aid for recreational travelers in avalanche terrain. In: J.A. Gleason (Editor), International Snow Science Workshop (ISSW), Telluride, CO, pp. 234-244.

McClung, D., 2000. Extreme avalanche runout in space and time. Canadian Geotechnical Journal, 37: 161-170.

McClung, D., 2001. Characteristics of terrain, snow supply and forest cover for avalanche initiation caused by logging. Annals of Glaciology, 32: 223-229.

McClung, D. and Lied, K., 1987. Statistical and geometric definition of snow avalanche runout. Cold Regions Science and Technology, 13: 107-119.

McClung, D. and Mears, A.I., 1991. Extreme value prediction of snow avalanche runout. Cold Regions Science and Technology, 19(163-175).

McClung, D. and Mears, A.I., 1995. Dry flowing avalanche run-up and run-out. Journal of Glaciology, 41(138): 359-372.

McClung, D., Mears, A.I. and Schaerer, P., 1989. Extreme avalanche runout: data from four mountain ranges. Annals of Glaciology, 13(180-184).

McClung, D. and Schaerer, P., 1993. The Avalanche Handbook. The Mountaineers, Seattle, WA, 271 pp.

McClung, D. and Schaerer, P., 2006. The Avalanche Handbook, 3rd Edition. The Mountaineers Books, Seattle, WA, 288 pp.

McClung, D. and Schweizer, J., 1999. Skier-triggering, snow temperatures and the stability index for dry-slab avalanche formation. Journal of Glaciology, 45(150): 190-200.

McCollister, C., Birkeland, K., Hansen, K., Aspinall, R. and Comey, R., 2002. A probabilistic technique for exploring multi-scale spatial patterns in historical avalanche data by combining GIS and meteorological nearest neighbors with an example from the Jackson Hole Ski Area, Wyoming, International Snow Science Workshop (ISSW), Penticton, BC, Canada, pp. 109-116.

McLaren, S., 2000. Suitability mapping of avalanche trigger sites on the North Shore Mountains, Vancouver using a digital elevation model and GIS.

Mears, A.I., 1988. Comparisons of Colorado, Eastern Sierra, coastal Alaska, and Western Norway runout data, International Snow Science Workshop (ISSW), Wistler, BC, pp. 232-238.

Mears, A.I., 1989. Regional comparisons of avalanche-profile and runout data. Arctic and Alpine Research, 21(3): 283-287.

Mears, A.I., 1992. Snow Avalanche Hazard Analysis for Land-Use Planning and Engineering, Bulletin 49. Colorado Geological Survey, Geological Survey, Dept. of Natural Resources, Denver, Colorado, 54 pp.

MELP, 1992. British Columbia Specifications and Guidelines for Geomatics: Content Series Volume 3 Digital Base Mapping at 1:20,000, Province of British Columbia, Ministry of Environment, Lands and Parks, Geographic Data BC, Victoria, BC.

Miles, J. and Shevlin, M., 2001. Applying Regression and Correlation. A guide for students and researchers. Sage Publications, Thousand Oaks, CA, 253 pp.

Mock, C.J. and Birkeland, K.W., 2000. Snow avalanche climatology of the western United States mountain ranges. Bulletin of the American Meteorological Society, 81(10): 2367-2392.

Molander, C.W., 2001. Photogrammetry. In: D.F. Maune (Editor), Digital Elevation Model Technologies and Applications: The DEM Users Manual. American Society for Photogrammetry and Remote Sensing (ASPRS), Bethesda, Maryland, pp. 121-142.

Moner, I. et al., 2004. Development of a GIS supported tool for the cartographic representation of the avalanche hazard bulletin. Institut Cartogràfic de Catalunya.

Munter, W., 1997. 3x3 Lawinen: Entscheiden in kritischen Situationen Agentur Pohl & Schellhammer, Garmisch Patenkirchen, Germany.

NATO, 2006. ISAF assists in relief efforts to help avalanche-hit village in Northern-Afgahanistan, North Atlantic Treaty Organization Press Release #2006-008, Kabul, Afghanistan.

Nixon, D.J. and McClung, D., 1993. Snow avalanche runout from two Canadian mountain ranges. Annals of Glaciology, 18: 1-6.

Norušis, M.J., 2006. SPSS 14.0 guide to data analysis. Prentice Hall, Upper Saddle River, NJ, 649 pp.

O'Gorman, D., Hein, P. and Leiss, W., 2003. Parks Canada's Backcountry Avalanche Risk Review, Parks Canada.

Paparoditis, N. and Polidori, L., 2001. Overview of Digital Surface Models. In: M. Kasser and Y. Egels (Editors), Digital Photogrammetry. Taylor & Francis Inc., New York, NY, pp. 159-164.

ParksCanada, 2004. Public Information Package for Custodial Groups Planning Winter Backcountry Travel. Parks Canada.

ParksCanada, 2007. Public Safety - Backcountry Avalanche Information. Government of Canada.

Paternoster, R., Brame, R., Mazerolle, P. and Piquero, A., 1998. Using the correct statistical test for the equality of regression coefficients. Criminology, 36(4): 859-866.

Purves, R.S., Barton, J.S., Mackaness, W.A. and Sugden, D.E., 1998. The development of a rule based spatial model of wind transport and deposition of snow. Annals of Glaciology, 26: 197-202.

Rasemann, S., Schmidt, J., Schrott, L. and Dikau, R., 2004. Geomorphometry in mountain terrain. In: M.P. Bishop and J.F.J. Shroder (Editors), Geographic Information Science and Mountain Geomorphology. Springer-Verlag, Berlin, pp. 101-145.

Royer, A. and Lemieux, S., 2006. Mapping and classification of potential avalanche sites in the Chic-Choc Mountains, Quebec, Canada, Using Geographic Information Systems, International Snow Science Workshop (ISSW), Telluride, Colorado, United States, pp. 411-418.

Russi, T., Ammann, W. and Stucki, T., 1998. Avalanche warning Switzerland 2000: a new concept and its implementation, International Snow Science Workshop (ISSW), Sunriver, OR., pp. 146-153.

Sailer, R., Rammer, L. and Sampl, P., 2002. Recalculation of an artifically released avalanche with SAMOS and validation with measurements from a pulsed Doppler radar. Natural Hazards and Earth Systems Sciences, 2: 211-216.

Sampl, P. and Zwinger, T., 2004. Avalanche simulations with SAMOS. Annals of Glaciology, 38: 393-396.

Schaerer, P., 1977. Analysis of snow avalanche terrain. Canadian Geotechnical Journal, 14(3): 281-287.

Schleiss, V.G., 1989. Rogers Pass Snow Avalanche Atlas, Glacier National Park, British Columbia, Canada. Canadian Parks Service, Revelstoke, B.C., 313 pp.

Schneider, J., Soon Lee, M. and Moore, A., 1997. A tutorial on using the Vizier memory-based learning system. Schenley Park Research Inc., Squirrel Hill, Pittsburgh, Pennsylvania.

Schweizer, J., 1999. Review of dry snow slab avalanche release. Cold Regions Science and Technology, 30: 43-57.

Schweizer, J., Bellaire, S., Fierz, C., Lehning, M. and Pielmeier, C., 2006a. Evaluating and improving the stability predications of the snow cover model SNOWPACK. Cold Regions Science and Technology, 46(1): 52-59.

Schweizer, J. and Jamieson, B., 2000. Field observations of skier-triggered avalanches, International Snow Science Workshop (ISSW). American Avalanche Association, Big Sky, Montana, USA, pp. 192-199.

Schweizer, J. and Jamieson, B., 2001. Snow cover properties for skier triggering of avalanches. Cold Regions Science and Technology, 33: 207-221.

Schweizer, J. and Jamieson, B., 2002. Contrasting stable and unstable snow profiles with respect to skier loading, International Snow Science Workshop (ISSW), Penticton, BC, Canada, pp. 499-501.

Schweizer, J., Jamieson, B. and Schneebeli, M., 2003. Snow avalanche formation. Reviews of Geophyics, 41(4): 2.1 - 2.25.

Schweizer, J., Kronholm, K., Jamieson, B. and Birkeland, K., 2006b. Spatial variability - so what?, International Snow Science Workshop (ISSW), Telluride, Colorado, pp. 365-376.

Scott, D., 2004. GIS Data Model (Poster Session), International Snow Science Workshop (ISSW), Jackson Hole, WY.

Scott, D., 2006. Using GIS and remote sensing to assess avalanche hazards for new road corridors in Alaska, International Snow Science Workshop (ISSW), Telluride, Colorado, United States, pp. 465-467.

Sigurdsson, F., Tomasson, G.G. and Sandersen, F., 2000. Avalanche defenses for Flateyri, Iceland. From hazard evaluation to construction of defenses. VST Consulting Engineers.

Smith, M.J. and McClung, D., 1997. Avalanche frequency and terrain characteristics at Roger's Pass, British Columbia, Canada. Journal of Glaciology, 43(143): 165-171.

SPSS, 2006. SPSS® 15.0 for Windows. SPSS Inc., Chicago, Illinois, USA.

Statham, G., McMahon, B. and Tomm, I., 2006a. The Avalanche Terrain Exposure Scale, International Snow Science Workshop (ISSW). Omnipress, Telluride, CO, pp. 491-497.

Statham, G., McMahon, B. and Tomm, I., 2006b. The Avalanche Terrain Exposure Scale. In: J.A. Gleason (Editor), Internation Snow Science Workshop (ISSW), Telluride, CO, pp. 491-497.

Stoffel, A., Brabec, B. and Stoeckli, U., 2001. GIS Applications at the Swiss Federal Institute for Snow and Avalanche Research, Proceedings of the 2001 ESRI International User Conference, San Diego.

Stoffel, A., Meister, R. and Schweizer, J., 1998. Spatial characteristics of avalanche activity in an alpine valley--a GIS approach. Annals of Glaciology, 26: 329-336.

Stucki, T., Ammann, W., Meister, R. and Brabec, B., 1998. A new concept for avalanche warning in Switzerland. In: E. Hestnes (Editor), 25 Years of Snow Avalanche Research. Norges Geotekniske Institutt/Norwegian Geotechnical Institute, Oslo, Norway, pp. 278-282.

Tomm, I., 2006. Building the Canadian Avalanche Data System - From concept to reality in fourteen days. Avalanche.ca, 78(Fall): 12-15.

Toppe, R., 1987. Terrain models: a tool for natural hazard mapping. In: B. Salm and H. Gubler (Editors), Avalanche Formation, Movements and Effects (Proceedings of the Davos Symposium, September 1986). International Association of Hydrological Sciences (IAHS), Wallingford, UK., pp. 629-638.

Tracy, L., 2001. Using GIS in Avalanche Hazard Management, Proceedings of the 2001 ESRI International User Conference, San Diego.

Visual Learning Systems, 2006. Feature Analyst Version 4.1 for ArcGIS, Reference Manual. Visual Learning Systems, Inc., Missoula, Montana, pp. 153.

Weir, P., 2002. Snow Avalanche Management in Forested Terrain, Land Management Handbook No. 55. Res., Br., B.C. Min. For., Victoria, BC, 208 pp.

Welch, R. and Jordan, T.R., 1996. Using Scanned Air Photographs. In: S. Morain and S.L. Baros (Editors), Raster Imagery in Geographic Information Systems. Onward Press, pp. 55-69.

Wilks, D.S., 1995. Statistical Methods in the Atmospheric Sciences: An Introduction 59. Academic Press, San Diego, CA, 465 pp.

Wilson, J.P. and Gallant, J.C. (Editors), 2000. Terrain Analysis - Principles and Applications. John Wiley and Sons, New York, 479 pp.

Woods, J.G., 1983. Snow War. An illustrated history of Rogers Pass, Glacier National Park, British Columbia. National and Provincial Parks Association of Canada, 52 pp.

Yamada, Y., Abe, O., Kosugi, K. and Watanabe, S., 2002. Avalanche release hazard mapping using GIS, The 11th Standing International Road Weather Commission, Sapporo, Japan.

APPENDIX A: FLIGHT REPORT

GEODESY REMOTE SENSING INC.

820 McTavish Road N.E., Calgary Alberta T2E 7G6 Ph:(403)291-9655 Fax:(403)291-4988

Aerial Photography Report

Camera Type	Film Type		Client Roll Number
Zeiss/Jena LMK 15	AGFA X100		A31888
Lens Number	Emulsion Number	Expiry Date	Geodesy Field Roll No.
7381342/C	677663143	05/2007	GRS04038/040/043
Calibrated Focal Length	Magazine No.	Filter Type and Number	Average Scale
152.092mm	266454	CLEAR	1:30,000

Project No.	Date	Annotated Neg No.'s	Line and Number Direction	Exposure No.		U.T.C.		True Altitude Above Sea Level	Camera Exposure	Remarks
				Start	Finish	Start	Finish			
										LEADER
	24/09/04	001-009	LN-1N	087	095	19:24	19:28	21,500	4.5/175	LLYK NAT. PARK
	24/09/04	010-020	LN-3W	096	106	19:33	19:38	21,500	4.5/175	LLYK NAT. PARK
	24/09/04	021-029	LN-2E	107	115	19:41	19:45	21,500	4.5/175	LLYK NAT. PARK
	24/09/04	030-038	LN-4N	001	009	19:58	20:01	23,500	4.5/175	LLYK NAT. PARK
	24/09/04	039-047	LN-5S	010	018	20:06	20:09	23,500	4.5/175	LLYK NAT. PARK
	24/09/04	048-056	LN-6N	019	027	20:12	20:16	23,500	4.5/175	LLYK NAT. PARK
	24/09/04	057-078	LN-8S	028	049	20:20	20:30	23,500	4.5/175	LLYK NAT. PARK
	24/09/04	079-084	LN-7N	050	055	20:33	20:36	23,500	4.5/175	LLYK NAT. PARK
	24/09/04	085-106	LN-9N	056	077	20:43	20:54	24,000	4.5/175	LLYK NAT. PARK
	24/09/04	107-128	LN-10S	078	099	20:58	21:07	24,000	4.5/175	LLYK NAT. PARK
	24/09/04	129-148	LN-11N	100	119	21:10	21:20	24,000	4.5/175	LLYK NAT. PARK
	24/09/04	149-166	LN-12S	120	137	21:23	21:31	23,500	4.5/175	LLYK NAT. PARK
	24/09/04	167-181	LN-5E	138	152	21:45	21:50	23,000	4.5/175	BANFF TOWNSITE
	27/09/04	182-191	LN-6W	001	010	18:26	18:29	22,500	4.5/125	BANFF TOWNSITE
	27/09/04	192-200	LN-1W	011	019	18:54	18:55	22,500	4.5/125	GLACIER NAT. PARK
	27/09/04	201-213	LN-2E	020	032	19:00	19:05	22,500	4.5/125	GLACIER NAT. PARK
	27/09/04	214-227	LN-3W	033	046	19:12	19:18	22,500	4.5/125	GLACIER NAT. PARK
	27/09/04	228-240	LN-4E	047	059	19:21	19:26	22,500	4.5/125	GLACIER NAT. PARK
	27/09/04	241-253	LN-5W	060	072	19:30	19:36	22,500	4.5/125	GLACIER NAT. PARK
	27/09/04	254-261	LN-6E	073	080	19:40	19:43	22,500	4.5/125	GLACIER NAT. PARK
	01/10/04	262-267	LN-7W	001	006	18:26	18:30	22,500	4.5/125	GLACIER NAT. PARK
										TRAILER

	Take Off	Land At	Take Off	Land At	Take Off	Land At	Take Off	Land At
Date	SEPT 24,04		SEPT 27,04					
	From	To	From	To	From	To	From	To
Base	YYC	YYC	YYC	YYC				
Time	18:40	22:10	17:30	20:50				

Aircraft Registration	Type	Photographer
C-GBLB	C-T310R	MATT LEGAULT / BILL FIRTH
Camera Port Category	Altimeter No.	Navigator
A	ARC 370	MATT LEGAULT / BILL FIRTH
Camera Port No.		Pilot
NRL 16-6-81-1		BOB HARRITY

APPENDIX B: AERIAL TRIANGULATION REPORT

March 6, 2006

Selkirk College
301 Frank Beinder Way
Castlegar, B.C.
V1N 3J1

Att: Donna Delparte

Re: Aerial Triangulation Report for Selkirk College Colour Photo: Job #050609

The photo for Glacier National Park was Aerial Triangulated by Integrated Mapping Technologies for the purpose of generating DiAP Viewer data. The work was performed in August 2005.

This report describes source materials, hardware, software and procedures used. Statistical results and accuracy's are also included and summarized for the 76 photos triangulated. Accompanying this report is the PAT-B output file.

1. Photographic Materials

Source, scale and date	Geodesy, ~1:30,000, Date 2004
Overlaps	~60% forward, ~30%
Roll Number	A31888

2. Control

a) Control Coordinates

TRIM I High Level Control (TRIM I Control has an absolute accuracy of +/- 3m.)

Classes and Weights

Control Points

Std. Dev. Set (metres)	Number of points used		Declared Standard Deviation	
	H	V	H	V
SDS1	26	25	5.0	2.0
SDS2		1	5.0	5.0

3. Equipment and Software

Image Resolution	25 microns
Mensuration	I.S.M. Digital Image Analytical Plotter Workstation With the Aerial Triangulation Module: ISM DiAP-ATM
Block Adjustment	K^2-Photogrammetry PAT-B

4. Methodology / Procedure

a) Pre-scanned images were provided at a resolution of 25 micron which results in a raw ground pixel size of 0.75 metres. No information was available on the film format scanned or quality of the scanner.

The mensuration of the scanned images was then carried out on an I.S.M. DiAP stereo workstation using I.S.M. ATM software.

Camera lens calibration corrections were applied at the time of measurement. Earth curvature/atmospheric refraction corrections were applied at the time of adjustment.

b). Block Data Cleaning Procedure

Standard deviations were assigned to the input data (image points & control points) based on the critical point list, the output statistics & the block geometry. These standard deviations split the observations into different classes according to their level of accuracy within the adjustment. Once the standard deviations of the observations are assigned, PAT-B then computes the corresponding weights along with the adjustment run. Appendix 1 shows these Block Adjustment Results.

The statistics of the final block-adjustment confirms that the assigned classes of standard deviations are in agreement with the output RMSE of the observations.

5. Quality of Adjustment

The results of the PAT-B adjustment show an average sigma value of 8.48 microns. Vertically (Z), the control used fits to within 1.4m. Horizontally (X/Y), the control fits to within 1.75m.

Relative accuracy of the block (each image adjusted to each other without taking the ground control into account) was .2m

The average redundancy of the block was 0.44.

6. Summary

The results of the PAT-B adjustment show this to be a structurally sound aerial survey database, both within itself and when adjusted using the provided control. Statistically, the results show a relative accuracy of less than .2m. The absolute accuracy of the block is in the order of 1.5 metres.

Sincerely,

Richard Marty
Vice President
Integrated Mapping Technologies
Suite 428, 800 West Pender Street,
Vancouver, BC, Canada V6C 2V6
Tel: +1 604 682 7376 • Fax: +1 604 682 7326
E-mail: imt@imtcan.com

APPENDIX C: COMPARING 2ND AND 4TH ORDER POLYNOMIAL FITS IN THE RUNOUT ZONE

In examining the best line of fit for the avalanche profiles of this dataset, the use of both 2nd and 4th order polynomials was explored. The purpose was to find a function that accurately represented the DEM profile in order to determine the regression parameters of H and Hy″θ necessary for the alpha-beta runout model. Second, a comparison was made between the position of the predicted alpha or maximum runout position by using extended 2nd and 4th order functions and the DEM profile.

To create 2nd and 4th order polynomials from the avalanche profile, the coordinate locations from the top of the profile to the expert identified maximum runout were utilized. Table 24 compares the H values from the polynomials to the actual measured drop on the DEM profile. H as measured on the 4th order polynomial is much closer to the DEM measured vertical drop on average for the 35 avalanche profiles and for paths A and B. Table 24. represents the runout portion of avalanche path B and shows the 2nd degree function dipping below the DEM profile. However this appears to be similar for other datasets and a difference in the H value measured on the 2nd degree polynomial compared to the true vertical drop is expected (Bakkehoi et al., 1983). Further, for this dataset, H and Hy″θ as measured on the 2nd degree polynomial are significant contributors along with beta to predict alpha.

Table 24. Comparison of H values from the 2nd and 4th degree polynomials to the actual measured drop

High resolution dataset (n=35)	Average	For Path A:	For Path B:
Vertical drop (DEM)	946.4	1025.0	1287.3
H (4th order) (m)	949.7	1060.6	1288.9
H (2nd order) (m)	1187.0	1571.4	1437.7

An important distinction must be made between calculating regression parameters from the 2nd degree polynomial for the regression equation and actually finding a final alpha predicted position on the avalanche profile. Ideally the extended DEM profile would be used to calculate the position at which the predicted alpha intersects it. To demonstrate the importance of using the DEM profile, Figure 47. displays the 2nd and 4th degree polynomial fits for avalanche path B in the runout zone. The 4th degree provides a much closer representation to the DEM avalanche profile and could potentially be used to estimate the position of alpha. The differences in the runout zone between the polynomial functions and the DEM profile is detailed in Table 25. For example, the full runout model for avalanche path B as based on the 4th degree model is 45.9 m too long and 1.4 m too low; in contrast, the 2nd degree function for the same value yields an overestimate of 145.7 too long and 44.6 m too low. Note that the dip in the DEM profile line (Figure 47) is due to the presence of a stream.

Table 25. Avalanche path B with calculated differences between the predicted alpha positions as measured on the 2nd degree polynomial, the 4th degree polynomial and the DEM profile

Equation and predicted alpha		2nd degree polynomial		4th degree polynomial		DEM profile	
Eq.	$\hat{\alpha}$ (°)	Distance (m)	Elevation (m)	Distance (m)	Elevation (m)	Distance (m)	Elevation (m)
2	23.38	145.7	-44.6	45.9	-1.4	43.3	-3.3
4	23.15	203.8	-55.3	84.6	-4.4	113.4	-16.7
7	22.68	327.5	-76.6	163.9	-8.2	204.8	-25.3

Thus, for this dataset, measuring H and $Hy''\theta$ on a 2nd order function contributed to finding an alpha-beta runout model which, along with beta, was used to estimate maximum runout. Finding the position of this point is ideally found along an extended DEM profile or if points beyond the surveyed maximum runout are not available, the 4th degree polynomial would be better to use than a 2nd degree polynomial as it provides a better fit for the runout portion of the profile.

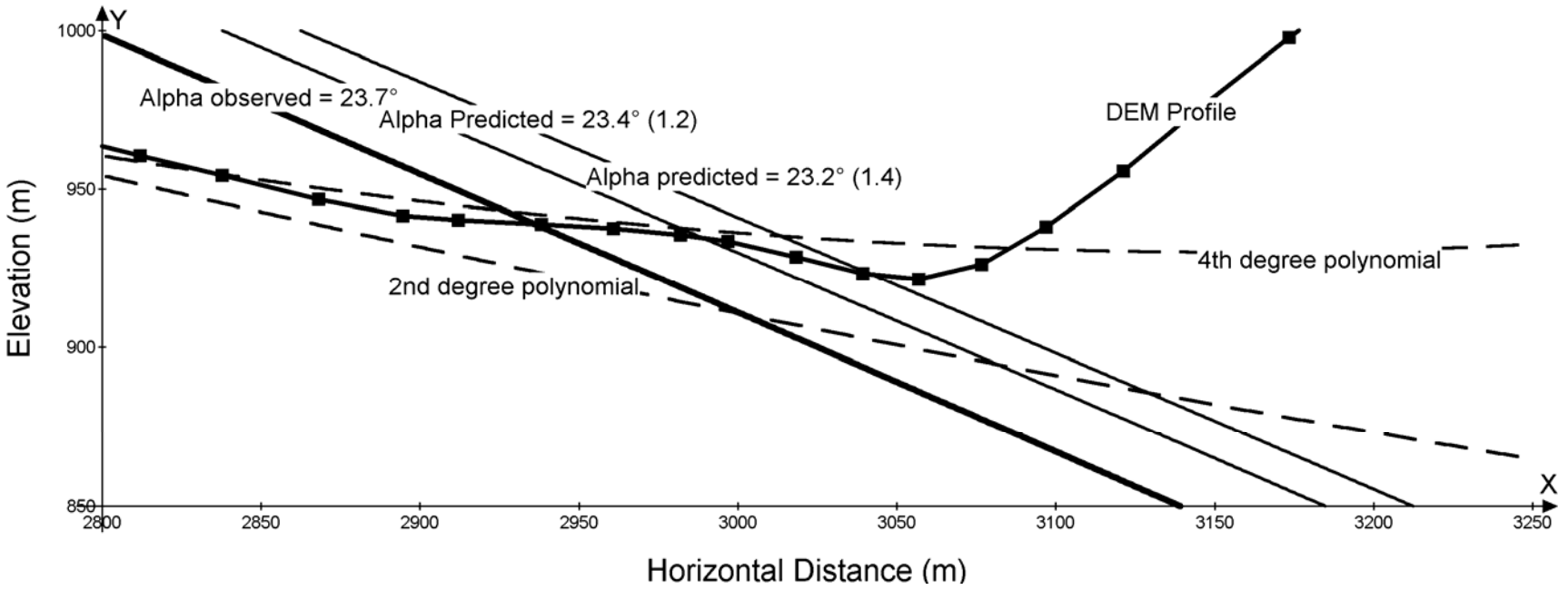

Figure 47. Avalanche path B runout zone comparing predicted alpha values as measured on the 2nd degree polynomial, 4th degree polynomial and the DEM profile. Table 25 provides a measure of the distances from the observed alpha location.